

Supplementary Information

A Crystalline Cyclic (Alkyl)(amino)carbene with a 1,1'-Ferrocenylene Backbone

Julia Volk,^a Myron Heinz,^b Michael Leibold,^a Clemens Bruhn,^a Tobias Bens,^c Biprajit Sarkar,^c Max C. Holthausen,^b and Ulrich Siemeling*^a

^a Institut für Chemie, Universität Kassel, Heinrich-Plett-Straße 40, 34132 Kassel, Germany

^b Institut für Anorganische und Analytische Chemie, Goethe-Universität, Max-von-Laue-Straße 7, 60438 Frankfurt am Main, Germany

^c Institut für Anorganische Chemie, Universität Stuttgart, Pfaffenwaldring 55, 50659 Stuttgart, Germany

Table of Contents

I	Experimental Section	S2
A	Compound Synthesis	S2
B	Determination of the Activation Barrier for the Formation of 10 from 8 ^{Mes}	S8
C	Electrochemistry and Spectroelectrochemistry	S10
D	X-Ray Crystallography	S12
E	Plots of NMR Spectra	S26
F	Plots of IR Spectra	S48
G	Percent Buried Volume (%V _{bur}) as Determined from [AuCl(L)] (L = 8 ^{Mes} , H , I , K)	S51
II	Computational Details	S55
	References	S63

A Compound Synthesis

General considerations

All reactions involving air-sensitive compounds were performed in an inert atmosphere (argon or dinitrogen) by using standard Schlenk techniques or a conventional glovebox. Starting materials were procured from standard commercial sources and used as received. 1,1'-Dibromoferrocene,^{S1} tosyl azide,^{S2} dimesityliodonium triflate^{S3} and [AuCl(THT)] (THT = tetrahydrothiophene)^{S4} were synthesised by adapted versions of the published procedures. NMR spectra were recorded at ambient temperature with Varian NMRS-500 and MR-400 spectrometers operating at 500 and 400 MHz, respectively, for ¹H. High-resolution (HR) electrospray ionisation (ESI) and direct-inlet probe atmospheric pressure chemical ionisation (APCI-DIP) mass spectra were obtained with a Bruker Daltonics micrOTOF time-of-flight mass spectrometer using an Apollo™ “ion funnel” ESI source. Mass calibration was performed immediately prior to the measurement. IR spectra were obtained with a Bruker ALPHA FT-IR spectrometer. Elemental analyses were carried out with a HEKAtech Euro EA-CHNS elemental analyser at the Institute of Chemistry, University of Kassel, Germany.

Synthesis of 2: A stirred solution of 1,1'-dibromoferrocene (**1**; 16.43 g, 47.8 mmol) in THF (60 mL) was cooled to –30 °C. *n*BuLi (1.59 M in hexane, 28.4 mL, 45.2 mmol) was added via syringe. Stirring was continued at this temperature for 1 h, leading to the formation of a light orange precipitate. A solution of benzophenone (7.84 g, 43.0 mmol) in THF (20 mL) was added via syringe. The cooling bath was removed and stirring was continued for 1 h. Volatile components were removed under reduced pressure. Diethyl ether (50 mL) and water (20 mL) were added sequentially. The mixture was stirred vigorously for 5 min. The organic layer was separated off. The aqueous layer was extracted with diethyl ether (50 mL). The combined organic layers were dried with MgSO₄. The drying agent was filtered off. The solvent was removed from the filtrate under reduced pressure, which afforded the crude product as a viscous red oil. Purification was achieved by column chromatography (silica gel). Unreacted starting material and impurities were removed by elution with *n*-hexane. The product was subsequently eluted with a mixture of *n*-hexane and diethyl ether (10:1). Volatile components were removed under reduced pressure, leaving the product as an orange crystalline solid. Yield 14.22 g (70 %). Anal. calcd for C₂₃H₁₉BrFeO (447.15): C 61.78, H 4.28 %; found C 62.02, H 4.43 %. ¹H NMR (400 MHz, C₆D₆): δ = 7.41 – 7.39 (m, 4 H, Ph), 7.11 – 7.01 (m, 6 H, Ph), 4.21, 4.01, 3.97, 3.69 (4 m, 4 × 2 H, cyclopentadienyl H), 2.96 ppm (s, 1 H, OH). ¹³C{¹H} NMR (101 MHz, C₆D₆): δ = 147.8 (Ph C_{ipso}), 127.8, 127.6, 127.1 (3 × Ph CH), 100.4, 77.9 (2 × cyclopentadienyl C_{ipso}), 71.7 (cyclopentadienyl CH), 71.2 (two closely spaced signals, 2 × cyclopentadienyl CH) 69.0 (Ph₂C), 68.2 ppm (cyclopentadienyl CH). HRMS/ESI(+): *m/z* = 445.9965 [M]⁺; 445.9969 calcd for [C₂₃H₁₉BrFeO]⁺.

Synthesis of 3: HBF₄·OEt₂ (3.63 g, 22.4 mmol) was added via syringe to a stirred solution of **2** (6.67 g, 14.9 mmol) in diethyl ether (30 mL). Stirring was discontinued after 15 min. The dark green precipitate was allowed to settle for 15 min. The supernatant was decanted off. The precipitate was washed with diethyl ether (3 × 20 mL) and was subsequently dried under reduced pressure, which afforded the product as a dark green powdery solid. Yield 4.77 g (62 %). Anal. calcd for C₂₃H₁₈BBrF₄Fe (516.94): C 53.44, H 3.51 %; found C 53.69, H 3.59 %. ¹H NMR (400 MHz, CD₂Cl₂): δ = 7.93 (br., 2 H, Ph), 7.53 – 7.48 (br., 8 H, Ph), 6.68, 5.52, 5.15, 4.75 ppm (4 br., 4 × 2 H, cyclopentadienyl H). ¹³C{¹H} NMR (101 MHz, CD₂Cl₂): δ = 184.4 (Ph₂C), 142.0 (Ph C_{ipso}), 134.8, 133.1, 130.4 (3 × Ph CH), 99.2 (cyclopentadienyl C_{ipso}), 96.0 (cyclopentadienyl CH), 86.9 (cyclopentadienyl C_{ipso}), 82.0, 81.1, 79.6 ppm (3 × cyclopentadienyl CH). ¹⁹F NMR (376 MHz, CD₂Cl₂): δ = –152.6 ppm. HRMS/APCI-DIP(+): *m/z* = 428.9938 [M – BF₄]⁺; 428.9941 calcd for [C₂₃H₁₈BrFe]⁺.

Synthesis of 4: A solution of NaCN (3.81 g, 77.7 mmol) in water (25 mL) was added to a vigorously stirred solution of **3** (13.40 g, 25.9 mmol) in dichloromethane (70 mL). Stirring was continued until

the dark green colour of the mixture had changed to brown (ca. 15 min). The organic layer was separated off, washed with water (3 × 30 mL) and was subsequently dried with MgSO₄. The drying agent was filtered off. The solvent was removed from the filtrate under reduced pressure. The crude product was purified by column chromatography (silica gel, dichloromethane/*n*-hexane 1:5). Volatile components were removed under reduced pressure, leaving the product as an orange powdery solid. Yield 10.13 g (86 %). Anal. calcd for C₂₄H₁₈NBrFe (456.16): C 63.19, H 3.98, N 3.07 %; found C 63.22, H 4.12, N 3.03 %. ¹H NMR (400 MHz, C₆D₆): δ = 7.27 – 7.25 (m, 4 H, Ph), 6.96 – 6.94 (m, 6 H, Ph), 4.29, 4.02, 4.00, 3.98 ppm (4 m, 4 × 2 H, cyclopentadienyl H). ¹³C{¹H} NMR (101 MHz, C₆D₆): δ = 141.7 (Ph C_{ipso}), 128.6, 128.3, 128.1 (3 × Ph CH), 122.5 (CN), 91.9, 78.1 (2 × cyclopentadienyl C_{ipso}), 72.6, 72.0, 71.2, 69.8 (4 × cyclopentadienyl CH), 53.3 (Ph₂C) ppm. HRMS/APCI-DIP(+): *m/z* = 454.9968 [M]⁺; 454.9972 calcd for [C₂₄H₁₈BrFeN]⁺.

Synthesis of 5: A stirred solution of **4** (2.32 g, 5.1 mmol) in THF (80 mL) was cooled to –90 °C. *t*BuLi (1.59 M in pentane, 3.2 mL, 5.1 mmol) was added rapidly in one portion. As soon as the colour of the mixture changed from yellow to dark green (ca. 2 s), tosyl azide (1.10 g, 5.6 mmol) was added in one portion, whereupon the colour changed immediately to dark red. Stirring was continued at –90 °C for 1 h. The cooling bath was removed and the mixture was allowed to warm up to room temperature. Water (40 mL) was added and stirring was continued for 30 min. The volume of the mixture was reduced to ca. 40 mL under reduced pressure. Diethyl ether (60 mL) was added. The organic layer was separated off, washed with water (2 × 20 mL) and was subsequently dried with MgSO₄. The drying agent was filtered off. The solvent was removed from the filtrate under reduced pressure, leaving a dark brown viscous oil (assumed to be the crude azidoferrocene [Fe(η⁵-C₅H₄CPh₂CN)(η⁵-C₅H₄N₃)]), which was not further analysed, but immediately used for a Staudinger reaction. For this purpose, the oil was dissolved in diethyl ether (40 mL) and toluene (20 mL). PPh₃ (1.67 g, 6.4 mmol) was added to the stirred mixture, leading to instantaneous gas evolution. Stirring was discontinued after 45 min. Insoluble material was removed by filtration. Volatile components were removed from the filtrate under reduced pressure. The remaining orange-brown viscous oil was taken up in diethyl ether (50 mL). Slow evaporation of the solvent under ambient conditions over the course of ca. 24 h afforded the product as a brown crystalline solid, which was separated from the mother liquor, washed with diethyl ether (3 × 4 mL) and subsequently dried under reduced pressure. Yield 1.99 g (60 %). Anal. calcd for C₄₂H₃₃N₂FeP (652.55): C 77.31, H 5.10, N 4.29 %; found C 77.32, H 5.19, N 4.23 %. ¹H NMR (400 MHz, C₆D₆): δ = 7.81 – 7.67 (m, 6 H, PPh), 7.46 – 7.35 (m, 4 H, PPh), 7.10 – 6.87 (m, 15 H, Ph), 4.21, 4.14 (2 m, 2 × 2 H, cyclopentadienyl H), 3.84 ppm (m, 4 H, cyclopentadienyl H). ¹³C{¹H} NMR (101 MHz, C₆D₆): δ = 142.7 (phenyl C_{ipso}), 133.1 (d, *J*_{CP} = 9.8 Hz, PPh CH), 131.8 (d, *J*_{CP} = 98.4 Hz, PC_{ipso}), 131.5 (d, *J*_{CP} = 2.8 Hz, PPh CH), 128.7 (Ph CH), 128.6 (d, *J*_{CP} = 11.8 Hz, PPh CH), 128.1, 127.8 (2 × Ph CH), 123.1 PhCCN), 113.1, 89.2 (2 × cyclopentadienyl C_{ipso}), 71.4, 69.0, 65.9 (3 × cyclopentadienyl CH), 63.8 (d, *J*_{CP} = 16.0 Hz, cyclopentadienyl CH), 53.8 ppm (Ph₂C). ³¹P{¹H} NMR (202 MHz, C₆D₆): δ = 1.3 ppm. HRMS/APCI-DIP(+): *m/z* = 653.1804 [M + H]⁺; 653.1809 calcd for [C₄₂H₃₄FeN₂P]⁺.

Synthesis of 6: An aqueous NaOH solution (20 mL, 15 %) was added to a suspension of **5** (4.60 g, 7.05 mmol) in toluene (60 mL) placed in a pressure Schlenk tube, which was subsequently sealed with a screw cap. The mixture was stirred vigorously at a bath temperature of 105 °C for 20 h. The heating bath was removed and the mixture was allowed to cool to room temperature. The organic layer was separated off and dried with K₂CO₃. The drying agent was filtered off. The solvent was removed from the filtrate under reduced pressure. The crude product was purified by column chromatography (silica gel, diethyl ether/*n*-hexane/triethyl amine 2:1:0.01). Volatile components were removed under reduced pressure, leaving the product as a yellow powdery solid. Yield 2.57 g (93 %). Anal. calcd for C₂₄H₂₀N₂Fe (392.28): C 73.48, H 5.14, N 7.14 %; found C 73.07, H 5.32, N 7.09 %. ¹H NMR (400 MHz,

C_6D_6): δ = 7.39 – 7.34 (m, 4 H, Ph), 7.01 – 6.93 (m, 6 H, Ph), 3.97, 3.89, 3.81, 3.75 (4 m, 4 × 2 H, cyclopentadienyl H), 2.19 ppm (s, 2 H, NH_2). $^{13}C\{^1H\}$ NMR (101 MHz, C_6D_6): δ = 142.2 (Ph C_{ipso}), 128.5, 128.5, 127.9 (3 × Ph CH), 123.4 (PhCCN), 108.3, 90.6 (2 × cyclopentadienyl C_{ipso}), 70.0, 69.7, 64.9, 59.7 (4 × cyclopentadienyl CH), 53.9 ppm (Ph_2C). HRMS/APCI-DIP(+): m/z = 393.1049 [$M + H$]⁺; 393.1054 calcd for [$C_{24}H_{21}FeN_2$]⁺.

Synthesis of 7: A stirred solution of **6** (1.00 g, 2.55 mmol) in toluene (10 mL) was cooled in an ice bath. Diisobutylaluminium hydride (1.0 M in toluene, 6.1 mL, 6.1 mmol) was added via syringe. The ice bath was removed after 5 min. Stirring was continued for 30 min. Water (20 mL) was added. The mixture was stirred vigorously for 15 min. The mixture was subsequently allowed to stand at complete rest for 1 h for phase separation. The organic layer was decanted off. The aqueous layer was extracted with toluene (ca. 4 × 10 mL) until the extract was colourless. $MgSO_4$ (20 g) was added to the combined extracts. The mixture was stirred for 1 h. Insoluble material was filtered off. The solvent was removed from the filtrate under reduced pressure. The resulting brown solid was washed with diethyl ether (2 × 2 mL) and subsequently dried under reduced pressure, which furnished the product as a yellow powdery solid. Yield 485 mg (51 %). Anal. calcd for $C_{24}H_{19}NFe$ (377.26): C 76.41, H 5.08, N 3.71 %; found C 76.38, H 5.22, N 3.56 %. 1H NMR (400 MHz, C_6D_6): δ = 8.62 (s, 1 H, N=CH), 7.36 – 7.34 (m, 4 H, Ph), 7.07 – 7.01 (m, 6 H, Ph), 4.04, 3.92, 3.85, 3.56 ppm (4 m, 4 × 2 H, cyclopentadienyl H). $^{13}C\{^1H\}$ NMR (101 MHz, C_6D_6): δ = 173.0 (N=CH), 144.6 (Ph C_{ipso}), 129.9, 128.5, 127.1 (3 × Ph CH), 111.6, 86.6 (2 × cyclopentadienyl C_{ipso}), 72.1, 70.6, 67.8, 62.6 (4 × cyclopentadienyl CH), 54.4 ppm (Ph_2C).

Synthesis of $8^{Me}H[BF_4]$: $Me_3O[BF_4]$ (19 mg, 0.13 mmol) was added to a stirred solution of **7** (50 mg, 0.13 mmol) in dichloromethane (4 mL). After 24 h volatile components were removed under reduced pressure. The solid residue was washed with diethyl ether (3 × 2 mL) and subsequently dried under reduced pressure, which furnished the product as a dark red microcrystalline solid. Yield 62 mg (97 %). Anal. calcd for $C_{25}H_{22}NBF_4Fe$ (479.10): C 62.67, H 4.63, N 2.92 %; found C 62.51, H 4.81, N 2.94 %. 1H NMR (400 MHz, CD_2Cl_2): δ = 9.64 (s, 1 H, N=CH), 7.57 – 7.49 (m, 6 H, Ph), 7.42 – 7.38 (m, 4 H, Ph), 4.87, 4.47, 4.42 (3 m, 3 × 2 H, cyclopentadienyl H), 4.36 (s, 3 H, CH_3), 4.28 ppm (m, 2 H, cyclopentadienyl H). $^{13}C\{^1H\}$ NMR (101 MHz, CD_2Cl_2): δ = 191.4 (N=CH), 140.0 (Ph C_{ipso}), 129.9 (Ph CH), 129.4 (two closely spaced signals, 2 × Ph CH), 100.5, 87.3 (2 × cyclopentadienyl C_{ipso}), 73.9 (two closely spaced signals, 2 × cyclopentadienyl CH), 71.6, 67.6 (2 × cyclopentadienyl CH), 60.6 (Ph_2C), 55.8 ppm (CH_3).

Synthesis of $8^{Et}H[BF_4]$: $Et_3O[BF_4]$ (25 mg, 0.13 mmol) was added to a stirred solution of **7** (50 mg, 0.13 mmol) in dichloromethane (4 mL). After 24 h volatile components were removed under reduced pressure. The solid residue was washed with diethyl ether (3 × 2 mL) and subsequently dried under reduced pressure, which furnished the product as a dark red powdery solid. Yield 53 mg (81 %). Anal. calcd for $C_{26}H_{24}NBF_4Fe$ (493.13): C 63.33, H 4.91, N 2.84 %; found C 63.37, H 5.00, N 2.81 %. 1H NMR (400 MHz, CD_2Cl_2): δ = 9.58 (s, 1H, N=CH), 7.50 – 7.41 (m, 6 H, Ph), 7.33 – 7.29 (m, 4 H, Ph), 4.82 (m, 2 H, cyclopentadienyl H), 4.62 (q, $^3J_{HH} = 7.3$ Hz, 2 H, CH_2), 4.43 (m, 4 H, cyclopentadienyl H), 4.23 (m, 2H, cyclopentadienyl H), 1.58 ppm (t, $^3J_{HH} = 7.1$ Hz, 3 H, CH_3). $^{13}C\{^1H\}$ NMR (101 MHz, CD_2Cl_2): δ = 189.8 (N=CH), 139.8 (Ph C_{ipso}), 129.9 (Ph CH), 129.4 (two closely spaced signals, 2 × Ph CH), 98.6, 87.2 (2 × cyclopentadienyl C_{ipso}), 73.9 (two closely spaced signals, 2 × cyclopentadienyl CH), 71.7, 68.4 (2 × cyclopentadienyl CH), 64.2 (CH_2), 60.3 (Ph_2C), 14.4 (CH_3) ppm.

Synthesis of $8^{Mes}H(OTf)$: THF (15 mL) was added to a mixture of **7** (270 mg, 0.72 mmol), CuCl (21 mg, 0.21 mmol) and $Mes_2I(OTf)$ (557 mg, 1.08 mmol). The stirred suspension was heated to 50 °C (oil bath) for 2 h, leading to a colour change from light yellow to dark red. The oil bath was removed and the mixture was allowed to cool down to room temperature. Volatile components were removed

under reduced pressure. Dichloromethane (4 mL) and diethyl ether (4 mL) were added to the residue. Insoluble material was removed by decanting the supernatant off after centrifugation. The solvents were removed from the supernatant under reduced pressure. The residue was suspended in a mixture of THF (4 mL) and diethyl ether (2 mL). The dark insoluble material was isolated by decanting the supernatant off after centrifugation. It was subsequently washed with diethyl ether (2 × 5 mL) and was finally dried under reduced pressure, which furnished the product as a violet powdery solid. Yield 220 mg (47 %). Anal. calcd for C₃₄H₃₀NSF₃FeO₃ (645.51): C 63.26, H 4.68, N 2.17, S 4.97 %; found C 63.30, H 4.63, N 2.13, S 4.32 %. ¹H NMR (400 MHz, CD₂Cl₂): δ = 9.76 (s, 1 H, N=CH), 7.54 – 7.45 (m, 6 H, Ph), 7.41 – 7.37 (m, 4 H, Ph), 7.08 (s, 2 H, C₆H₂Me₃), 4.96, 4.55, 4.49, 4.45 (4 m, 4 × 2 H, Cp), 2.34 ppm (s, 9 H, CH₃). ¹³C{¹H} NMR (101 MHz, CD₂Cl₂): δ = 195.4 (N=CH), 142.9, 142.2, 140.3, 131.8, 131.6, 130.3, 129.8, 129.3 (8 × aryl C), 98.8, 88.4 (2 × cyclopentadienyl C_{ipso}), 74.6, 74.4, 72.3, 69.2 (4 × cyclopentadienyl CH), 62.1 (Ph₂C), 21.3, 19.1 ppm (2 × CH₃); CF₃ not detected. ¹⁹F NMR (376 MHz, CD₂Cl₂): δ = -78.4 ppm. HRMS/ESI(+): *m/z* = 496.1713 [M – OTf]⁺; 496.1728 calcd for [C₃₃H₃₀FeN]⁺.

Synthesis of 8^{Mes}: *n*-Hexane (4 mL) and diethyl ether (2 mL) were added to a mixture of 8^{Mes}H(OTf) (75 mg, 0.12 mmol) and (Me₃Si)₂NK (25 mg, 0.13 mmol). The mixture was stirred for 2 min and subsequently filtered through Celite to remove insoluble material. The volume of the filtrate was reduced to ca. 2 mL under reduced pressure. Storage of the solution at -40 °C for 6 h afforded the product as light yellow crystals, which could be stored at this temperature without any signs of decomposition for several weeks, but decomposed at room temperature within 1 d. The crystals were isolated by removing the mother liquor with a syringe and washed with diethyl ether (3 × 2 mL). The product was subsequently dried briefly under reduced pressure. Yield 39 mg (68 %). ¹H NMR (400 MHz, C₆D₆): δ = 7.99 – 7.97, 7.22 – 7.18 (2 m, 2 × 4 H, Ph), 7.08 – 7.04 (m, 2 H, Ph), 6.72 (s, 2 H, C₆H₂Me₃), 4.27, 4.04, 3.89, 3.73 (4 m, 4 × 2 H, cyclopentadienyl H), 2.31 (s, 6 H, *o,o'*-CH₃), 2.11 ppm (s, 3 H, *p*-CH₃). ¹H NMR (400 MHz, THF-*d*₈): δ = 7.65 – 7.63, 7.24 – 7.20 (2 m, 2 × 4H, Ph), 7.15 – 7.11 (m, 2 H, Ph), 6.90 (s, 2 H, C₆H₂Me₃), 4.46, 4.18, 3.99, 3.81 (4 m, 4 × 2 H, cyclopentadienyl H), 2.31 (s, 6 H, *o,o'*-CH₃), 2.25 ppm (s, 3 H, *p*-CH₃). ¹³C{¹H} NMR (101 MHz, C₆D₆): δ = 360.2 (C_{carbene}), 148.3, 147.7, 136.0, 132.5, 131.1, 130.4, 128.0, 126.4 (8 × aryl C), 111.7, 94.7 (2 × cyclopentadienyl C_{ipso}), 72.3, 70.9, 67.9, 66.6 (4 × cyclopentadienyl CH), 63.5 (Ph₂C), 20.8, 19.5 ppm (2 × CH₃). ¹³C{¹H} NMR (101 MHz, THF-*d*₈): δ = 359.2 (C_{carbene}), 147.7, 147.0, 135.4, 132.0, 130.4, 129.5, 127.0, 125.5 (8 × aryl C), 111.3, 94.0 (2 × cyclopentadienyl C_{ipso}), 71.5, 70.0, 67.1, 66.0 (4 × cyclopentadienyl CH), 62.7 (Ph₂C), 19.8, 18.5 ppm (2 × CH₃).

Synthesis of [AuCl(8^{Mes})]: 8^{Mes} was generated from 8^{Mes}H(OTf) (20 mg, 0.03 mmol) and (Me₃Si)₂NK (7 mg, 0.04 mmol) in benzene (0.7 mL). The suspension was filtered through Celite. [AuCl(THT)] (12 mg, 0.04 mmol) was added to the filtrate, leading to instantaneous formation of a yellow precipitate. The solid was separated from the mother liquor after centrifugation, washed with diethyl ether (2 × 2 mL) and dried under reduced pressure. The crude product was taken up in CD₂Cl₂ (0.6 mL). Small amounts of insoluble material were removed by filtration through Celite. The filtrate was placed in a 5 mm NMR tube and subjected to spectroscopic analysis. Subsequently diethyl ether (2 mL) was added. The volume of the solution was reduced to ca. 2 mL by slow evaporation of the solvents under ambient conditions. The product was obtained as red crystals, which were separated from the mother liquor and subsequently dried under reduced pressure. Yield 9 mg (40 %). ¹H NMR (400 MHz, CD₂Cl₂): δ = 7.75 – 7.73 (m, 4 H, Ph), 7.46 – 7.38 (m, 6 H, Ph), 6.98 (s, 2 H, C₆H₂Me₃), 4.67, 4.30, 4.25, 4.21 (4 m, 4 × 2 H, cyclopentadienyl H), 2.43 (s, 6 H, *o,o'*-CH₃), 2.29 ppm (s, 3 H, *p*-CH₃). ¹³C{¹H} NMR (101 MHz, CD₂Cl₂): δ = 246.3 (C_{carbene}), 147.2, 143.8, 139.4, 131.7, 131.6, 131.0, 128.7, 128.5 (8 × aryl C), 105.9, 90.1 (2 × cyclopentadienyl C_{ipso}), 73.0 (two closely spaced signals), 70.5 (3 × cyclopentadienyl CH), 66.7 (Ph₂C), 66.4 (cyclopentadienyl CH), 21.2, 19.7 ppm (2 × CH₃).

Synthesis of [CuCl(8**^{Mes})]:** CuCl (10 mg, 0.10 mmol) was added to a solution of **8**^{Mes} (20 mg, 0.04 mmol) in THF (4 mL). The suspension was stirred for 24 h. Volatile components were removed under reduced pressure. The remaining solid was extracted with C₆D₆ (0.6 mL). Insoluble material was removed by filtration through Celite. The filtrate was placed in a 5 mm NMR tube and subjected to spectroscopic analysis. After standing for 15 h, yellow crystals had formed, which were separated from the mother liquor, washed with *n*-hexane (2 × 1 mL) and subsequently dried under reduced pressure. Yield 12 mg (50 %). ¹H NMR (400 MHz, CD₂Cl₂): δ = 7.66 – 7.64 (m, 4 H, Ph), 7.43 – 7.34 (m, 6 H, Ph), 6.99 (s, 2 H, C₆H₂Me₃), 4.61, 4.32, 4.23, 4.21 (4 m, 4 × 2 H, cyclopentadienyl H), 2.41 (s, 6 H, *o,o'*-CH₃), 2.30 ppm (s, 3 H, *p*-CH₃). ¹³C{¹H} NMR (101 MHz, CD₂Cl₂): δ = 263.5 (C_{carbene}), 146.5, 144.8, 139.4, 132.0, 131.1, 131.1, 128.9, 128.3 (8 × aryl C), 105.7, 90.6 (2 × cyclopentadienyl C_{ipso}), 73.1, 72.7, 70.0, 67.0 (4 × cyclopentadienyl CH), 65.3 (Ph₂C), 21.2, 19.7 ppm (2 × CH₃).

Synthesis of **8^{Mes}Se:** THF (2 mL) was added to a mixture of **8**^{Mes}H(OTf) (45 mg, 0.07 mmol), (Me₃Si)₂NK (18 mg, 0.09 mmol) and grey selenium (11 mg, 0.14 mmol). The mixture was stirred for 30 min. Volatile components were removed under reduced pressure. The residue was subjected to separation by column chromatography (silica gel). Impurities were eluted with *n*-hexane. The product was subsequently eluted with toluene. Evaporation of the eluent under reduced pressure afforded the product as an orange-red powdery solid. Yield 22 mg (55 %). Anal. calcd for C₃₃H₂₉NFeSe (574.40): C 69.00, H 5.09, N 2.44 %; found C 69.15, H 5.31, N 2.39 %. ¹H NMR (400 MHz, C₆D₆): δ = 7.93 – 7.91, 7.16 – 7.14 (2 m, 2 × 4 H, Ph), 7.12 – 7.08 (m, 2 H, Ph), 6.71 (s, 2 H, C₆H₂Me₃), 4.43, 4.25, 4.05, 3.68 (4 m, 4 × 2 H, cyclopentadienyl H), 2.44 (s, 6 H, *o,o'*-CH₃), 2.06 ppm (s, 3 H, *p*-CH₃). ¹³C{¹H} NMR (101 MHz, C₆D₆): δ = 219.8 (CSe), 148.1, 147.9, 136.9, 132.7, 132.4, 130.8, 127.1, 126.8 (8 × aryl C), 99.6, 91.2 (2 × cyclopentadienyl C_{ipso}), 73.0, 72.4 (2 × cyclopentadienyl CH), 71.6 (Ph₂C), 69.6, 66.4 (2 × cyclopentadienyl CH), 20.9, 20.0 ppm (2 × CH₃). ⁷⁷Se NMR (95 MHz, acetone-*d*₆): δ = 1039 ppm. HRMS/APCI-DIP(+): *m/z* = 576.0891 [M + H]⁺; 576.0893 calcd for [C₃₃H₃₀FeNSe]⁺.

Synthesis of **8^{Mes}S:** Benzene (1 mL) was added to a mixture of **8**^{Mes}H(OTf) (30 mg, 0.05 mmol), (Me₃Si)₂NK (10 mg, 0.05 mmol) and freshly sublimed sulfur (3 mg, 0.09 mmol S) in a 5 mm NMR tube. The mixture was shaken for 1 min. Volatile components were removed under reduced pressure. The residue was subjected to separation by column chromatography (silica gel). Impurities were eluted with *n*-hexane. The product was subsequently eluted with toluene. Slow evaporation of the eluent under ambient conditions afforded the product as yellow crystals. Yield 17 mg, 69 %. ¹H NMR (500 MHz, C₆D₆): δ = 7.85 – 7.82, 7.15 – 7.13 (2 m, 2 × 4 H, Ph), 7.09 – 7.07 (m, 2 H, Ph), 6.72 (s, 2H, C₆H₂Me₃), 4.42, 4.22, 4.08, 3.71 (4 m, 4 × 2 H, cyclopentadienyl H), 2.41 (s, 6 H, *o,o'*-CH₃), 2.06 ppm (s, 3 H, *p*-CH₃). ¹³C{¹H} NMR (126 MHz, C₆D₆): δ = 212.4 (CS), 148.2, 146.1, 136.8, 133.2, 132.3, 130.8, 127.0, 126.9 (8 × aryl C), 98.0, 91.1 (2 × cyclopentadienyl C_{ipso}), 72.8, 72.3, 69.6 (3 × cyclopentadienyl CH), 68.6 (Ph₂C), 67.0 (cyclopentadienyl CH), 20.9, 19.8 ppm (2 × CH₃).

Synthesis of [Rh(9**)(CO)₂]:** THF (6 mL) was cooled to –60 °C and added to a mixture of **8**^{Mes}H(OTf) (70 mg, 0.11 mmol), (Me₃Si)₂NK (43 mg, 0.22 mmol) and [Rh(μ-Cl)(COD)]₂ (27 mg, 0.05 mmol) kept at the same temperature. The mixture was stirred at –60 °C for 2 h. The cooling bath was removed and stirring was continued for 18 h. The mixture was frozen (liquid N₂) and the atmosphere in the reaction vessel replaced with CO. The mixture was allowed to warm up to room temperature and was stirred for 1 h, during which time a colour change from dark red to orange occurred. Volatile components were removed under reduced pressure. *n*-Hexane (6 mL) was added to the residue. Insoluble material was removed by filtration through Celite. The volume of the filtrate was reduced to ca. 3 mL under reduced pressure. Storage of the solution at –40 °C for 24 h afforded the product as red crystals, which were separated from the mother liquor and subsequently dried under reduced pressure. Yield 12 mg (17 %). Anal. calcd for C₃₅H₂₈NFeO₂Rh (653.35): C 64.34, H 4.32, N 2.14 %;

found C 64.36, H 4.42, N 2.18 %. ^1H NMR (400 MHz, C_6D_6): δ = 8.06 – 8.03 (m, 1 H, aryl), 7.52 – 7.50 (m, 2 H, aryl), 7.43 – 7.41 (m, 1 H, aryl), 7.23 – 7.18 (m, 2 H, aryl), 7.15 – 7.14 (m, 2 H, aryl), 7.03 – 6.99 (m, 1 H, aryl), 6.68, 6.65 (2 s, 2 \times 1 H, $\text{C}_6\text{H}_2\text{Me}_3$), 4.52, 4.17 (2 m, 2 \times 1H, cyclopentadienyl H), 3.96 – 3.94 (m, 2 H, cyclopentadienyl H), 3.90 (m, 1 H, cyclopentadienyl H), 3.70 (m, 2 H, cyclopentadienyl H), 3.55 (m, 1 H, cyclopentadienyl H), 2.48, 2.29, 1.99 ppm (3 s, 3 \times 3 H, CH_3). $^{13}\text{C}\{^1\text{H}\}$ NMR (101 MHz, C_6D_6): δ = 275.8 (d, $^1J_{\text{CRh}} = 49.9$ Hz, $\text{C}_{\text{carbene}}$), 195.7 (d, $^1J_{\text{CRh}} = 61.3$ Hz, CO), 191.7 (d, $^1J_{\text{CRh}} = 53.8$ Hz, CO), 167.2 (d, $^1J_{\text{CRh}} = 31.4$ Hz, RhC_{aryl}), 160.0, 148.5, 147.0, 141.5, 138.5, 134.2, 131.1, 130.7, 130.6, 129.1, 128.6, 127.9, 126.9 (13 \times aryl C), 126.2 (d, $^2J_{\text{CRh}} = 2.3$ Hz, aryl C), 125.1 (aryl C), 106.1, 91.0 (2 \times cyclopentadienyl C_{ipso}), 75.0 (d, $^2J_{\text{CRh}} = 5.1$ Hz, PhC), 74.5, 72.4, 71.5, 71.2, 70.0, 68.2, 67.5, 65.9 (8 \times cyclopentadienyl CH), 20.8, 20.4, 20.2 (3 \times CH_3) ppm. IR(ATR): $\tilde{\nu}(\text{CO}) = 2026$, 1961 cm^{-1} ; $\tilde{\nu}_{\text{av}}(\text{CO}) = 1994\text{ cm}^{-1}$. IR(CH_2Cl_2): $\tilde{\nu}(\text{CO}) = 2040$, 1979 cm^{-1} ; $\tilde{\nu}_{\text{av}}(\text{CO}) = 2010\text{ cm}^{-1}$.

Synthesis of $[\text{RhCl}(\text{CO})_2(\mathbf{8}^{\text{Mes}})]$: HCl in diethyl ether (3.0 M, 2 drops) was added to a solution of *cis*- $[\text{Rh}(\mathbf{9})(\text{CO})_2]$ (10 mg, 0.02 mmol) in C_6D_6 (0.6 mL) in a 5 mm NMR tube. The mixture was shaken, which resulted in an immediate colour change from orange to light yellow due to quantitative conversion to the product according to ^1H NMR spectroscopic analysis. The solution was reduced to dryness under reduced pressure. The yellow solid was dried only briefly in order to avoid conversion to $[\text{Rh}(\mu\text{-Cl})(\mathbf{8}^{\text{Mes}})(\text{CO})]_2$ by loss of CO (vide infra) and was subjected to immediate spectroscopic and elemental analysis. No isolated yield determined (assumed to be essentially quantitative). Anal. calcd for $\text{C}_{35}\text{H}_{29}\text{NClFeO}_2\text{Rh}$ (689.82): C 60.94, H 4.24, N 2.03 %; found C 60.70, H 4.67, N 1.71 %. ^1H NMR (400 MHz, C_6D_6): δ = 8.09 – 8.07 (m, 2 H, Ph), 7.81 (br., 2 H, Ph), 7.27 – 7.23 (m, 2 H, Ph), 7.13 – 7.01 (m, 4 H, Ph), 6.71, 6.68 (2 s, 2 \times 1 H, $\text{C}_6\text{H}_2\text{Me}_3$), 4.63, 4.38 (2 m, 2 \times 1 H, cyclopentadienyl H), 4.12 (m, 2 H, cyclopentadienyl H), 4.06, 3.92, 3.70, 3.49 (4 m, 4 \times 1 H, cyclopentadienyl H), 2.90, 2.41, 1.98 ppm (3 s, 3 \times 3 H, CH_3). $^{13}\text{C}\{^1\text{H}\}$ NMR (101 MHz, C_6D_6): δ = 286.0 (d, $^1J_{\text{CRh}} = 40.6$ Hz, $\text{C}_{\text{carbene}}$), 187.5 (d, $^1J_{\text{CRh}} = 53.0$ Hz, CO), 182.7 (d, $^1J_{\text{CRh}} = 78.1$ Hz, CO), 149.2, 146.2, 144.9, 138.7, 134.4, 132.7, 131.8, 131.4, 131.2, 130.0, 128.0 (two closely spaced signals), 127.6, 127.4 (14 \times aryl C), 103.7, 92.9 (2 \times cyclopentadienyl C_{ipso}), 76.4, 74.1, 71.6, 71.3 (4 \times cyclopentadienyl CH), 70.5 (d, $^2J_{\text{CRh}} = 1.7$ Hz, Ph_2C), 70.5, 68.5, 67.8, 65.6 (4 \times cyclopentadienyl CH), 21.8, 20.9, 20.8 ppm (3 \times CH_3). IR(ATR): $\tilde{\nu}(\text{CO}) = 2060$, 1986 cm^{-1} ; $\tilde{\nu}_{\text{av}}(\text{CO}) = 2023\text{ cm}^{-1}$. IR(CH_2Cl_2): $\tilde{\nu}(\text{CO}) = 2071$, 2002 cm^{-1} ; $\tilde{\nu}_{\text{av}}(\text{CO}) = 2036\text{ cm}^{-1}$.

Synthesis of $[\text{Rh}(\mu\text{-Cl})(\text{CO})(\mathbf{8}^{\text{Mes}})]_2$: The dichloromethane solution of $[\text{RhCl}(\mathbf{8}^{\text{Mes}})(\text{CO})_2]$ used for IR spectroscopy was reduced to dryness under reduced pressure. The yellow solid was taken up in C_6D_6 (0.6 mL) and subjected to ^1H NMR spectroscopic analysis, which confirmed its identity. Slow evaporation of the solvent under ambient conditions over the course of one week afforded a red solid, which was washed with benzene (2 \times 0.5 mL) and subsequently dried under reduced pressure. Yield not determined (assumed to be essentially quantitative). ^1H NMR (400 MHz, CD_2Cl_2): δ = 7.76 – 7.74 (m, 8 H, Ph), 7.64 – 7.60 (m, 4 H, Ph), 7.57 – 7.54 (m, 8 H, Ph), 7.03 (s, 4 H, $\text{C}_6\text{H}_2\text{Me}_3$), 4.57, 4.30, 4.27, 3.99 (4 m, 4 \times 4 H, cyclopentadienyl H), 2.75 (s, 12 H, *o,o'*- CH_3), 2.32 ppm (s, 6 H, *p*- CH_3). $^{13}\text{C}\{^1\text{H}\}$ NMR (101 MHz, CD_2Cl_2): δ = 246.3 (d, $^1J_{\text{CRh}} = 38.0$ Hz, $\text{C}_{\text{carbene}}$), 181.0 (d, $^1J_{\text{CRh}} = 115.3$ Hz, CO), 140.0, 133.4, 131.4, 130.9, 130.3, 128.6, 128.3, 128.1 (8 \times aryl C), 102.2, 92.5 (2 \times cyclopentadienyl C_{ipso}), 73.5, 73.1, 69.6 (3 \times cyclopentadienyl CH), 68.5 (d, $^2J_{\text{CRh}} = 4.6$ Hz, Ph_2C), 67.1 (cyclopentadienyl CH), 21.2, 20.7 ppm (2 \times CH_3). IR(ATR): $\tilde{\nu}(\text{CO}) = 1955\text{ cm}^{-1}$.

Synthesis of $\mathbf{8}^{\text{Mes}}\text{CO}$: *n*-Hexane (8 mL) and THF (2 mL) were added to $\mathbf{8}^{\text{Mes}}\text{H}(\text{OTf})$ (60 mg, 0.09 mmol) and $(\text{Me}_3\text{Si})_2\text{NK}$ (20 mg, 0.10 mmol). The suspension was stirred for 10 min and was subsequently frozen (liquid N_2). The atmosphere in the reaction vessel was replaced with CO. The mixture was allowed to warm up to room temperature and was stirred for 1 h. Volatile components were removed under reduced pressure. *n*-Hexane (5 mL) was added to the residue. Insoluble material was removed by filtration through Celite. The volume of the filtrate was reduced to ca. 2.5 mL under

reduced pressure. After storage of the solution at $-40\text{ }^{\circ}\text{C}$ for 12 h, a yellow solid had formed, which was separated from the mother liquor and subsequently dried under reduced pressure. Yield 23 mg (47 %). ^1H NMR (400 MHz, C_6D_6): δ = 7.52 – 7.49 (m, 4 H, Ph), 7.06 – 7.01 (m, 6 H, Ph), 6.69 (s, 2 H, $\text{C}_6\text{H}_2\text{Me}_3$), 4.51, 4.41, 4.10, 3.93 (4 m, 4×2 H, cyclopentadienyl H), 2.14 (s, 6 H, o,o' - CH_3), 2.06 ppm (s, 3 H, p - CH_3). $^{13}\text{C}\{^1\text{H}\}$ NMR (101 MHz, CD_2Cl_2): δ = 220.7 (C=C=O), 146.1, 143.0, 137.4, 136.6, 130.7, 130.3, 128.2, 127.5 ($8 \times$ aryl C), 105.7, 91.3 ($2 \times$ cyclopentadienyl C_{ipso}), 77.8 (C=C=O), 74.5, 69.4, 68.7, 68.0 ($4 \times$ cyclopentadienyl CH), 53.6 (Ph_2C), 20.8, 19.9 ppm ($2 \times \text{CH}_3$). IR(ATR): $\tilde{\nu}(\text{CO}) = 2084\text{ cm}^{-1}$.

Synthesis of 10: A solution of $\mathbf{8}^{\text{Mes}}$ (15 mg, 0.03 mmol) in C_6D_6 (0.6 mL) was stored at room temperature for 48 h. Essentially quantitative conversion to the product had occurred during this time according to NMR spectroscopic analysis. Volatile components were removed under reduced pressure. Diethyl ether (2 mL) was added to the solid residue. After storage of the solution at room temperature for 16 h, light yellow crystals had formed, which were separated from the mother liquor and subsequently dried under reduced pressure. Yield 6 mg (40 %). Anal. calcd for $\text{C}_{33}\text{H}_{29}\text{NFe}$ (495.44): C 80.00, H 5.90, N 2.83 %; found C 79.80, H 6.24, N 2.30 %. ^1H NMR (400 MHz, C_6D_6): δ = 8.58 – 7.54 (br., 2 H, Ph), 7.53 – 7.47 (m, 2 H, Ph), 7.10 – 7.03 (m, 6 H, Ph), 6.63, 6.57 (2 s, 2×1 H, $\text{C}_6\text{H}_2\text{Me}_2\text{CH}_2$), 4.86 (dd, $J_{\text{HH}} = 12.6, 8.6$ Hz, 1 H, CHCH_2), 4.33, 4.30, 4.10 (3 m, 3×1 H, cyclopentadienyl H), 4.01 (m, 2 H, cyclopentadienyl H), 3.99, 3.92, 3.84 (3 m, 3×1 H, cyclopentadienyl H), 3.36 (dd, $J_{\text{HH}} = 15.9, 12.4$ Hz, 1 H, CHCH_2), 2.64 (dd, $J_{\text{HH}} = 15.7, 8.7$ Hz, 1 H, CHCH_2), 2.16, 2.08 ppm (2 s, 2×3 H, CH_3). $^{13}\text{C}\{^1\text{H}\}$ NMR (101 MHz, C_6D_6): δ = 160.2, 147.2, 144.0, 144.0, 133.0 (br.), 132.9 (br.), 132.1, 130.6, 129.7, 129.6, 128.2, 127.9, 127.7, 127.3, 126.6, 126.6, 123.4, 119.3 ($18 \times$ aryl C), 97.9, 96.0 ($2 \times$ cyclopentadienyl C_{ipso}), 84.3 (CHCH_2), 74.0, 73.1, 70.8, 69.7, 69.0, 68.9, 67.7, 65.9 ($8 \times$ cyclopentadienyl CH), 52.9 (PhC), 34.6 (CHCH_2), 20.8, 19.9 ppm ($2 \times \text{CH}_3$).

B Determination of the Activation Barrier for the Formation of 10 from $\mathbf{8}^{\text{Mes}}$

The first-order kinetics of the reaction was established by monitoring four samples of different concentration in C_6D_6 at 298 K by ^1H NMR spectroscopy. The rate constant was found to be independent of the concentration ($k_{298} = 5 \cdot 10^{-5}\text{ s}^{-1}$). The results of a representative experiment are exemplarily shown in Figures S1 and S2. Subsequently, the reaction was monitored at several higher temperatures using 5 K intervals. The results are collected in Table S1. An Arrhenius diagram based on the data collected in Table S1 is shown in Figure S3.

According to the Arrhenius equation in its logarithmic form:

$$\ln k = -E_a/RT + \text{const.}$$

the energy barrier E_a can be obtained from the slope of the best-fit straight line:

$$E_a = -mR$$

With $R = 1.987\text{ cal K}^{-1}\text{ mol}^{-1}$ the energy barrier for the formation of **10** from $\mathbf{8}^{\text{Mes}}$ in C_6D_6 is calculated as $22.6\text{ kcal mol}^{-1}$. The standard deviation of this value is $\pm 0.6\text{ kcal mol}^{-1}$.

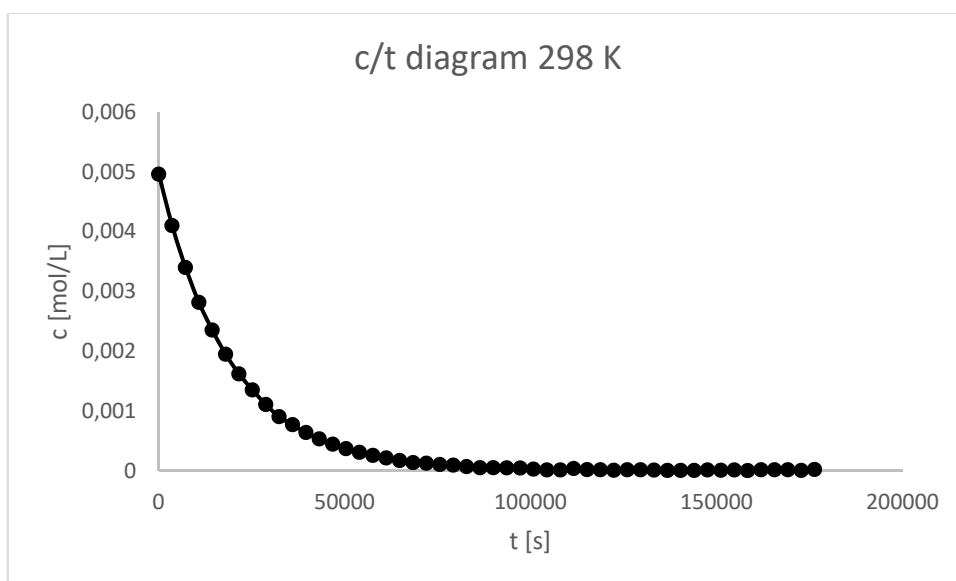


Figure S1. Concentration of 8^{Mes} vs. time at 298 K (initial concentration $c_0 = 5 \text{ mM}$).

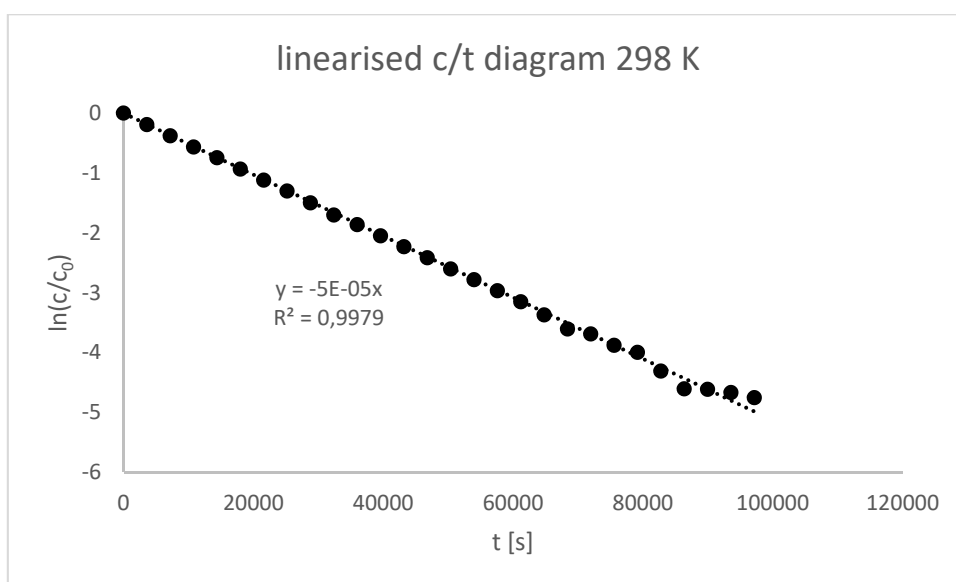


Figure S2. Determination of the rate constant for the example shown in Figure S1 ($k_{298} = 5 \cdot 10^{-5} \text{ s}^{-1}$).

Table S1. Rate constants and half-life times determined for the reaction of 8^{Mes} to 10 in C_6D_6 at different temperatures.

$k_{\text{T}} [\text{s}^{-1}]$	$T [\text{K}]$	$t_{1/2} [\text{h}]$
0.00005	298	3.85
0.00009	303	2.14
0.0002	308	0.96
0.0003	313	0.64
0.0006	318	0.32
0.0009	323	0.21
0.0017	328	0.11

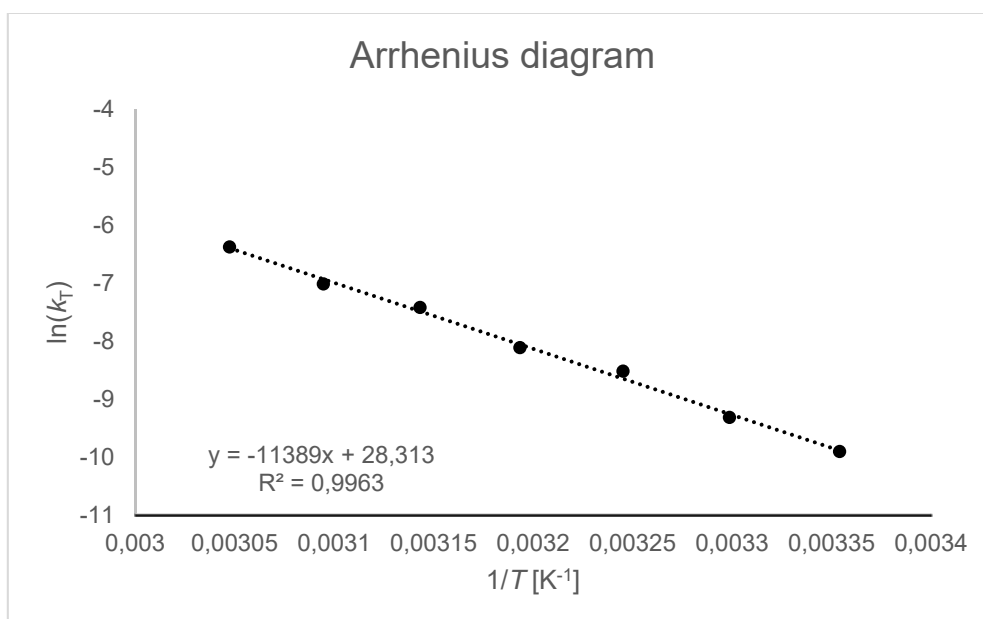


Figure S3. Arrhenius diagram for the formation of **10** from **8**^{Mes} in C₆D₆.

C Electrochemistry and Spectroelectrochemistry

General: All measurements were carried out under an inert atmosphere of argon (Linde Argon 4.8, purity 99.998%) using standard Schlenk techniques. Commercially available chemicals were used without further purification. MeCN for cyclic voltammetry was dried and freshly distilled under argon from CaH₂ and degassed by common techniques prior to use.

Electrochemistry: Cyclic voltammograms were recorded with a PalmSens4 potentiostat with a conventional three-electrode configuration consisting of a freshly polished (0.05 μm polishing alumina) glassy carbon working electrode (∅ = 3 mm, CH Instruments Inc.), a Pt auxiliary electrode, and coiled Ag wire as pseudoreference electrode. The decamethylferrocene/decamethylferrocenium couple was used as internal reference. All measurements were performed at room temperature with a scan rate between 25 and 1000 mV/s. The experiments were carried out in MeCN containing 0.1 M *n*Bu₄NPF₆ (Sigma-Aldrich, ≥ 99.0%, electrochemical grade) as the supporting electrolyte.

Spectroelectrochemistry: IR spectra were recorded with a BRUKER INVENIOS FT-MIR spectrometer; the program used was OPUS Version 8.5. IR-spectroelectrochemical measurements were carried out in an optically transparent thin-layer electrochemical (OTTLE)⁵⁵ cell (CaF₂ windows) with a Pt mesh working electrode, a Pt mesh counter electrode, and an Ag foil pseudoreference electrode. The experiments were carried out in MeCN containing 0.1 M *n*Bu₄NPF₆ (Sigma-Aldrich, ≥ 99.0%, electrochemical grade) as the supporting electrolyte.

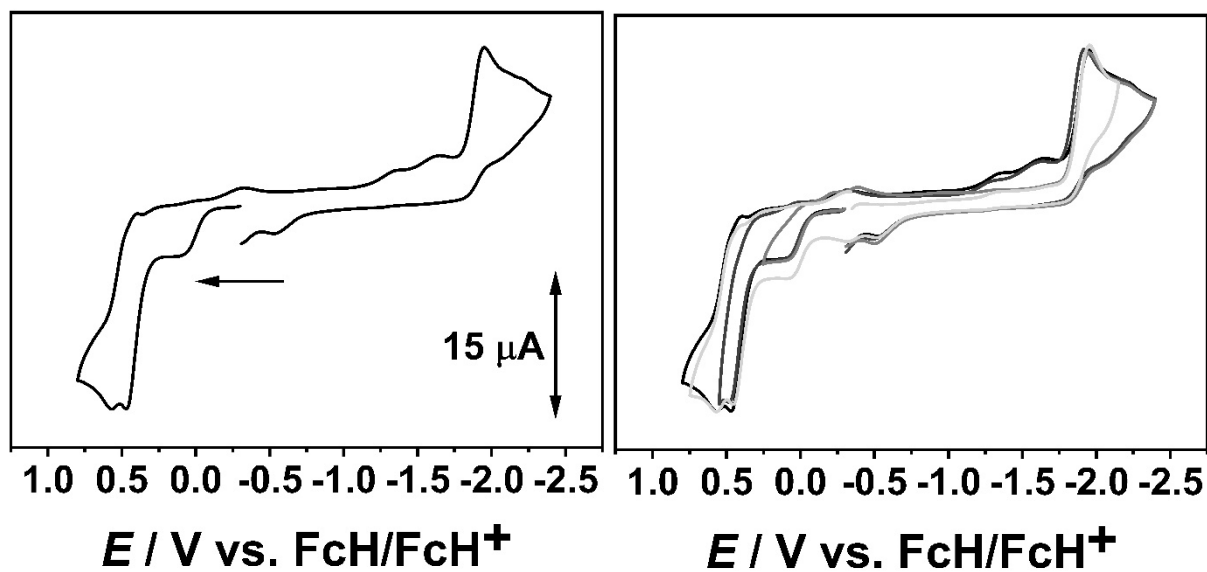


Figure S4. Cyclic voltammograms of $[\text{RhCl}(\text{CO})_2(\mathbf{8}^{\text{Mes}})]$ at 100 mV/s in MeCN/0.1 M $n\text{Bu}_4\text{NPF}_6$ with a glassy carbon working electrode.

Table S2. Redox potentials of $[\text{RhCl}(\text{CO})_2(\mathbf{8}^{\text{Mes}})]$ in MeCN/0.1 M $n\text{Bu}_4\text{NPF}_6$ at 100 mV/s.

$E_{pa,ox}$ [V]	Oxidation	$E_{pc,red}$ [V]	Reduction
+0.13	irreversible	-1.95	irreversible
+0.47	irreversible	-2.20	quasi-reversible
+0.57	quasi-reversible		

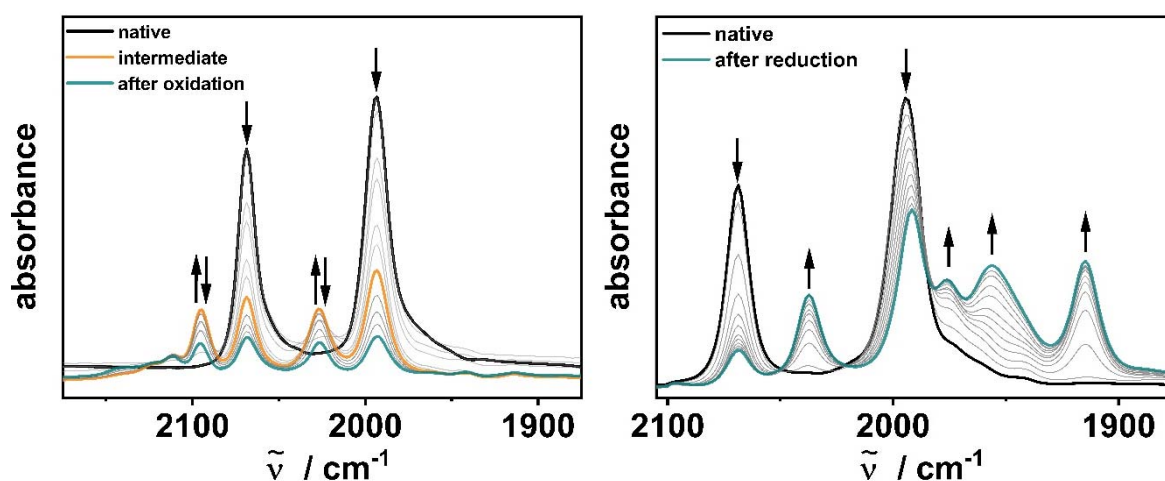


Figure S5. Changes in the IR spectra of $[\text{RhCl}(\text{CO})_2(\mathbf{8}^{\text{Mes}})]$ in MeCN/0.1 M $n\text{Bu}_4\text{NPF}_6$ with a Pt working electrode during the first oxidation (left) and first reduction (right).

Table S3. Changes in the CO frequencies of $[\text{RhCl}(\text{CO})_2(\mathbf{8}^{\text{Mes}})]$ in MeCN/0.1 M Bu_4NPF_6 with a Pt working electrode during the first oxidation and first reduction.

$\tilde{\nu} [\text{cm}^{-1}]$		
$[\text{RhCl}(\text{CO})_2(\mathbf{8}^{\text{Mes}})]$	$[\text{RhCl}(\text{CO})_2(\mathbf{8}^{\text{Mes}})]^+$	$[\text{RhCl}(\text{CO})_2(\mathbf{8}^{\text{Mes}})]^-$
2069	2095	2037
1994	2025	1992
		1976
		1956
		1914

D X-Ray Crystallography

For each data collection a single crystal was mounted on a micro-mount and all geometric and intensity data were taken from this sample at 100(2) K. Data collections were carried out either on a Stoe IPDS2 diffractometer equipped with a 2-circle goniometer and an area detector or a Stoe StadiVari diffractometer equipped with a 4-circle goniometer and a DECTRIS Pilatus 200K detector. The data sets were corrected for absorption, Lorentz and polarisation effects. The structures were solved by direct methods (SHELXT) and refined using alternating cycles of least-squares refinements against F^2 (SHELXL2014/7).⁵⁶ C-bonded H atoms were included in the models in calculated positions, heteroatom-bonded H atoms have been found in the difference Fourier lists. All H atoms were treated with the 1.2-fold or 1.5-fold isotropic displacement parameter of their bonding partner. Experimental details for each diffraction experiment are given in Table S4.

Deposition numbers CCDC 2183320 – 2183338 contain the supplementary crystallographic data for this paper. These data are provided free of charge by the joint Cambridge Crystallographic Data Centre and Fachinformationszentrum Karlsruhe Access Structure service.

Table S4. X-ray crystallographic details.

	2	3	4	5	6	7
Empirical formula	C ₂₃ H ₁₉ BrFeO	C ₂₃ H ₁₈ BBrF ₄ Fe	C ₂₄ H ₁₈ BrFeN	C ₄₂ H ₃₃ FeN ₂ P	C ₂₄ H ₂₀ FeN ₂	C ₂₄ H ₁₉ FeN
Formula weight	447.14	516.94	456.15	652.52	392.27	377.25
Crystal system	monoclinic	monoclinic	monoclinic	triclinic	monoclinic	monoclinic
Space group	<i>P</i> 2 ₁ / <i>c</i>	<i>P</i> 2 ₁ / <i>n</i>	<i>P</i> 2 ₁ / <i>n</i>	<i>P</i> -1	<i>P</i> 2 ₁ / <i>c</i>	<i>C</i> 2/ <i>c</i>
<i>a</i> /Å	8.4213(3)	9.2002(5)	13.1689(6)	10.1852(8)	8.5730(5)	22.178(4)
<i>b</i> /Å	15.4832(9)	19.8156(13)	16.7690(10)	12.9446(11)	16.7375(6)	8.7425(9)
<i>c</i> /Å	14.0343(6)	10.6277(6)	16.6399(7)	13.390(2)	14.4353(8)	17.501(3)
<i>α</i> /°	90	90	90	85.398(10)	90	90
<i>β</i> /°	94.125(3)	92.430(4)	100.403(4)	71.395(9)	94.502(4)	100.855(14)
<i>γ</i> /°	90	90	90	70.741(7)	90	90
Volume/Å ³	1825.17(15)	1935.8(2)	3614.2(3)	1578.9(3)	2064.94(18)	3332.6(9)
<i>Z</i>	4	4	8	2	4	8
ρ_{calc} /cm ³	1.627	1.774	1.677	1.373	1.262	1.504
μ /mm ⁻¹	3.024	2.888	3.054	0.563	0.740	0.912
<i>F</i> (000)	904.0	1032.0	1840.0	680.0	816.0	1568.0
Crystal size/mm ³	0.37 × 0.18 × 0.06	0.23 × 0.12 × 0.04	0.14 × 0.08 × 0.02	0.17 × 0.12 × 0.03	0.33 × 0.26 × 0.17	0.13 × 0.08 × 0.02
Radiation used	Mo K α (λ = 0.71073 Å)	Mo K α (λ = 0.71073 Å)	Mo K α (λ = 0.71073 Å)	Mo K α (λ = 0.71073 Å)	Mo K α (λ = 0.71073 Å)	Mo K α (λ = 0.71073 Å)
2 θ range for data collection/°	3.922 to 49.992	4.11 to 50.992	3.478 to 50.996	3.210 to 52.538	3.732 to 53.568	3.740 to 53.660
	-10 ≤ <i>h</i> ≤ 10	-11 ≤ <i>h</i> ≤ 10	-15 ≤ <i>h</i> ≤ 15	-12 ≤ <i>h</i> ≤ 11	-10 ≤ <i>h</i> ≤ 10	-28 ≤ <i>h</i> ≤ 27
Index ranges	-17 ≤ <i>k</i> ≤ 18	-24 ≤ <i>k</i> ≤ 23	-18 ≤ <i>k</i> ≤ 20	-16 ≤ <i>k</i> ≤ 15	-20 ≤ <i>k</i> ≤ 21	-11 ≤ <i>k</i> ≤ 10
	-16 ≤ <i>l</i> ≤ 14	-12 ≤ <i>l</i> ≤ 12	-17 ≤ <i>l</i> ≤ 20	-16 ≤ <i>l</i> ≤ 16	-14 ≤ <i>l</i> ≤ 18	-16 ≤ <i>l</i> ≤ 22
Refl. collected	6646	12442	16195	11950	12497	8309
Independent refl.	3193 [<i>R</i> _{int} = 0.0518]	3603 [<i>R</i> _{int} = 0.0299]	6718 [<i>R</i> _{int} = 0.0307]	6340 [<i>R</i> _{int} = 0.0319]	4373 [<i>R</i> _{int} = 0.0806]	3523 [<i>R</i> _{int} = 0.0700]
Data/restr./param.	3193/0/236	3603/0/271	6718/0/487	6340/0/415	4373/0/252	3523/0/235
Goodness-of-fit on <i>F</i> ²	1.052	1.068	1.145	1.056	1.054	1.024
Final <i>R</i> indexes	<i>R</i> ₁ = 0.0774	<i>R</i> ₁ = 0.0745	<i>R</i> ₁ = 0.0439	<i>R</i> ₁ = 0.0365	<i>R</i> ₁ = 0.0743	<i>R</i> ₁ = 0.0679
[<i>I</i> > 2 σ (<i>I</i>)]	<i>wR</i> ₂ = 0.2037	<i>wR</i> ₂ = 0.2243	<i>wR</i> ₂ = 0.1027	<i>wR</i> ₂ = 0.0906	<i>wR</i> ₂ = 0.2069	<i>wR</i> ₂ = 0.1568
Final <i>R</i> indexes	<i>R</i> ₁ = 0.0814	<i>R</i> ₁ = 0.0800	<i>R</i> ₁ = 0.0648	<i>R</i> ₁ = 0.0496	<i>R</i> ₁ = 0.0794	<i>R</i> ₁ = 0.1172
[all data]	<i>wR</i> ₂ = 0.2131	<i>wR</i> ₂ = 0.2302	<i>wR</i> ₂ = 0.1160	<i>wR</i> ₂ = 0.0959	<i>wR</i> ₂ = 0.2153	<i>wR</i> ₂ = 0.1878
Largest diff. peak/hole /e Å ⁻³	2.48/-1.34	1.69/-2.49	0.94/-0.39	0.54/-0.39	1.46/-1.17	0.82/-0.43
CCDC No.	2183320	2183321	2183322	2183323	2183324	2183325

Table S4 (continued). X-ray crystallographic details.

	$\mathbf{8}^{\text{Me}}\text{H}[\text{BF}_4]\cdot\text{C}_6\text{H}_6$	$\mathbf{8}^{\text{Et}}\text{H}[\text{BF}_4]\cdot\frac{1}{2}\text{PhMe}$	$\mathbf{8}^{\text{Mes}}\text{H}(\text{OTf})$	$\mathbf{8}^{\text{Mes}}$	$[\text{AuCl}(\mathbf{8}^{\text{Mes}})]$	$[\text{CuCl}(\mathbf{8}^{\text{Mes}})]$
Empirical formula	$\text{C}_{31}\text{H}_{28}\text{BF}_4\text{FeN}$	$\text{C}_{59}\text{H}_{56}\text{B}_2\text{F}_8\text{Fe}_2\text{N}_2$	$\text{C}_{34}\text{H}_{30}\text{F}_3\text{FeNO}_3\text{S}$	$\text{C}_{33}\text{H}_{29}\text{FeN}$	$\text{C}_{33}\text{H}_{29}\text{AuClFeN}$	$\text{C}_{33}\text{H}_{29}\text{ClCuFeN}$
Formula weight	557.20	1078.37	645.50	495.42	727.84	594.41
Crystal system	triclinic	triclinic	orthorhombic	monoclinic	monoclinic	monoclinic
Space group	<i>P</i> -1	<i>P</i> -1	<i>Pbca</i>	<i>P</i> ₂ ₁ / <i>c</i>	<i>P</i> ₂ ₁ / <i>n</i>	<i>C</i> ₂ / <i>c</i>
<i>a</i> /Å	9.2168(7)	8.9255(9)	10.2684(3)	9.6742(15)	14.0999(6)	21.4874(15)
<i>b</i> /Å	12.0164(10)	11.1122(14)	16.9671(7)	16.056(3)	12.5596(4)	11.2129(13)
<i>c</i> /Å	13.5831(10)	14.004(4)	33.7760(11)	15.509(3)	14.9583(5)	23.4835(16)
α /°	64.005(6)	66.471(18)	90	90	90	90
β /°	72.937(6)	77.129(18)	90	90.684(13)	98.956(3)	96.238(6)
γ /°	88.830(7)	76.442(9)	90	90	90	90
Volume/Å ³	1282.37(19)	1224.9(4)	5884.6(4)	2408.8(7)	2616.66(17)	5624.5(9)
<i>Z</i>	2	1	8	4	4	8
$\rho_{\text{calc}}/\text{g cm}^{-3}$	1.443	1.462	1.457	1.366	1.848	1.404
μ/mm^{-1}	0.639	0.666	5.251	5.174	6.281	1.389
<i>F</i> (000)	576.0	558.0	2672.0	1040.0	1424.0	2448.0
Crystal size/mm ³	0.19 × 0.15 × 0.10	0.15 × 0.13 × 0.10	0.11 × 0.07 × 0.02	0.10 × 0.07 × 0.04	0.22 × 0.21 × 0.21	0.20 × 0.16 × 0.13
Radiation used	Mo K α ($\lambda = 0.71073$ Å)	Mo K α ($\lambda = 0.71073$ Å)	Cu K α ($\lambda = 1.54186$ Å)	Cu K α ($\lambda = 1.54186$ Å)	Mo K α ($\lambda = 0.71073$ Å)	Mo K α ($\lambda = 0.71073$ Å)
2 θ range for data collection/°	3.516 to 51.994	4.744 to 65.010	10.082 to 142.102	7.926 to 137.948	4.916 to 64.942	3.814 to 51.562
	−11 ≤ <i>h</i> ≤ 10	−13 ≤ <i>h</i> ≤ 11	−5 ≤ <i>h</i> ≤ 12	−11 ≤ <i>h</i> ≤ 11	−20 ≤ <i>h</i> ≤ 18	−26 ≤ <i>h</i> ≤ 26
Index ranges	−14 ≤ <i>k</i> ≤ 14	−13 ≤ <i>k</i> ≤ 15	−20 ≤ <i>k</i> ≤ 16	−13 ≤ <i>k</i> ≤ 18	−18 ≤ <i>k</i> ≤ 15	−13 ≤ <i>k</i> ≤ 13
	−16 ≤ <i>l</i> ≤ 15	−20 ≤ <i>l</i> ≤ 19	−37 ≤ <i>l</i> ≤ 40	−18 ≤ <i>l</i> ≤ 13	−20 ≤ <i>l</i> ≤ 20	−28 ≤ <i>l</i> ≤ 23
Refl. collected	9526	12097	13119	9691	26745	13397
Independent refl.	5017 [<i>R</i> _{int} = 0.0280]	7225 [<i>R</i> _{int} = 0.0328]	5484 [<i>R</i> _{int} = 0.0261]	4379 [<i>R</i> _{int} = 0.0698]	8262 [<i>R</i> _{int} = 0.0251]	5353 [<i>R</i> _{int} = 0.0317]
Data/restr./param.	5017/0/344	7225/0/336	5484/0/391	4379/0/319	8262/0/337	5353/0/337
Goodness-of-fit on <i>F</i> ²	1.057	1.017	1.030	1.082	1.019	1.059
Final <i>R</i> indexes	<i>R</i> ₁ = 0.0348	<i>R</i> ₁ = 0.0421	<i>R</i> ₁ = 0.0435	<i>R</i> ₁ = 0.0797	<i>R</i> ₁ = 0.0255	<i>R</i> ₁ = 0.0370
[<i>I</i> ≥ 2 σ (<i>I</i>)]	<i>wR</i> ₂ = 0.0892	<i>wR</i> ₂ = 0.0939	<i>wR</i> ₂ = 0.1040	<i>wR</i> ₂ = 0.1790	<i>wR</i> ₂ = 0.0582	<i>wR</i> ₂ = 0.1038
Final <i>R</i> indexes	<i>R</i> ₁ = 0.0434	<i>R</i> ₁ = 0.0666	<i>R</i> ₁ = 0.0637	<i>R</i> ₁ = 0.1251	<i>R</i> ₁ = 0.0363	<i>R</i> ₁ = 0.0421
[all data]	<i>wR</i> ₂ = 0.0940	<i>wR</i> ₂ = 0.1033	<i>wR</i> ₂ = 0.1163	<i>wR</i> ₂ = 0.2101	<i>wR</i> ₂ = 0.0615	<i>wR</i> ₂ = 0.1069
Largest diff. peak/hole /e Å ^{−3}	0.42/−0.28	0.69/−0.39	0.36/−0.41	0.52/−0.50	1.28/−1.75	0.71/−0.52
CCDC No.	2183326	2183327	2183328	2183329	2183330	2183331

Table S4 (continued). X-ray crystallographic details.

	$\mathbf{8}^{\text{Mes}}\text{Se}$	$\mathbf{8}^{\text{Mes}}\text{S}$	$[\text{Rh}(\mathbf{9})(\text{CO})_2]$	$[\text{RhCl}(\text{CO})_2(\mathbf{8}^{\text{Mes}})]$	$[\text{Rh}(\mu\text{-Cl})(\text{CO})(\mathbf{8}^{\text{Mes}})]_2$	$\mathbf{8}^{\text{Mes}}\text{CO}$	$\mathbf{10}$
Empirical formula	$\text{C}_{33}\text{H}_{29}\text{FeNSe}$	$\text{C}_{33}\text{H}_{29}\text{FeNS}$	$\text{C}_{35}\text{H}_{28}\text{FeNO}_2\text{Rh}$	$\text{C}_{42}\text{H}_{37}\text{ClFeNO}_2\text{Rh}$	$\text{C}_{68}\text{H}_{58}\text{Cl}_2\text{Fe}_2\text{N}_2\text{O}_2\text{Rh}_2$	$\text{C}_{34}\text{H}_{29}\text{FeNO}$	$\text{C}_{33}\text{H}_{29}\text{FeN}$
Formula weight	574.38	527.48	653.34	781.93	1323.58	523.43	495.42
Crystal system	orthorhombic	monoclinic	triclinic	monoclinic	triclinic	monoclinic	monoclinic
Space group	$Pna2_1$	$P2_1/n$	$P-1$	$P2_1/c$	$P-1$	$P2_1/c$	$P2_1/c$
$a/\text{\AA}$	14.8451(9)	12.2260(7)	9.7854(6)	14.3896(19)	8.9516(6)	7.6164(3)	24.8763(7)
$b/\text{\AA}$	13.9999(11)	8.7422(4)	16.1188(10)	13.9176(15)	12.6216(9)	24.9493(8)	11.9118(2)
$c/\text{\AA}$	12.1839(9)	23.4931(14)	18.4923(12)	18.1112(17)	12.8792(10)	13.6510(6)	24.1323(7)
$\alpha/^\circ$	90	90	108.724(5)	90	104.324(6)	90	90
$\beta/^\circ$	90	97.775(5)	89.850(5)	109.420(9)	96.718(6)	91.328(3)	92.528(2)
$\gamma/^\circ$	90	90	102.090(5)	90	105.380(5)	90	90
Volume/ \AA^3	2532.2(3)	2487.9(2)	2694.5(3)	3420.7(7)	1333.19(17)	2593.32(17)	7144.0(3)
Z	4	4	4	4	1	4	12
$\rho_{\text{calc}}/\text{g cm}^{-3}$	1.507	1.408	1.611	1.518	1.649	1.341	1.382
μ/mm^{-1}	2.056	0.714	1.185	8.316	1.293	0.609	5.234
$F(000)$	1176.0	1104.0	1328.0	1600.0	672.0	1096.0	3120.0
Crystal size/ mm^3	$0.11 \times 0.09 \times 0.06$	$0.11 \times 0.08 \times 0.04$	$0.30 \times 0.21 \times 0.11$	$0.13 \times 0.07 \times 0.03$	$0.07 \times 0.05 \times 0.02$	$0.30 \times 0.25 \times 0.07$	$0.47 \times 0.21 \times 0.07$
Radiation used	Mo $K\alpha$ ($\lambda = 0.71073 \text{ \AA}$)	Mo $K\alpha$ ($\lambda = 0.71073 \text{ \AA}$)	Mo $K\alpha$ ($\lambda = 0.71073 \text{ \AA}$)	Cu $K\alpha$ ($\lambda = 1.54186$)	Mo $K\alpha$ ($\lambda = 0.71073 \text{ \AA}$)	Mo $K\alpha$ ($\lambda = 0.71073 \text{ \AA}$)	Cu $K\alpha$ ($\lambda = 1.54186 \text{ \AA}$)
2θ range for data collection/ $^\circ$	3.998 to 51.560	3.500 to 51.568	4.568 to 54.000	8.194 to 143.616	3.328 to 51.662	4.424 to 55.994	7.114 to 143.346
Index ranges	$-16 \leq h \leq 17$ $-17 \leq k \leq 15$ $-12 \leq l \leq 14$	$-14 \leq h \leq 14$ $-10 \leq k \leq 9$ $-28 \leq l \leq 28$	$-12 \leq h \leq 12$ $-20 \leq k \leq 16$ $-23 \leq l \leq 23$	$-14 \leq h \leq 17$ $-14 \leq k \leq 16$ $-21 \leq l \leq 8$	$-10 \leq h \leq 10$ $-15 \leq k \leq 15$ $-15 \leq l \leq 15$	$-10 \leq h \leq 9$ $-32 \leq k \leq 17$ $-18 \leq l \leq 16$	$-28 \leq h \leq 30$ $-14 \leq k \leq 6$ $-29 \leq l \leq 27$
Refl. collected	7462	15068	22007	15108	9326	11402	50485
Independent refl.	4414 [$R_{\text{int}} = 0.0362$]	4741 [$R_{\text{int}} = 0.0329$]	11551 [$R_{\text{int}} = 0.0692$]	6373 [$R_{\text{int}} = 0.0656$]	5034 [$R_{\text{int}} = 0.0534$]	6178 [$R_{\text{int}} = 0.0521$]	13668 [$R_{\text{int}} = 0.0249$]
Data/restr./param.	4414/1/328	4741/0/328	11551/0/715	6373/9/437	5034/0/355	6178/0/337	13668/0/952
Goodness-of-fit on F^2	1.045	1.049	1.038	1.055	1.027	0.963	1.035
Final R indexes [$I \geq 2\sigma(I)$]	$R_1 = 0.0481$ $wR_2 = 0.1103$	$R_1 = 0.0373$ $wR_2 = 0.0954$	$R_1 = 0.0740$ $wR_2 = 0.1855$	$R_1 = 0.0722$ $wR_2 = 0.1869$	$R_1 = 0.0517$ $wR_2 = 0.1060$	$R_1 = 0.0538$ $wR_2 = 0.1145$	$R_1 = 0.0352$ $wR_2 = 0.0853$
Final R indexes [all data]	$R_1 = 0.0689$ $wR_2 = 0.1333$	$R_1 = 0.0494$ $wR_2 = 0.1009$	$R_1 = 0.1227$ $wR_2 = 0.2167$	$R_1 = 0.1044$ $wR_2 = 0.2188$	$R_1 = 0.0848$ $wR_2 = 0.1208$	$R_1 = 0.1042$ $wR_2 = 0.1330$	$R_1 = 0.0454$ $wR_2 = 0.0914$
Largest diff. peak/hole / $e \text{ \AA}^{-3}$	0.67/−0.98	0.52/−0.46	1.67/−1.45	1.03/−1.66	0.66/−1.00	0.40/−0.33	0.28/−0.42
Flack parameter	−0.013(17)						
CCDC No.	2183332	2183333	2183334	2183335	2183336	2183337	2183338

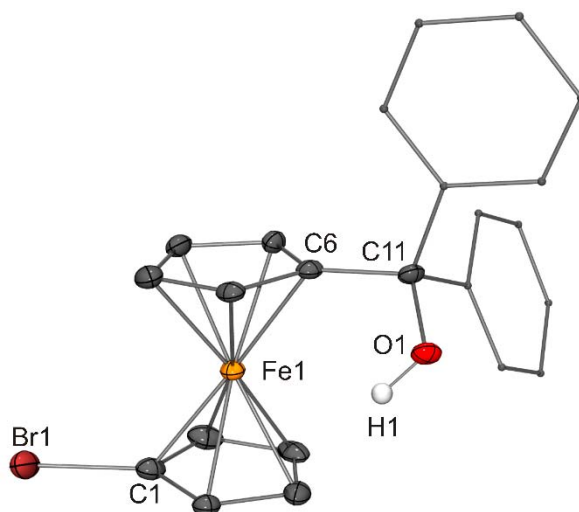


Figure S6. Molecular structure of **2** in the crystal (ORTEP with ellipsoids drawn at the 50 % probability level, C-bonded H atoms omitted for clarity, phenyl groups drawn as capped sticks). Selected bond lengths [Å] and angle [°]: Br1–C1 1.870(6), O1–C11 1.436(6), C6–C11 1.508(7); O1–C11–C6 108.8(4).

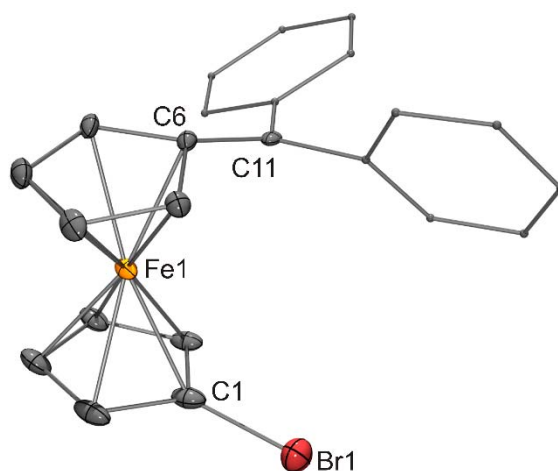


Figure S7. Molecular structure of the cation of **3** in the crystal (ORTEP with ellipsoids drawn at the 50 % probability level, H atoms omitted for clarity, phenyl groups drawn as capped sticks). Selected bond lengths [Å]: Br1–C1 1.799(8), C6–C11 1.401(8).

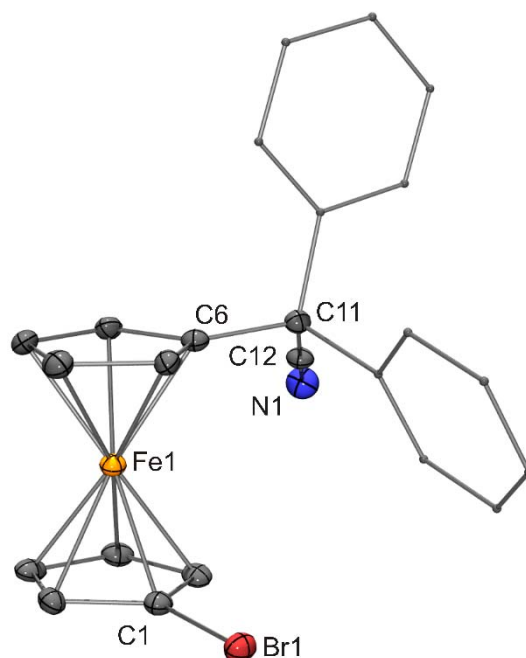


Figure S8. Molecular structure of **4** in the crystal (ORTEP with ellipsoids drawn at the 50 % probability level, H atoms omitted for clarity, phenyl groups drawn as capped sticks; two molecules with very similar bond parameters present in the asymmetric unit, molecule 1 shown arbitrarily). Selected bond lengths [Å] and angles [°]: Br1–C1 1.877(4), N1–C12 1.116(6), C6–C11 1.505(6), C11–C12 1.470(5); C6–C11–C12 108.1(3), N1–C12–C11 179.1(5).

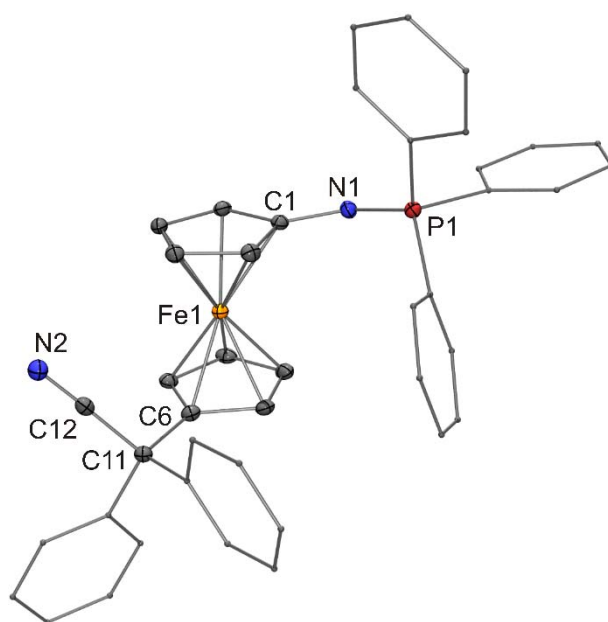


Figure S9. Molecular structure of **5** in the crystal (ORTEP with ellipsoids drawn at the 50 % probability level, H atoms omitted for clarity, phenyl groups drawn as capped sticks). Selected bond lengths [Å] and angles [°]: P1–N1 1.5748(18), N1–C1 1.389(3), N2–C12 1.146(3), C6–C11 1.519(3), C11–C12 1.484(3); P1–N1–C1 123.23(15), N2–C12–C11 178.7(2).

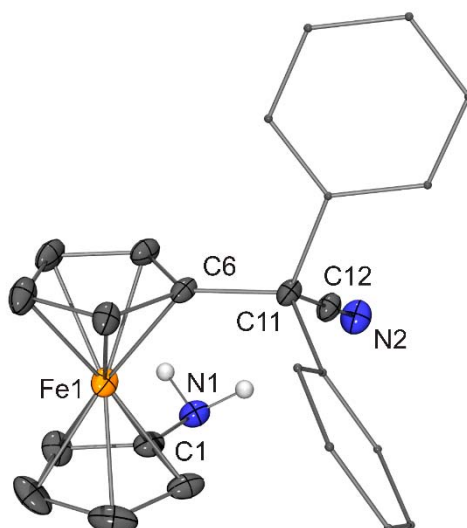


Figure S10. Molecular structure of **6** in the crystal (ORTEP with ellipsoids drawn at the 50 % probability level, C-bonded H atoms omitted for clarity, phenyl groups drawn as capped sticks). Selected bond lengths [Å] and angles [°]: N1–C1 1.386(4), N2–C12 1.144(4), C6–C11 1.524(3), C11–C12 1.481(4); C6–C11–C12 106.3(2), N2–C12–C11 178.7(3).

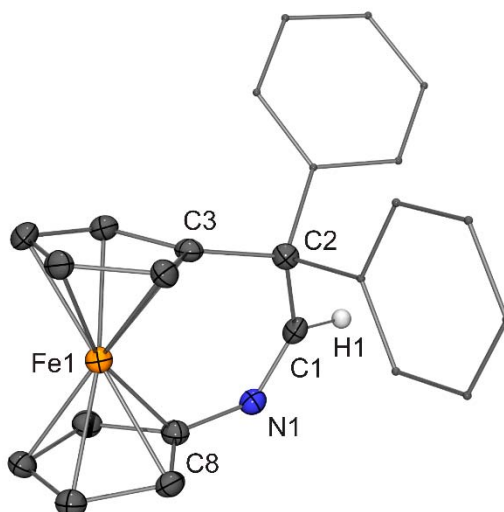


Figure S11. Molecular structure of **7** in the crystal (ORTEP with ellipsoids drawn at the 50 % probability level, H atoms except that at C1 omitted for clarity, phenyl groups drawn as capped sticks). Selected bond lengths [Å] and angles [°]: N1–C1 1.277(6), N1–C8 1.420(7), C1–C2 1.550(7), C2–C3 1.515(7); C1–N1–C8 122.9(4), N1–C1–C2 133.2(5), C1–C2–C3 115.0(4).

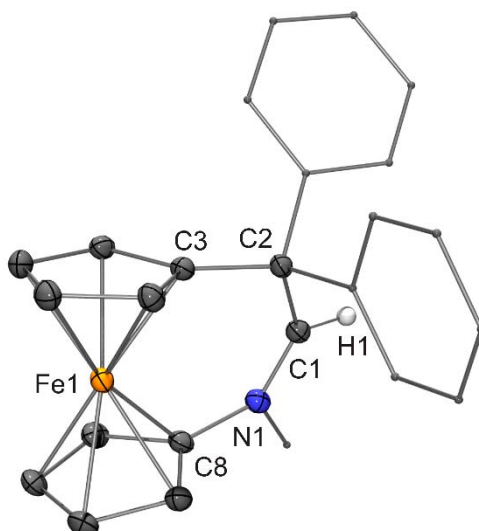


Figure S12. Molecular structure of the cation of $8^{\text{Me}}\text{H}[\text{BF}_4] \cdot \text{C}_6\text{H}_6$ in the crystal (ORTEP with ellipsoids drawn at the 50 % probability level, solvent molecule and H atoms except that at C1 omitted for clarity, methyl and phenyl groups drawn as capped sticks). Selected bond lengths [Å] and angles [°]: N1–C1 1.284(3), N1–C8 1.439(3), C1–C2 1.521(3), C2–C3 1.526(3); C1–N1–C8 126.16(17), N1–C1–C2 131.33(18), C1–C2–C3 114.80(16).

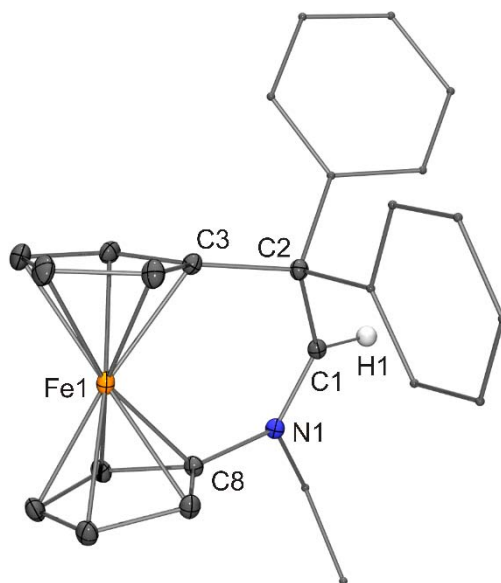


Figure S13. Molecular structure of the cation of $8^{\text{Et}}\text{H}[\text{BF}_4] \cdot \frac{1}{2} \text{PhMe}$ in the crystal (ORTEP with ellipsoids drawn at the 50 % probability level, solvent molecule and H atoms except that at C1 omitted for clarity, ethyl and phenyl groups drawn as capped sticks). Selected bond lengths [Å] and angles [°]: N1–C1 1.292(2), N1–C8 1.438(2), C1–C2 1.528(2), C2–C3 1.528(2); C1–N1–C8 125.69(15), N1–C1–C2 130.66(15), C1–C2–C3 113.96(14).

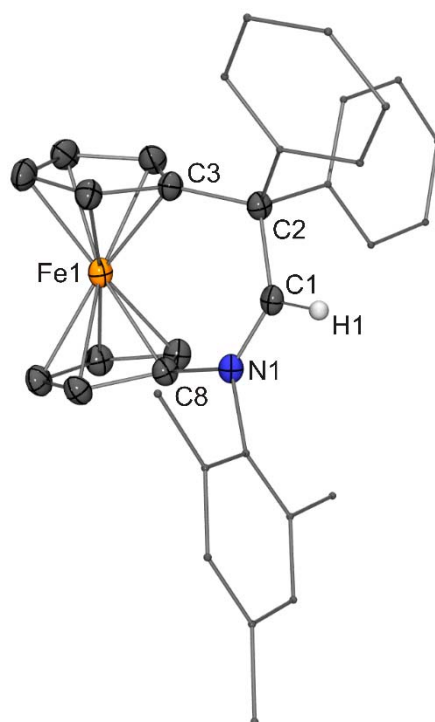


Figure S14. Molecular structure of the cation of $8^{\text{MesH}}(\text{OTf})$ in the crystal (ORTEP with ellipsoids drawn at the 50 % probability level, H atoms except that at C1 omitted for clarity, mesityl and phenyl groups drawn as capped sticks). Selected bond lengths [\AA] and angles [$^\circ$]: N1–C1 1.292(3), N1–C8 1.444(3), C1–C2 1.525(4), C2–C3 1.526(4); C1–N1–C8 126.5(2), N1–C1–C2 130.7(2), C1–C2–C3 114.2(2).

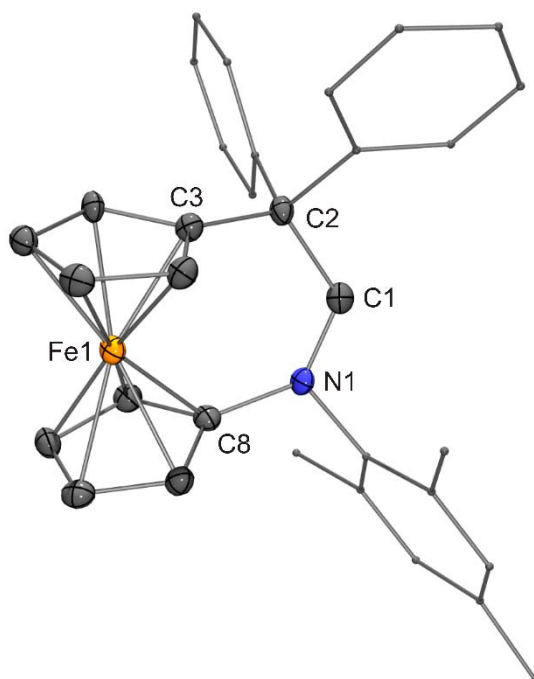


Figure S15. Molecular structure of 8^{Mes} in the crystal (ORTEP with ellipsoids drawn at the 50 % probability level, H atoms omitted for clarity, mesityl and phenyl groups drawn as capped sticks). Selected bond lengths [\AA] and angles [$^\circ$]: N1–C1 1.306(8), N1–C8 1.467(8), C1–C2 1.571(8), C2–C3 1.541(8); C1–N1–C8 132.7(5), N1–C1–C2 121.5(5), C1–C2–C3 118.9(5).

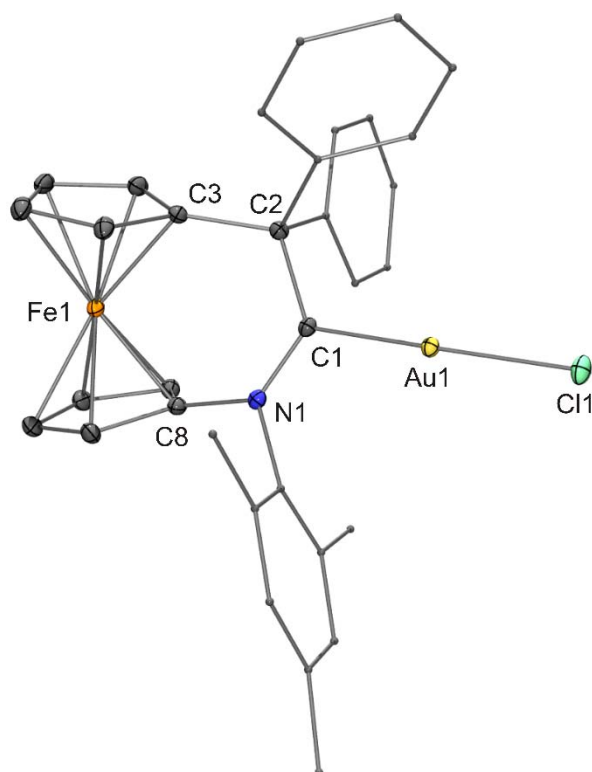


Figure S16. Molecular structure of $[\text{AuCl}(\mathbf{8}^{\text{Mes}})]$ in the crystal (ORTEP with ellipsoids drawn at the 50 % probability level, H atoms omitted for clarity, mesityl and phenyl groups drawn as capped sticks). Selected bond lengths [\AA] and angles [$^\circ$]: Au1–C1 1.994(2), Au1–Cl1 2.2903(6), C1–N1 1.325(3), C1–C2 1.560(3), C2–C3 1.534(3), C8–N1 1.450(3); C1–Au1–Cl1 176.67(7), C1–N1–C8 129.5(2), N1–C1–C2 122.4(2), C1–C2–C3 116.3(2).

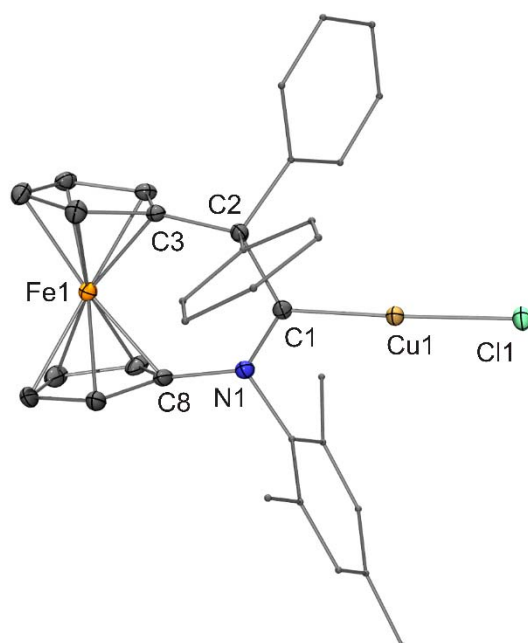


Figure S17. Molecular structure of $[\text{CuCl}(\mathbf{8}^{\text{Mes}})]$ in the crystal (ORTEP with ellipsoids drawn at the 50 % probability level, H atoms omitted for clarity, mesityl and phenyl groups drawn as capped sticks). Selected bond lengths [\AA] and angles [$^\circ$]: Cu1–Cl1 2.0990(6), Cu1–C1 1.889(2), N1–C1 1.313(3), N1–C8 1.447(3), C1–C2 1.547(3), C2–C3 1.533(3); Cl1–Cu1–C1 177.81(7), C1–N1–C8 130.18(18), Cu1–C1–N1 119.83(16), Cu1–C1–C2 116.17(14), N1–C1–C2 123.79(19), C1–C2–C3 119.09(17).

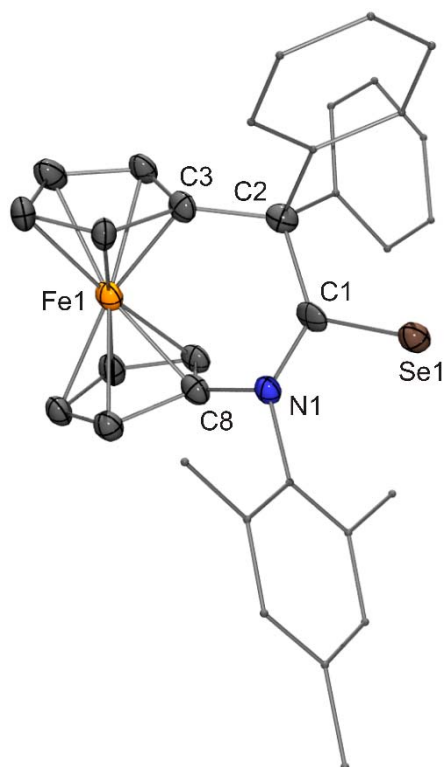


Figure S18. Molecular structure of 8^{MesSe} in the crystal (ORTEP with ellipsoids drawn at the 50 % probability level, H atoms omitted for clarity, mesityl and phenyl groups drawn as capped sticks). Selected bond lengths [\AA] and angles [$^\circ$]: Se1–C1 1.798(10), N1–C1 1.370(11), N1–C8 1.449(12), C1–C2 1.566(13), C2–C3 1.511(14); C1–N1–C8 128.0(8), Se1–C1–N1 117.8(7), Se1–C1–C2 120.7(6), N1–C1–C2 121.2(8), C1–C2–C3 115.1(8).

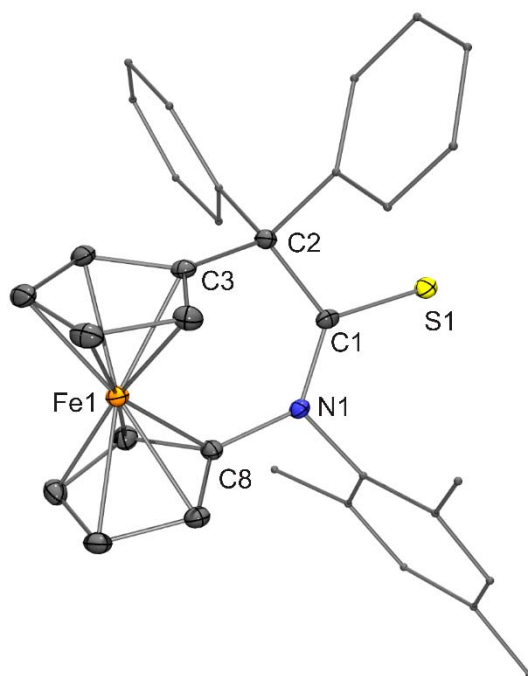


Figure S19. Molecular structure of 8^{MesS} in the crystal (ORTEP with ellipsoids drawn at the 50 % probability level, H atoms omitted for clarity, mesityl and phenyl groups drawn as capped sticks). Selected bond lengths [\AA] and angles [$^\circ$]: S1–C1 1.657(2), N1–C1 1.361(3), N1–C8 1.433(3), C1–C2 1.576(3), C2–C3 1.546(3); C1–N1–C8 128.61(18), S1–C1–N1 119.52(16), S1–C1–C2 117.21(16), N1–C1–C2 123.17(19), C1–C2–C3 117.35(18).

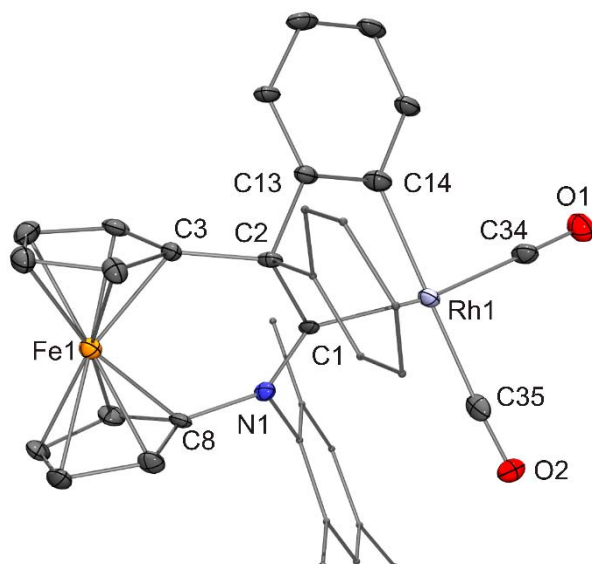


Figure S20. Molecular structure of $[\text{Rh}(\mathbf{9})(\text{CO})_2]$ in the crystal (ORTEP with ellipsoids drawn at the 50 % probability level, H atoms omitted for clarity, mesityl and phenyl groups drawn as capped sticks; two molecules with very similar bond parameters present in the asymmetric unit, molecule 1 shown arbitrarily). Selected bond lengths [\AA] and angles [$^\circ$]: Rh1–C1 2.056(7), Rh1–C14 2.045(8), Rh1–C34 1.885(8), Rh1–C35 1.915(9), O1–C34 1.154(10), O2–C35 1.135(10), N1–C1 1.306(9), N1–C8 1.436(9), C1–C2 1.568(10), C2–C3 1.511(10), C2–C13 1.547(9), C13–C14 1.407(10); C1–Rh1–C14 78.6(3), C34–Rh1–C35 93.2(3), C1–N1–C8 130.7(6), N1–C1–Rh1 125.3(5), C2–C1–Rh1 113.0(5), N1–C1–C2 121.6(6), C1–C2–C3 120.0(6), C1–C2–C13 102.1(5), C2–C13–C14 117.9(6), Rh1–C14–C13 114.8(5), Rh1–C34–O1 178.1(8), Rh1–C35–O2 171.1(8).

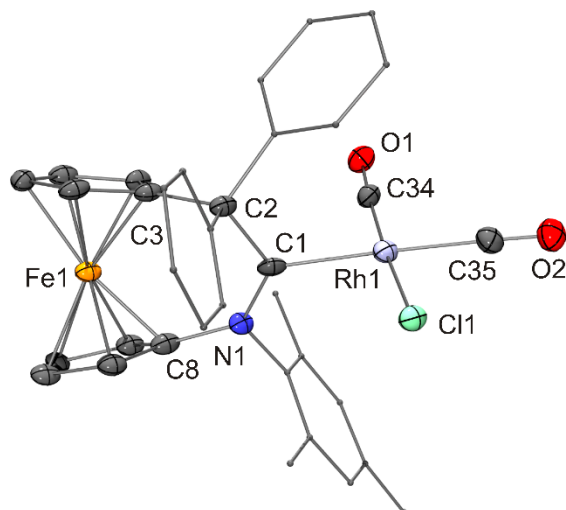


Figure S21. Molecular structure of $[\text{RhCl}(\text{CO})_2(\mathbf{8}^{\text{Mes}})] \cdot \text{PhMe}$ in the crystal (ORTEP with ellipsoids drawn at the 50 % probability level, solvent molecule and H atoms omitted for clarity, mesityl and phenyl groups drawn as capped sticks). Selected bond lengths [\AA] and angles [$^\circ$]: Rh1–Cl1 2.3705(19), Rh1–C1 2.084(8), Rh1–C34 1.821(8), Rh1–C35 1.915(10), O1–C34 1.144(9), O2–C35 1.130(11), N1–C1 1.316(9), N1–C8 1.454(11), C1–C2 1.585(10), C2–C3 1.537(10); C1–Rh1–C34 89.3(3), C1–Rh1–C35 178.3(3), C1–N1–C8 130.1(7), Rh1–C1–N1 120.7(6), Rh1–C1–C2 118.2(5), N1–C1–C2 121.1(7), C1–C2–C3 114.3(6), Rh1–C34–O1 175.1(7), Rh1–C35–O2 178.4(9).

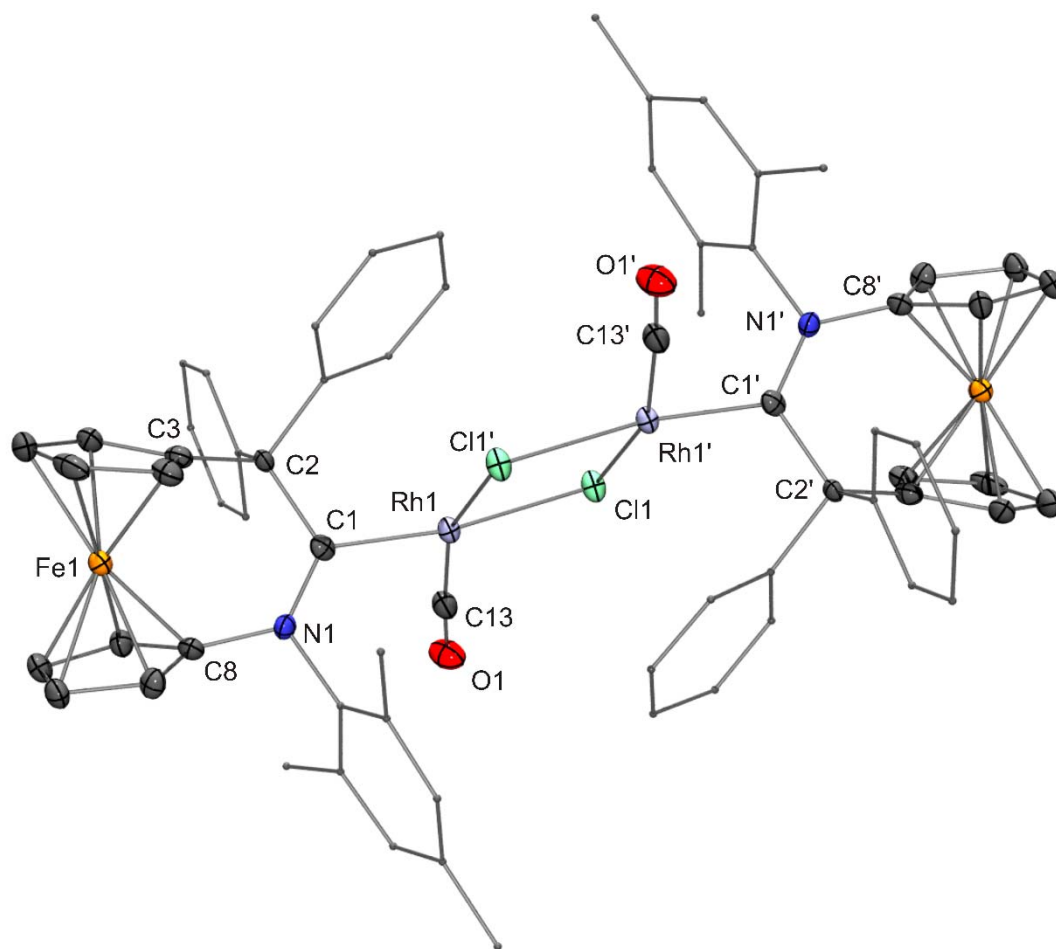


Figure S22. Molecular structure of $[\text{Rh}(\mu\text{-Cl})(\mathbf{8}^{\text{Mes}})(\text{CO})]_2$ in the crystal (ORTEP with ellipsoids drawn at the 50 % probability level, H atoms omitted for clarity, mesityl and phenyl groups drawn as capped sticks). Selected bond lengths [Å] and angles [°]: Rh1–Cl1 2.4377(15), Rh1–Cl1' 2.4535(14), Rh1–C1 1.953(6), Rh1–C13 1.778(7), O1–C13 1.167(7), N1–C1 1.333(7), N1–C8 1.442(7), C1–C2 1.587(8), C2–C3 1.517(8); C1–Rh1–C13 91.4(3), C1–N1–C8 129.0(5), Rh1–C1–N1 124.2(4), Rh1–C1–C2 114.4(4), N1–C1–C2 121.2(5), C1–C2–C3 115.0(4), Rh1–C13–O1 175.7(6).

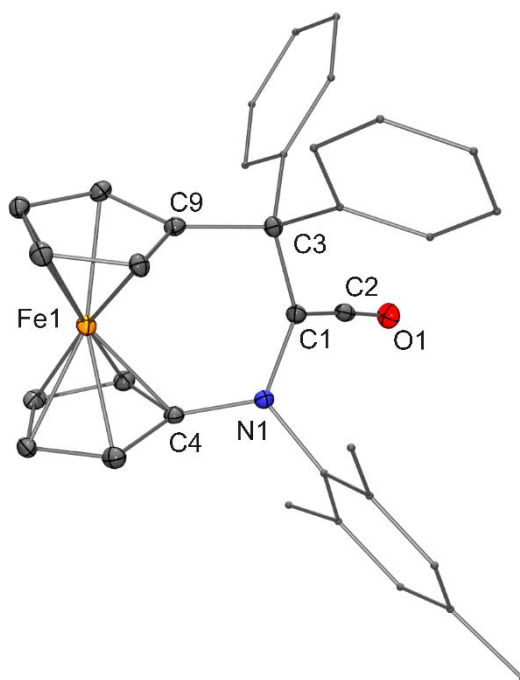


Figure S23. Molecular structure of 8^{MesCO} in the crystal (ORTEP with ellipsoids drawn at the 50 % probability level, H atoms omitted for clarity, mesityl and phenyl groups drawn as capped sticks). Selected bond lengths [\AA] and angles [$^\circ$]: O1–C2 1.171(3), N1–C1 1.437(4), N1–C4 1.410(4), C1–C2 1.320(4), C1–C3 1.553(4), C3–C9 1.547(4); C1–N1–C4 116.3(2), N1–C1–C2 115.9(3), N1–C1–C3 123.9(2), O1–C2–C1 175.6(3), C1–C3–C9 111.2(2).

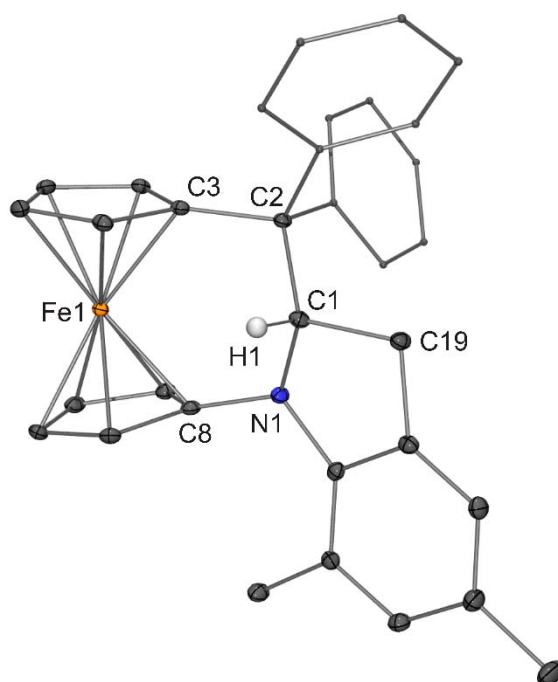
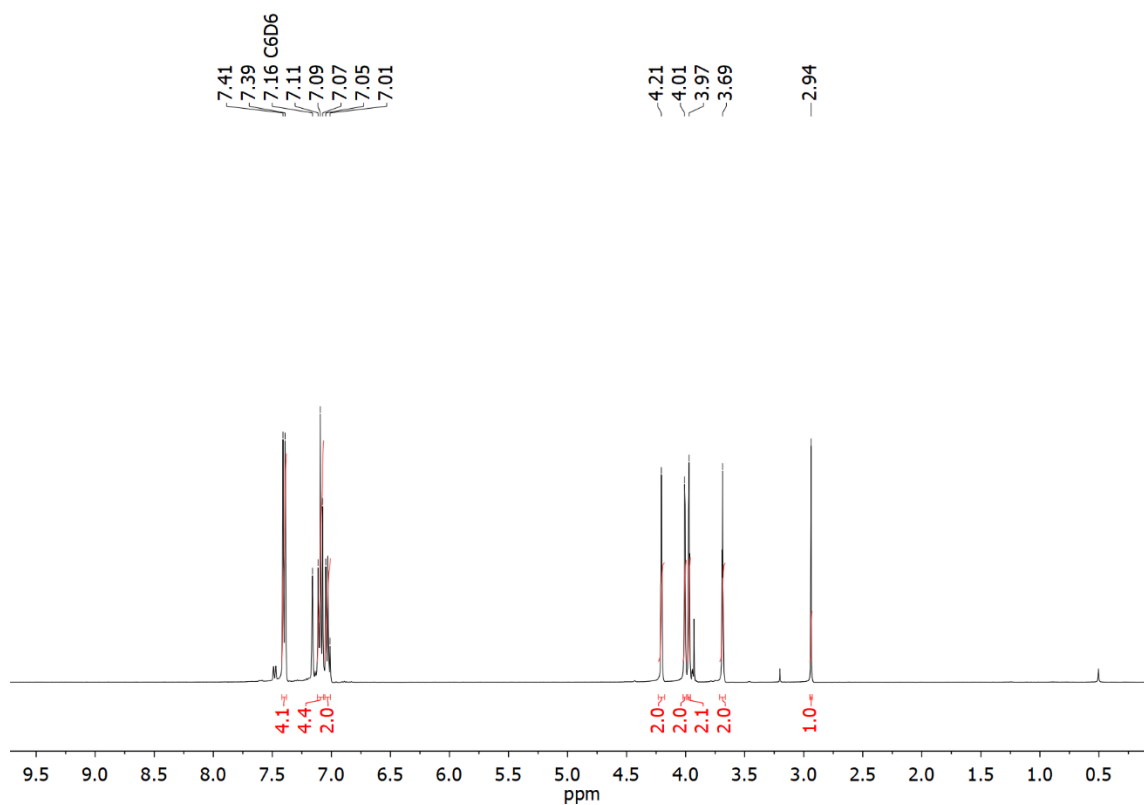
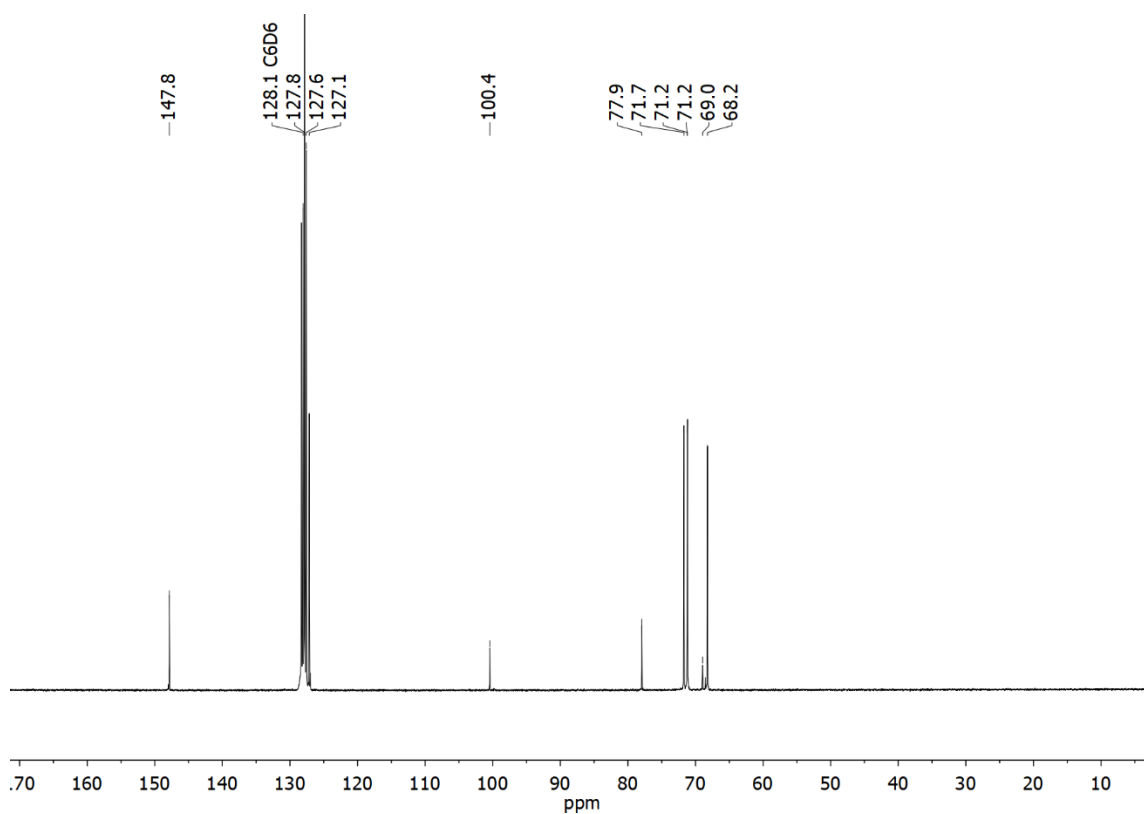


Figure S24. Molecular structure of **10** in the crystal (ORTEP with ellipsoids drawn at the 50 % probability level, H atoms except that at C1 omitted for clarity, phenyl groups drawn as capped sticks; three molecules with very similar bond parameters present in the asymmetric unit, molecule 1 shown arbitrarily). Selected bond lengths [\AA] and angles [$^\circ$]: N1–C1 1.497(2), N1–C8 1.418(2), C1–C2 1.570(2), C1–C19 1.543(2), C2–C3 1.531(2); C1–N1–C8 119.11(14), N1–C1–C2 115.46(14), N1–C1–C19 103.14(14), C2–C1–C19 116.25(14), C1–C2–C3 108.91(14).

E Plots of NMR Spectra

Figure S25. ^1H NMR spectrum (400 MHz, C_6D_6) of **2**.Figure S26. $^{13}\text{C}\{^1\text{H}\}$ NMR spectrum (101 MHz, C_6D_6) of **2**.

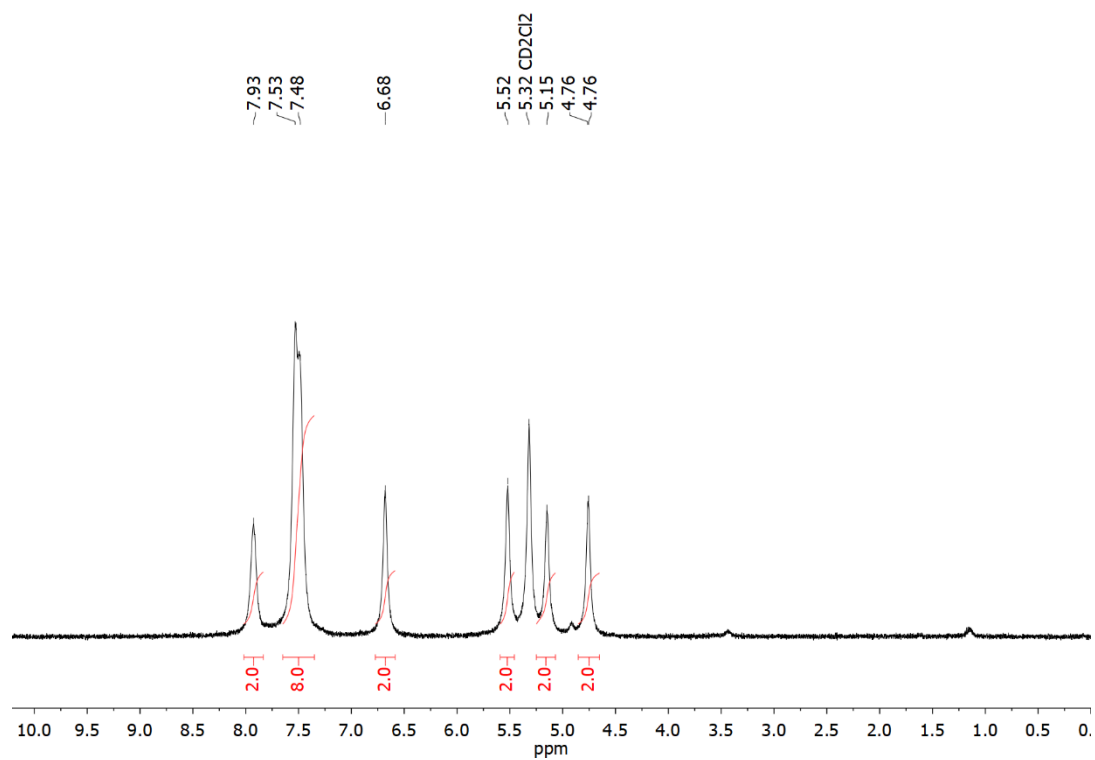


Figure S27. ^1H NMR spectrum (400 MHz, CD_2Cl_2) of **3**.

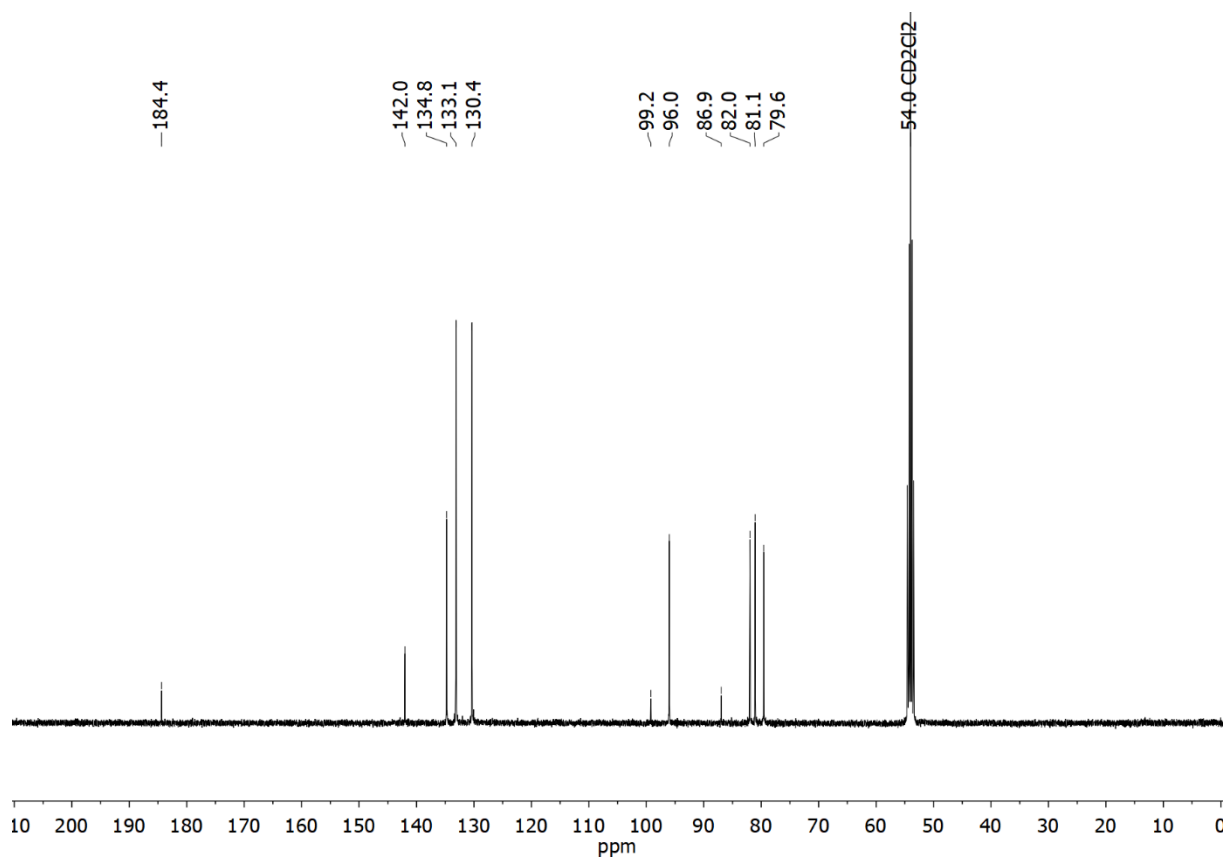


Figure S28. $^{13}\text{C}\{^1\text{H}\}$ NMR spectrum (101 MHz, CD_2Cl_2) of **3**.

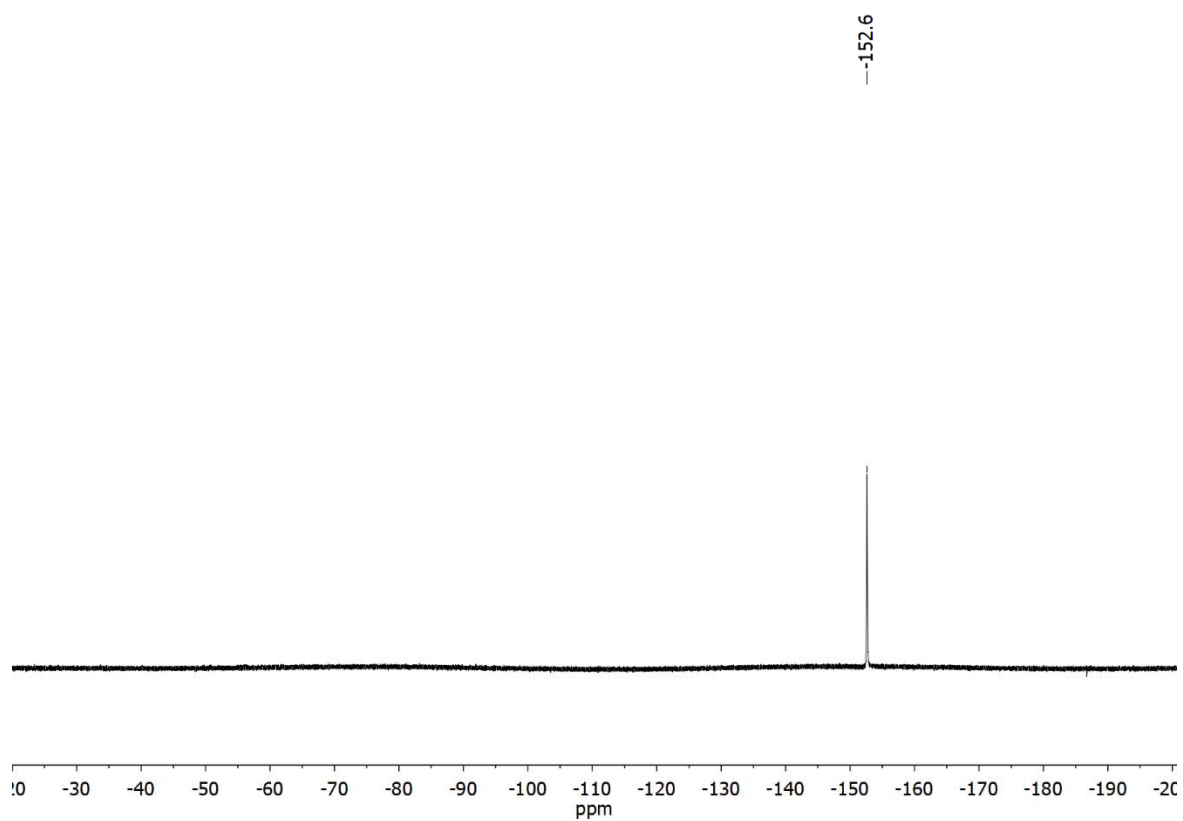


Figure S29. ^{19}F NMR spectrum (376 MHz, CD_2Cl_2) of **3**.

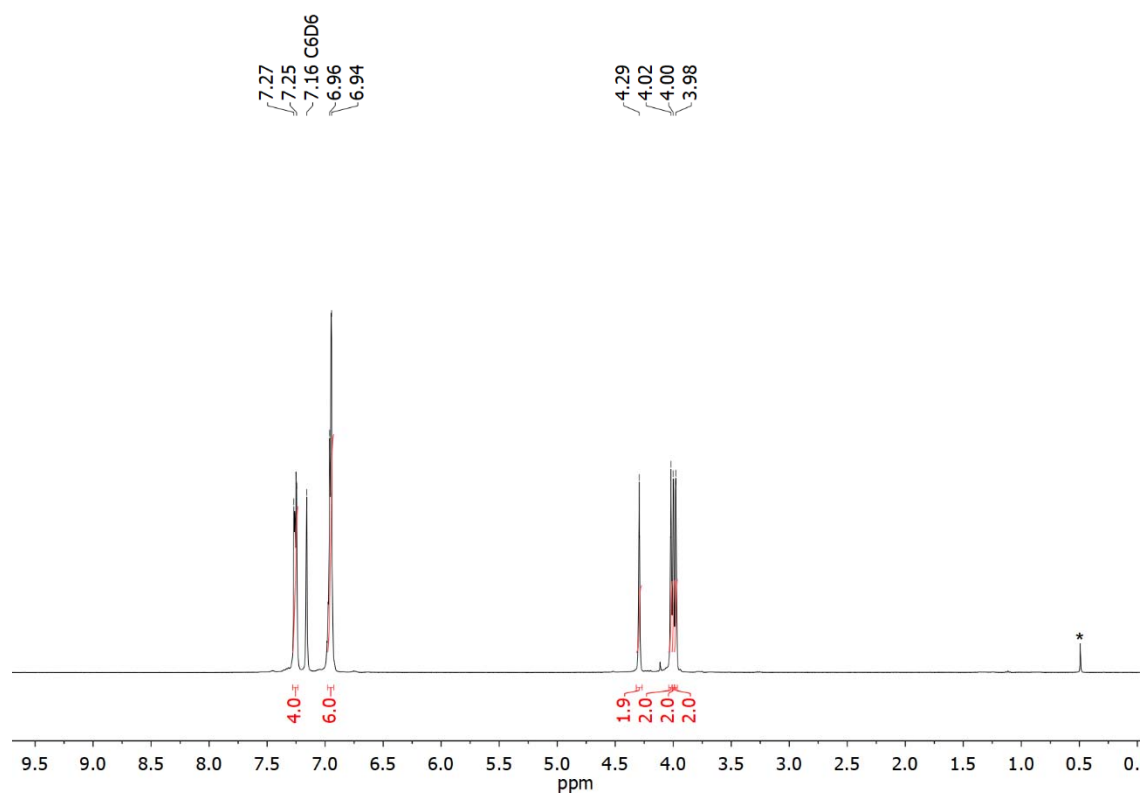


Figure S30. ^1H NMR spectrum (400 MHz, C_6D_6) of **4**. The signal marked (*) is due to trace amounts of water.

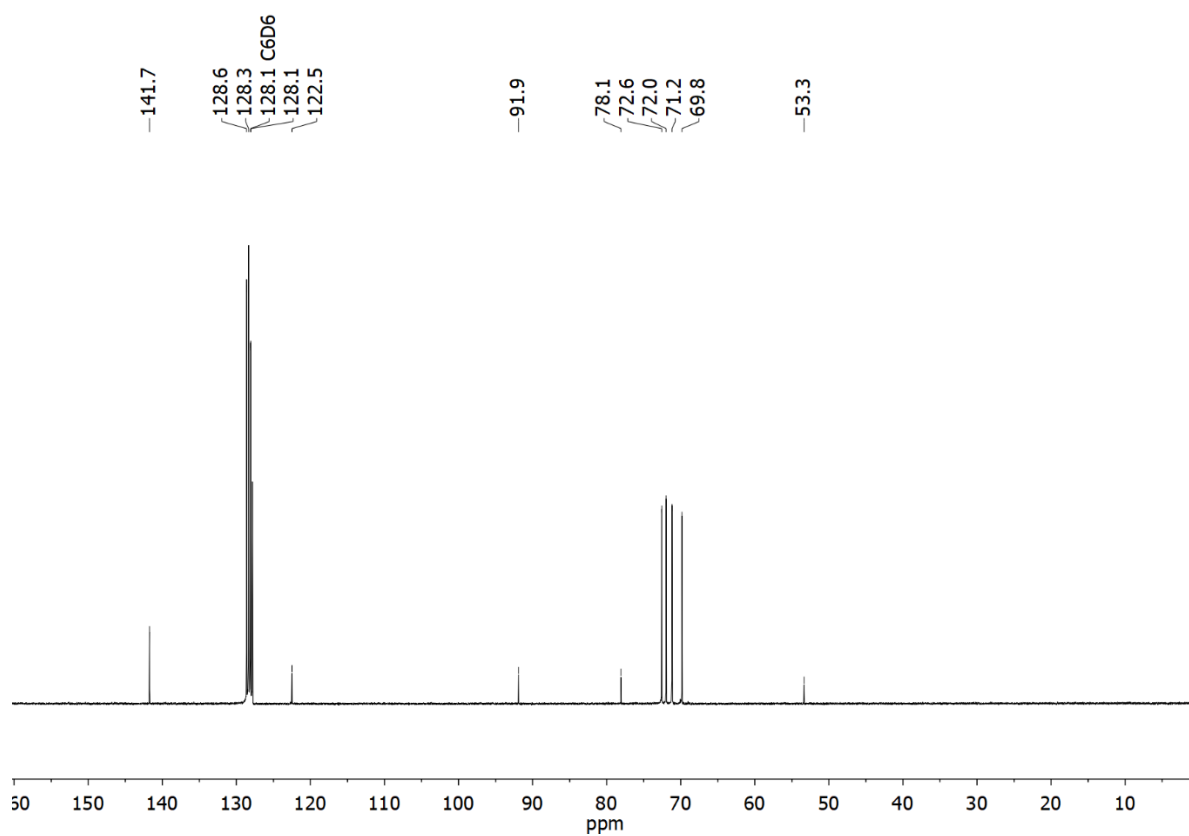


Figure S31. $^{13}\text{C}\{^1\text{H}\}$ NMR (101 MHz, C_6D_6) of **4**.

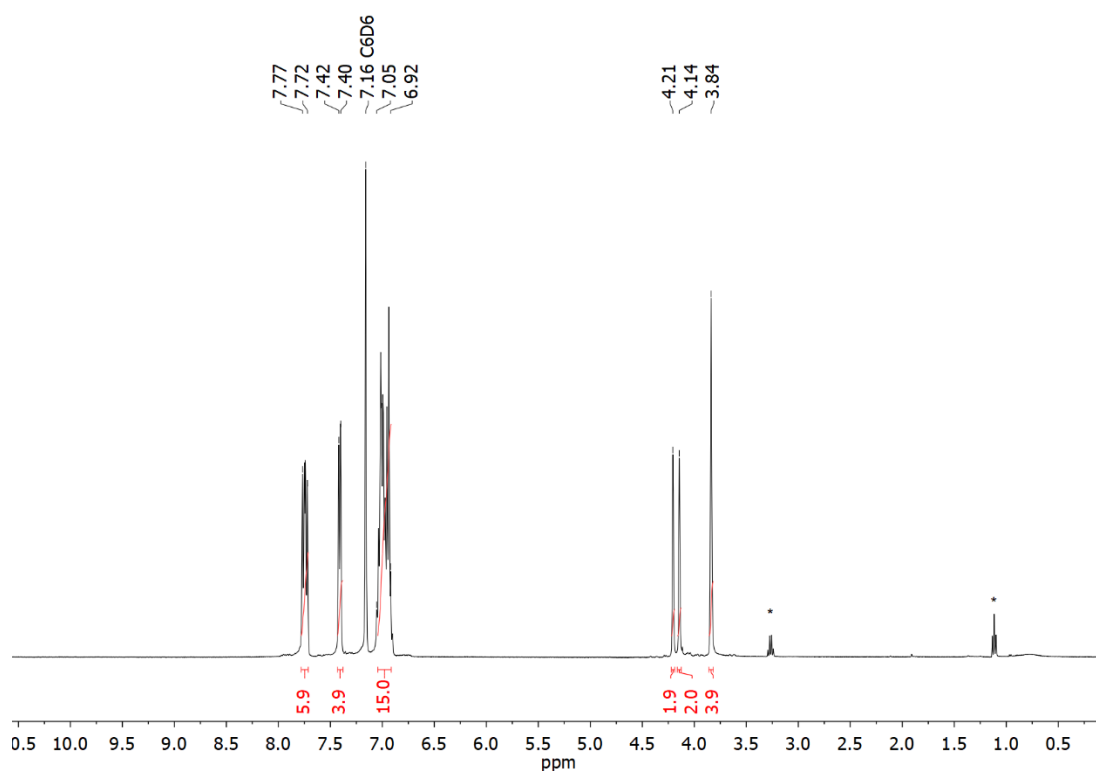


Figure S32. ^1H NMR spectrum (400 MHz, C_6D_6) of **5**. Signals marked (*) belong to residual diethyl ether.

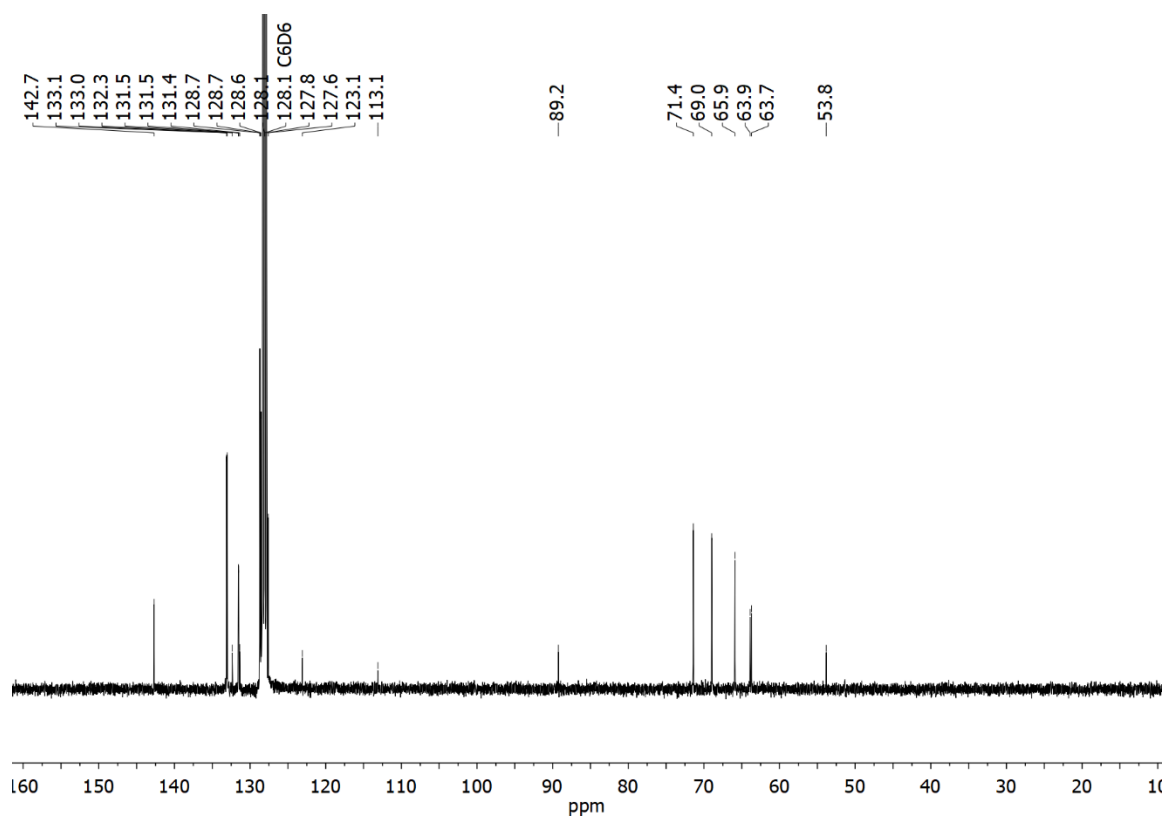


Figure S33. $^{13}\text{C}\{^1\text{H}\}$ NMR (101 MHz, C_6D_6) of 5.

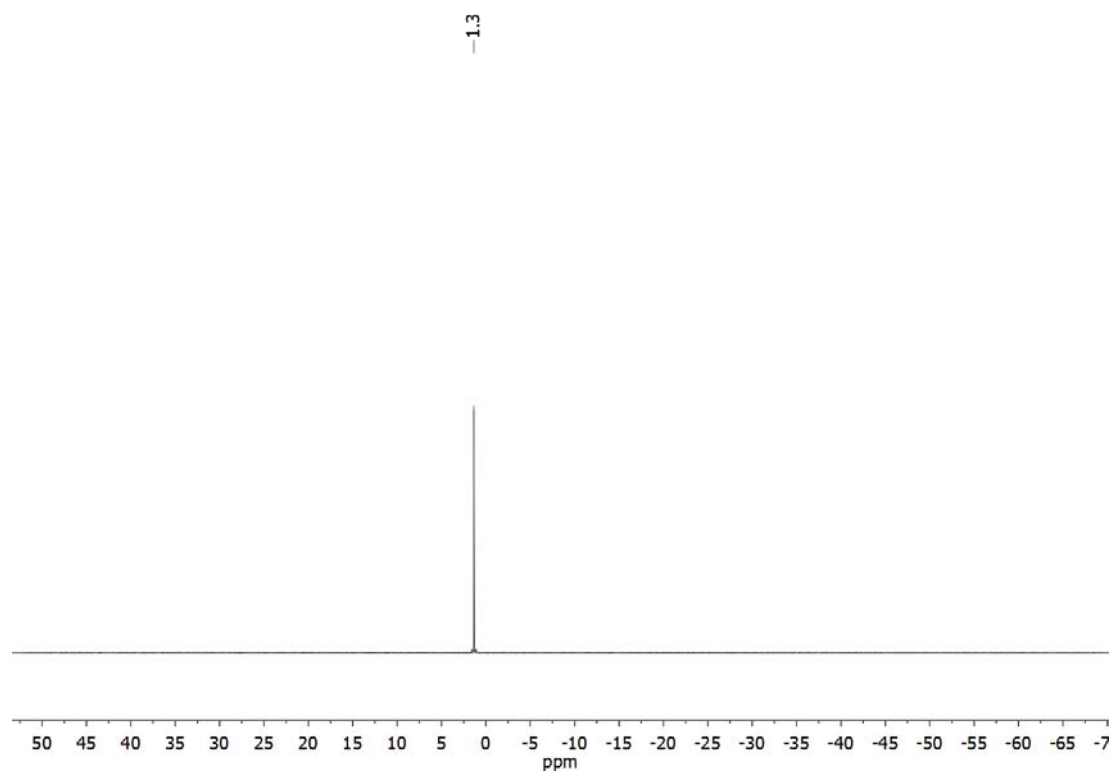


Figure S34. $^{31}\text{P}\{^1\text{H}\}$ NMR (202 MHz, C_6D_6) of 5.

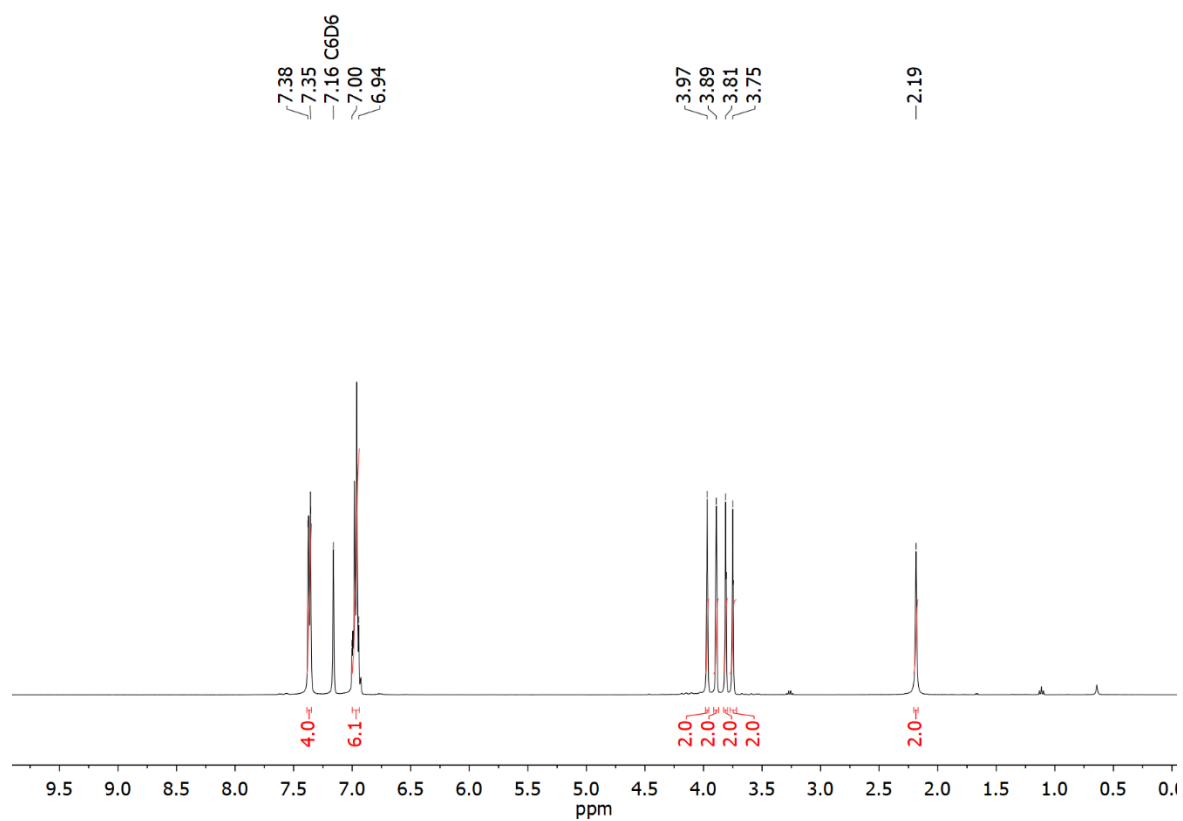


Figure S35. ¹H NMR spectrum (400 MHz, C₆D₆) of **6**.

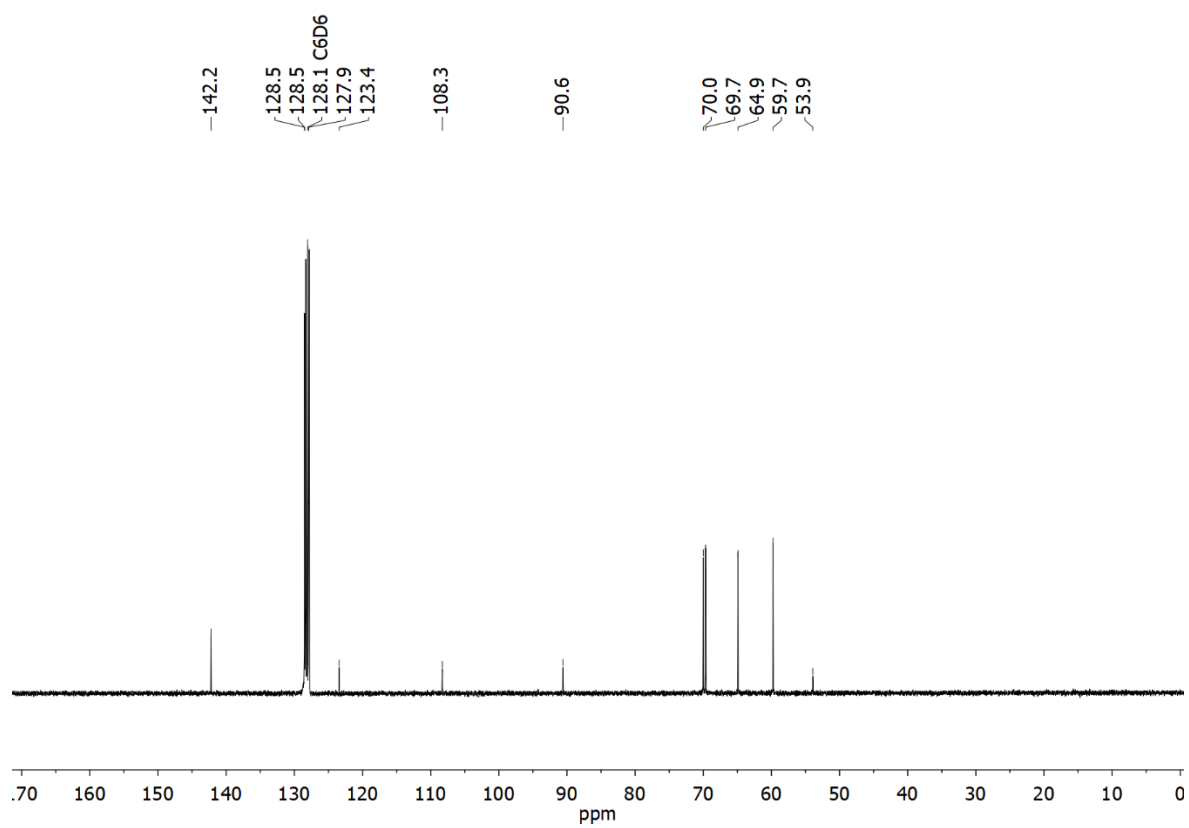


Figure S36. ¹³C{¹H} NMR (101 MHz, C₆D₆) of **6**.

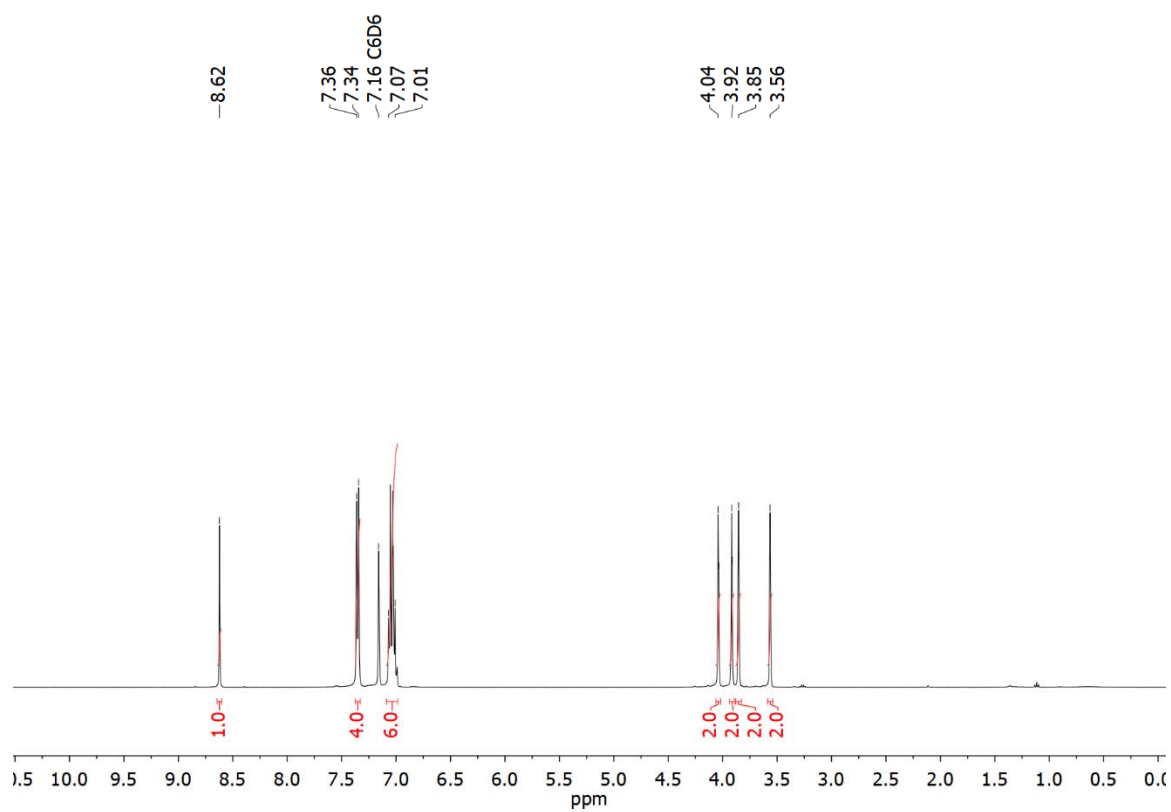


Figure S37. ^1H NMR spectrum (400 MHz, C_6D_6) of 7.

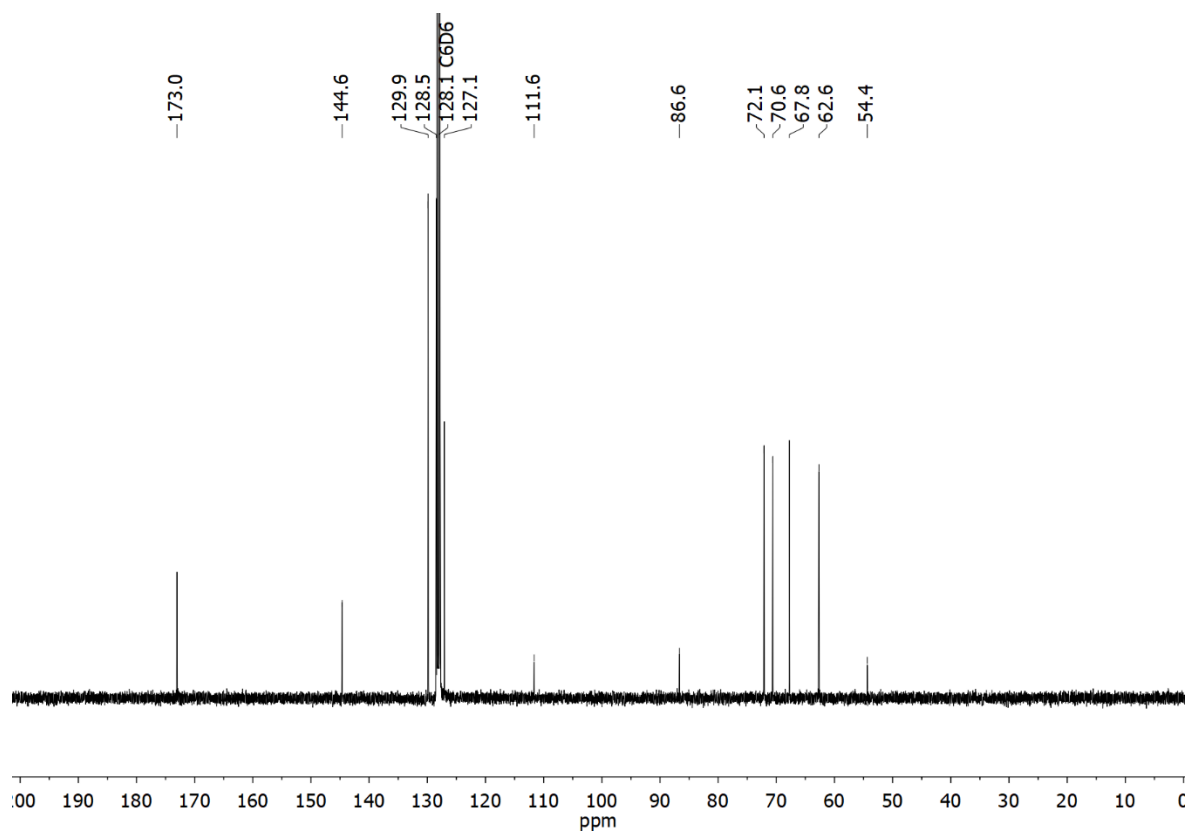


Figure S38. $^{13}\text{C}\{^1\text{H}\}$ NMR (101 MHz, C_6D_6) of 7.

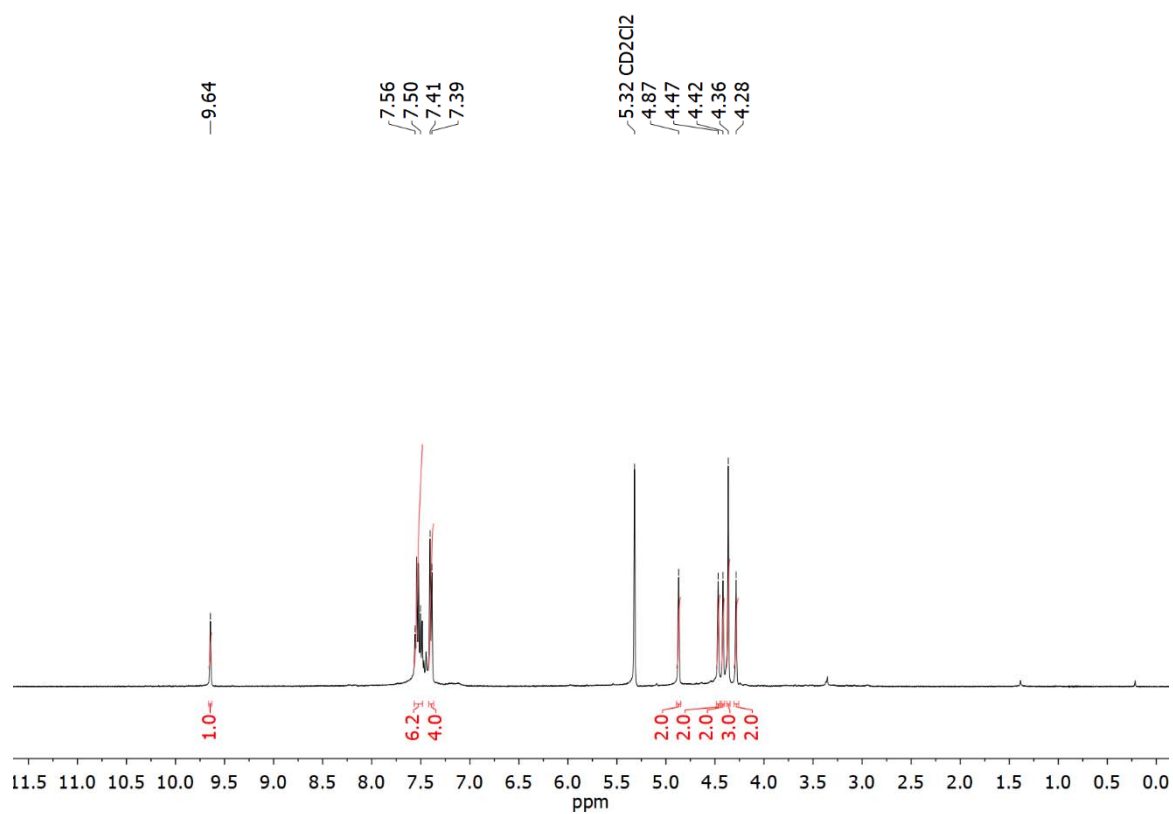


Figure S39. ^1H NMR spectrum (400 MHz, CD_2Cl_2) of $8^{\text{MeH}}[\text{BF}_4]$.

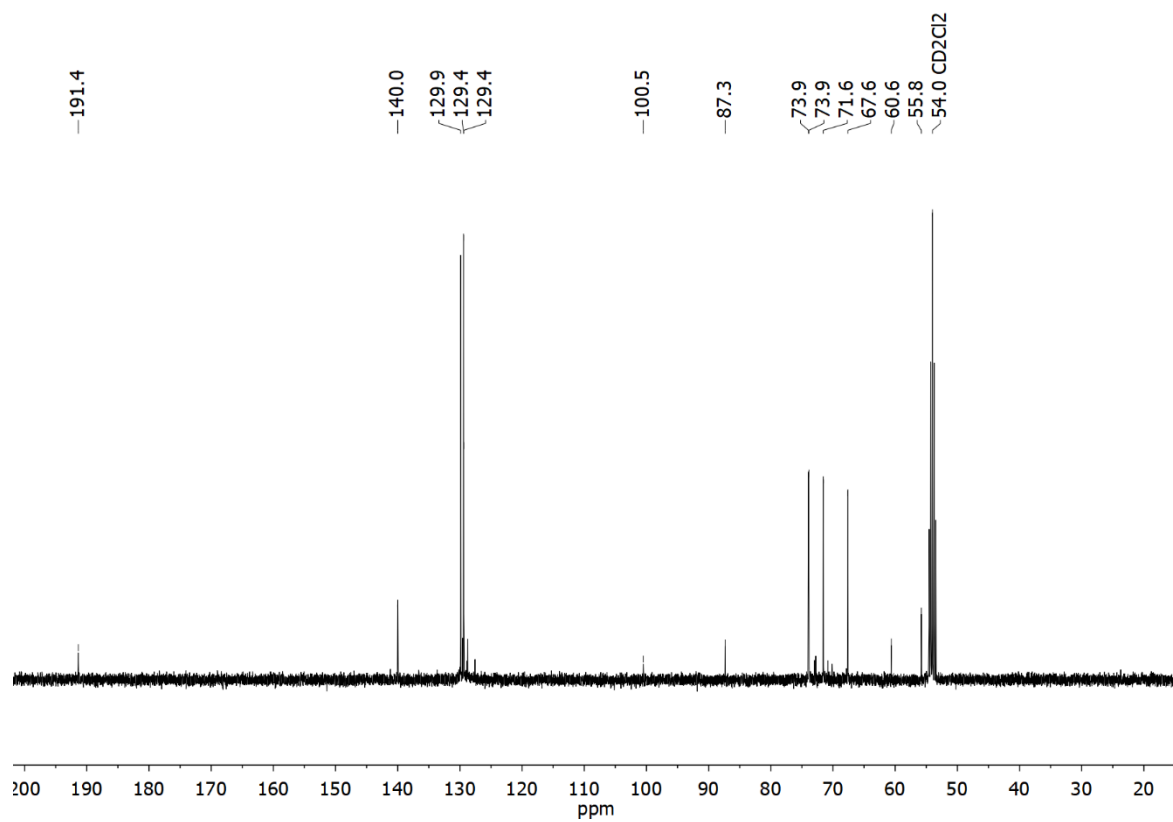


Figure S40. $^{13}\text{C}\{^1\text{H}\}$ NMR (101 MHz, CD_2Cl_2) of $8^{\text{MeH}}[\text{BF}_4]$.

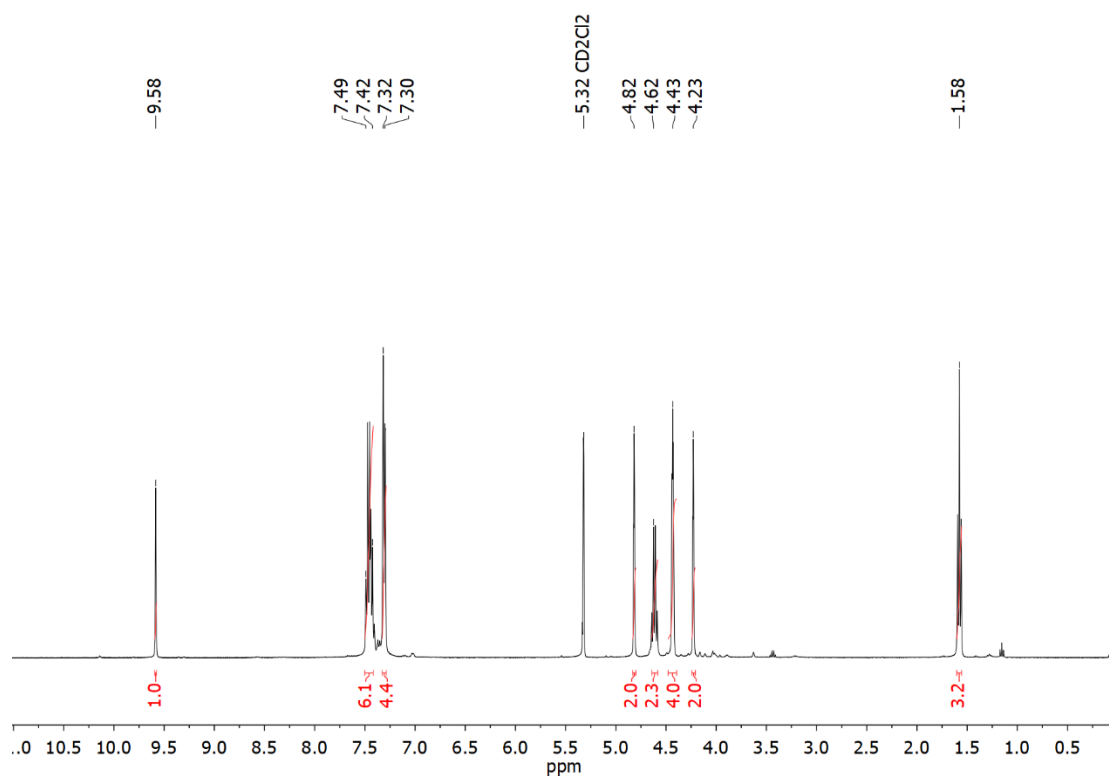


Figure S41. ^1H NMR spectrum (400 MHz, CD_2Cl_2) of $8^{\text{Et}}\text{H}[\text{BF}_4]$.

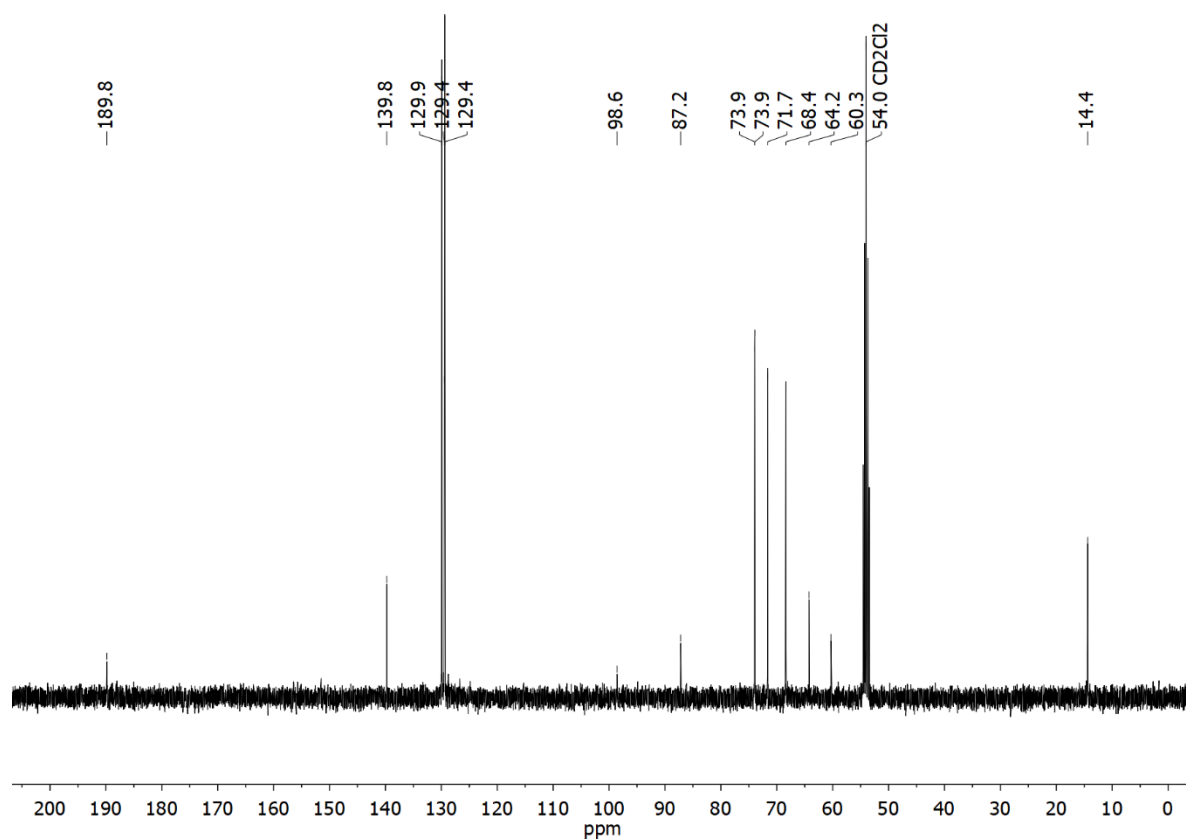


Figure S42. $^{13}\text{C}\{^1\text{H}\}$ NMR (101 MHz, CD_2Cl_2) of $8^{\text{Et}}\text{H}[\text{BF}_4]$.

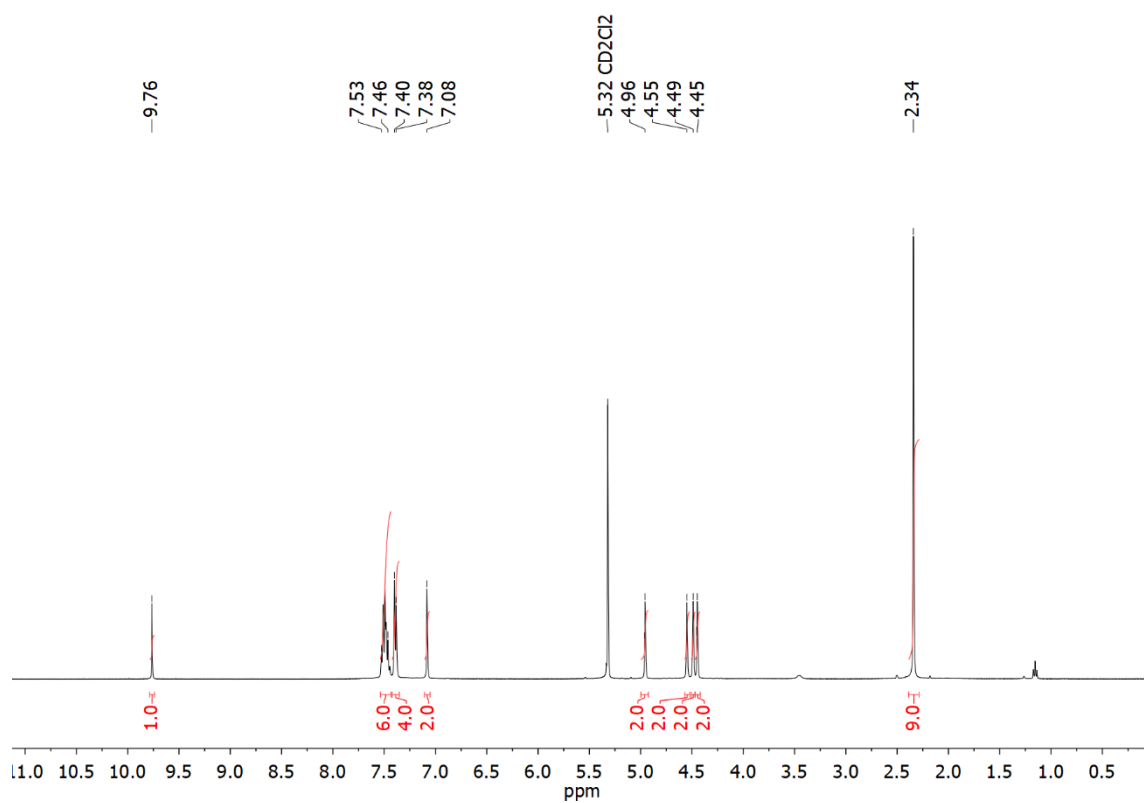


Figure S43. ^1H NMR spectrum (400 MHz, CD_2Cl_2) of $8^{\text{Mes}}\text{H}(\text{OTf})$.

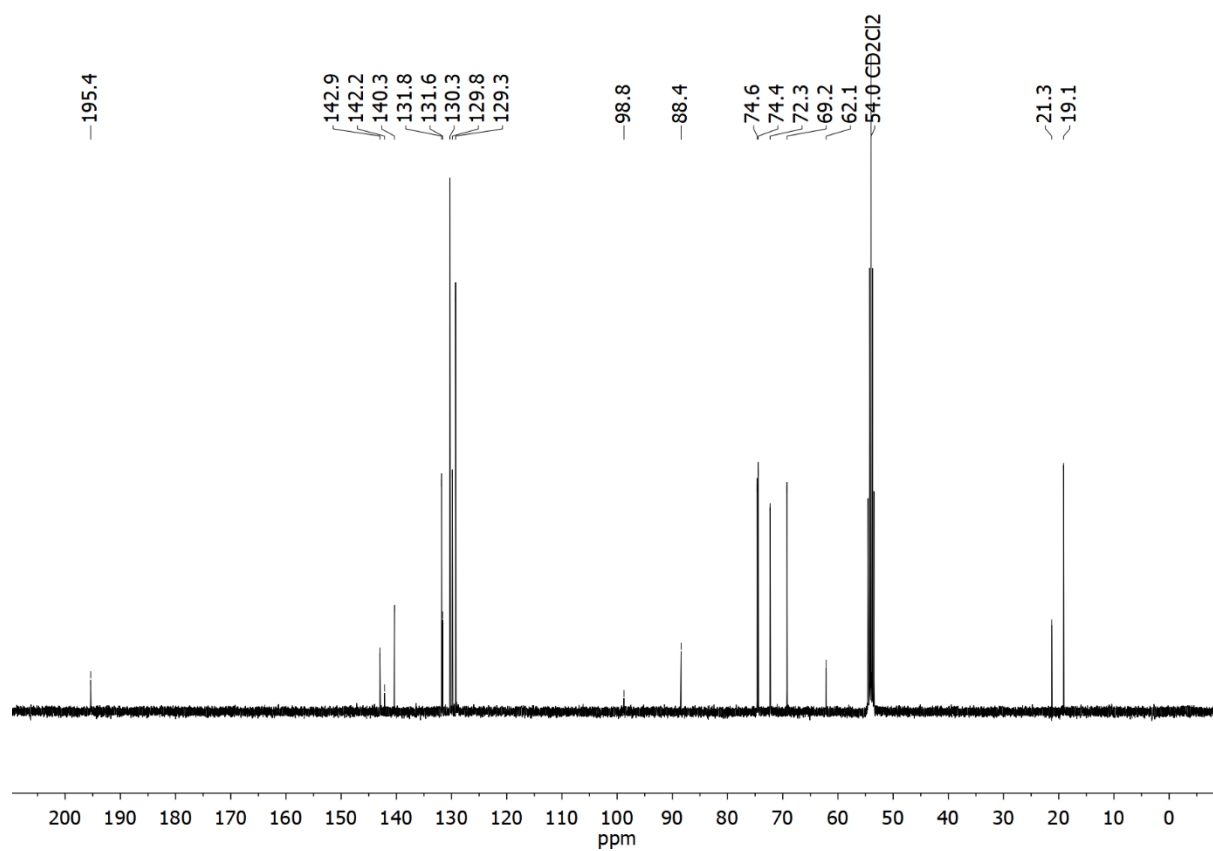


Figure S44. $^{13}\text{C}\{^1\text{H}\}$ NMR (101 MHz, CD_2Cl_2) of $8^{\text{Mes}}\text{H}(\text{OTf})$.

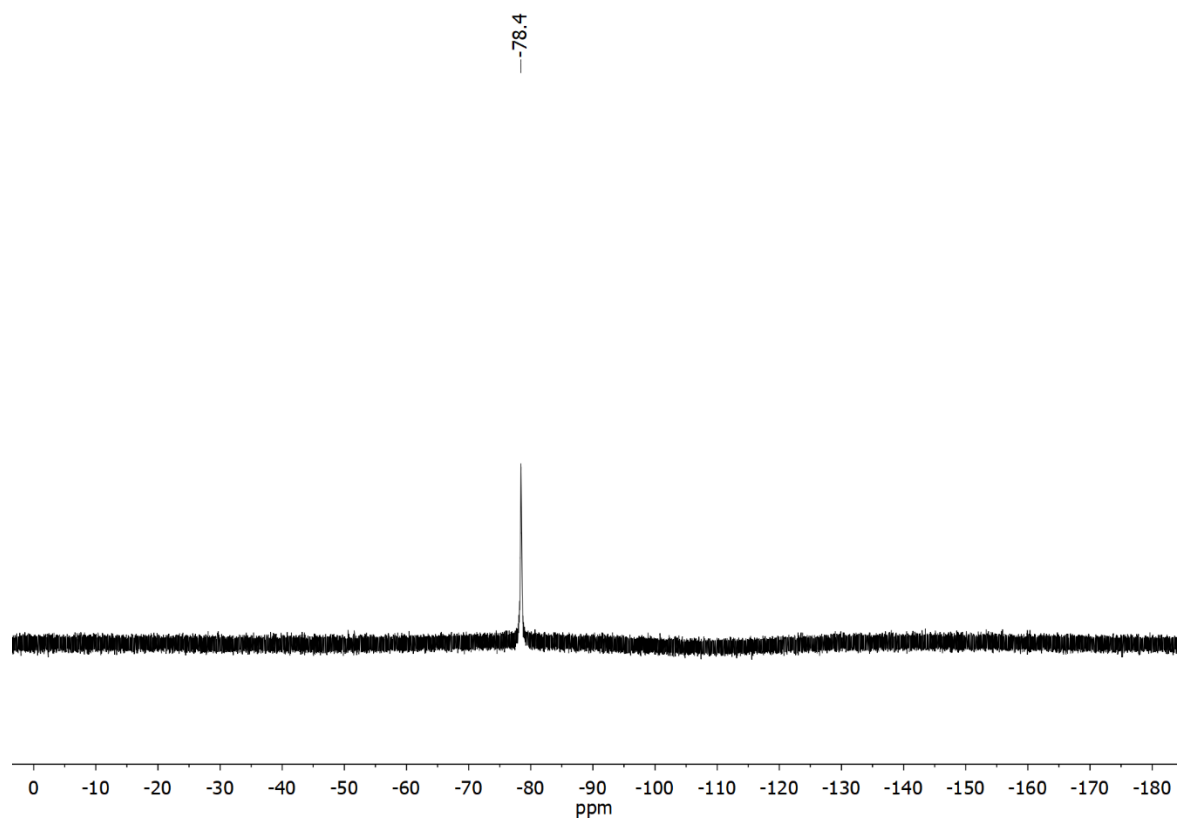


Figure S45. ^{19}F NMR (376 MHz, CD_2Cl_2) of $8^{\text{Mes}}\text{H}(\text{OTf})$.

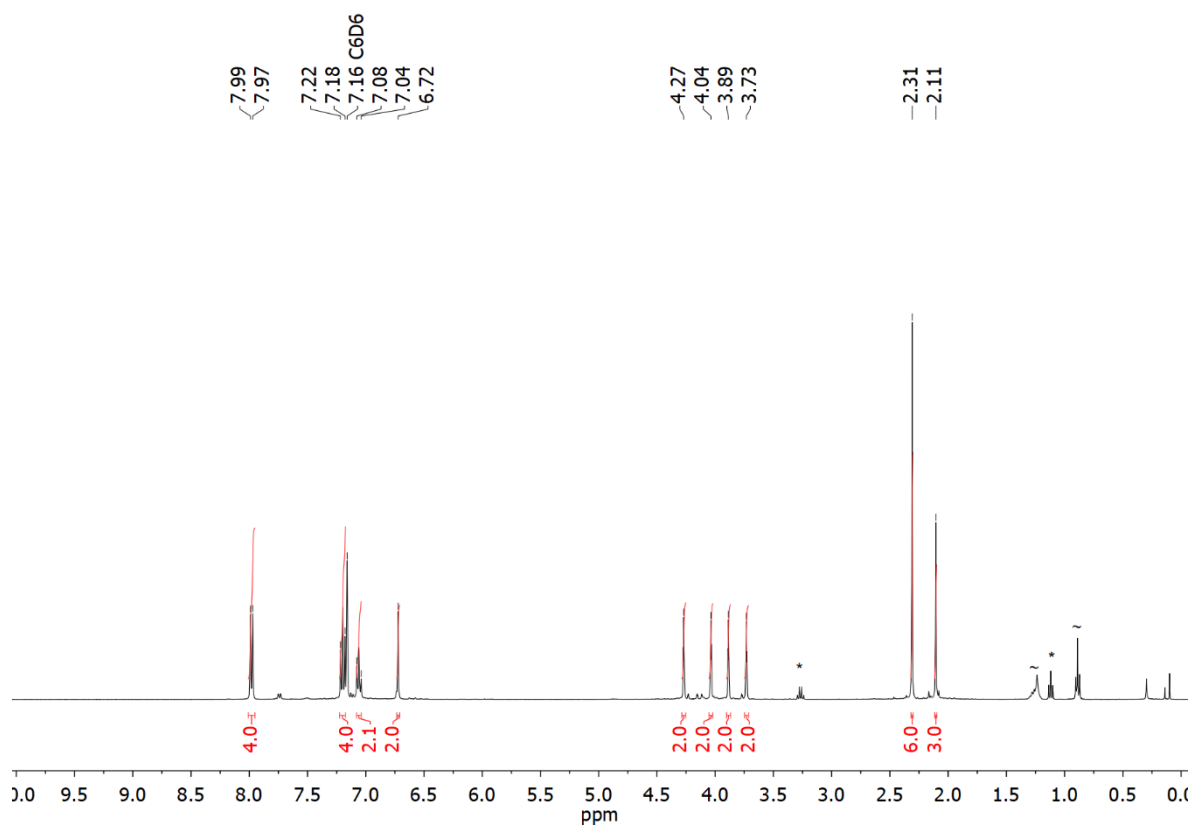


Figure S46. ^1H NMR spectrum (400 MHz, C_6D_6) of 8^{Mes} . Signals marked belong to residual diethyl ether (*) and *n*-hexane (~).

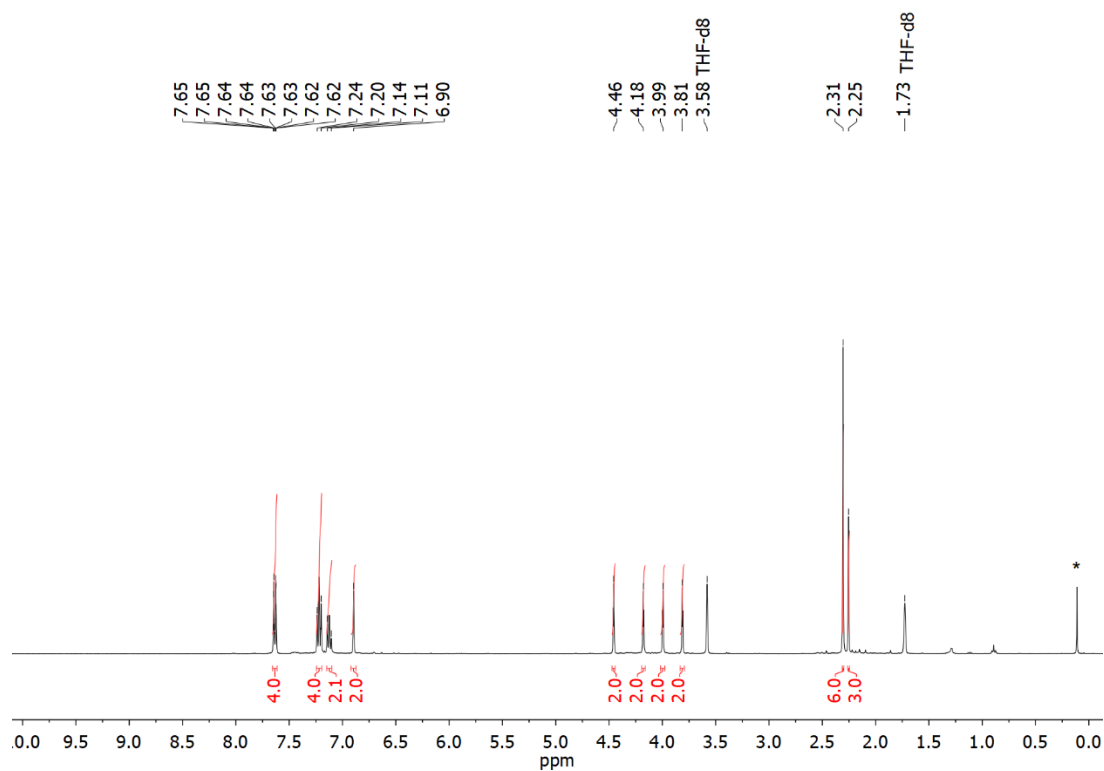


Figure S47. ^1H NMR spectrum (400 MHz, THF-d_8) of $\mathbf{8}^{\text{Mes}}$. The signal marked (*) belongs to silicon grease.

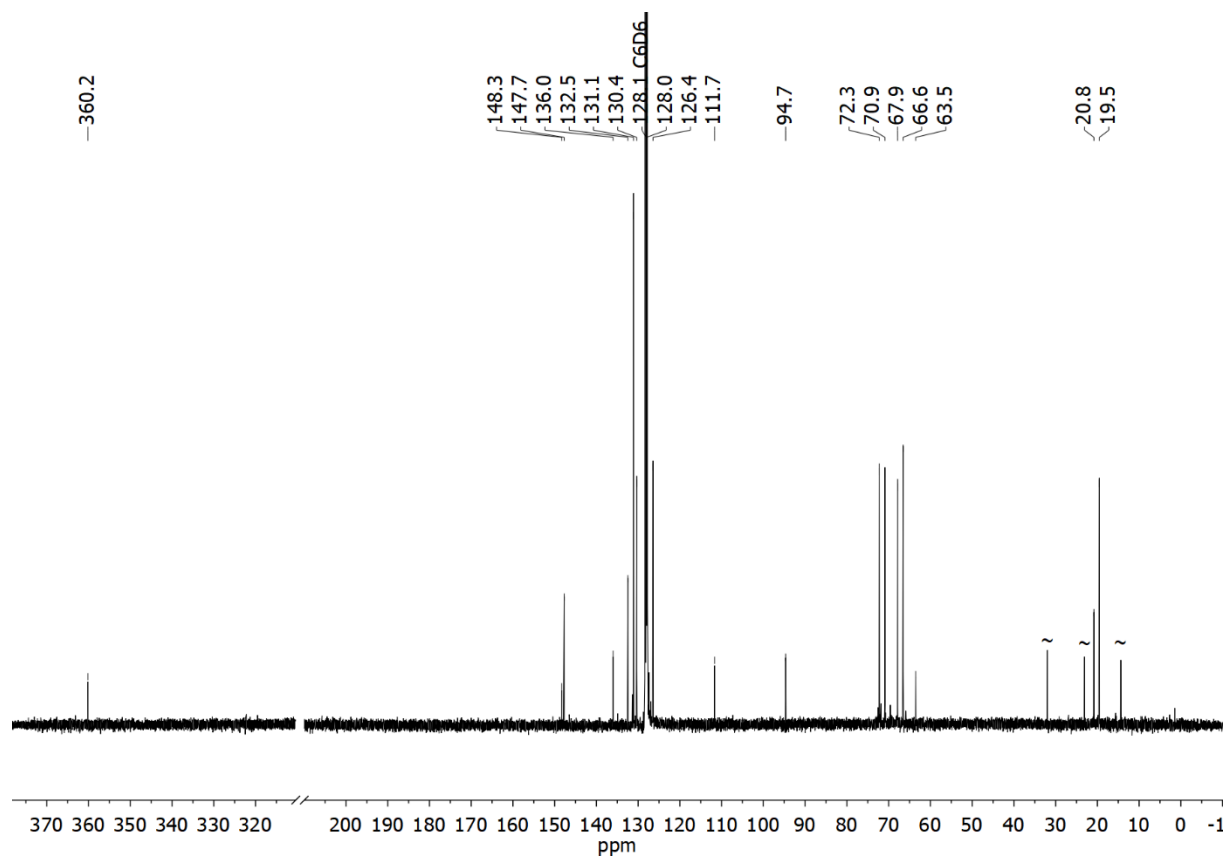


Figure S48. $^{13}\text{C}\{^1\text{H}\}$ NMR (101 MHz, C_6D_6) of $\mathbf{8}^{\text{Mes}}$. Signals marked (~) belong to residual *n*-hexane.

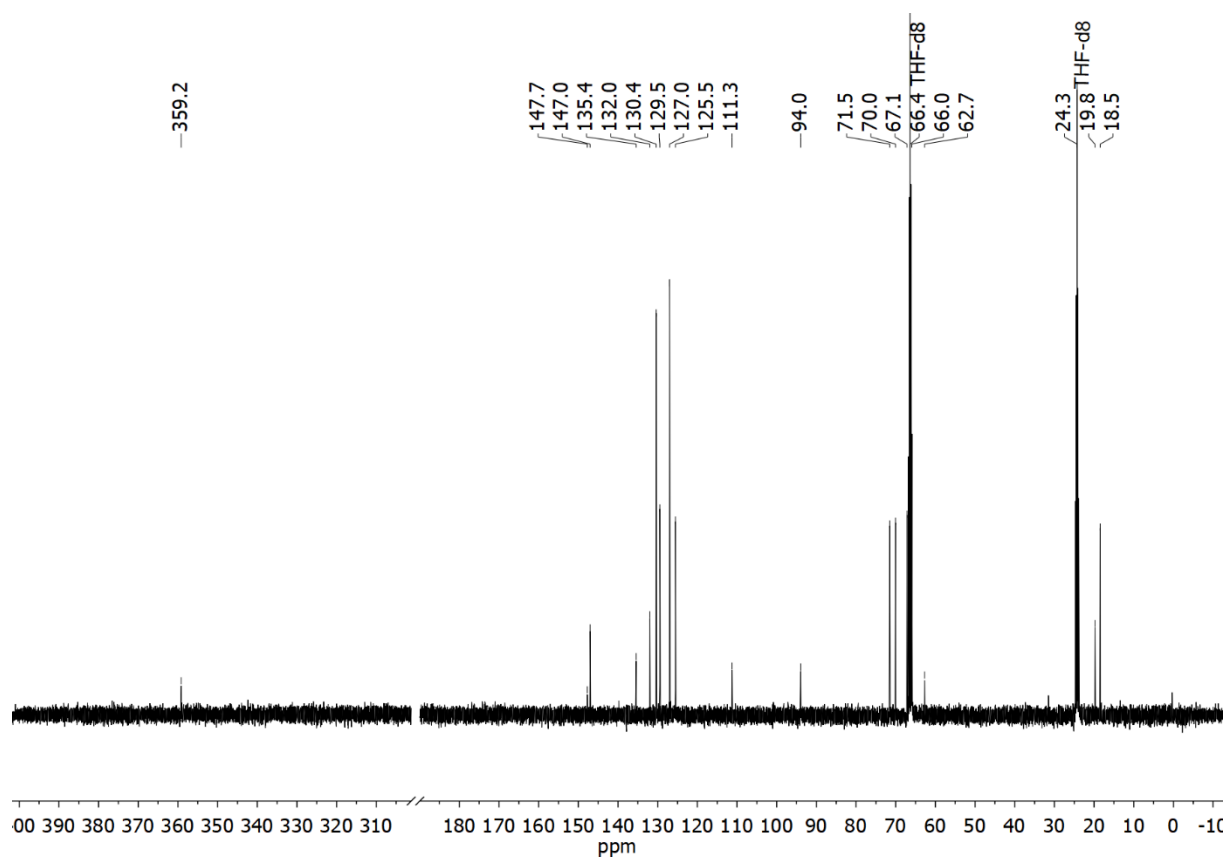


Figure S49. $^{13}\text{C}\{^1\text{H}\}$ NMR (101 MHz, THF- d_8) of $\mathbf{8}^{\text{Mes}}$.

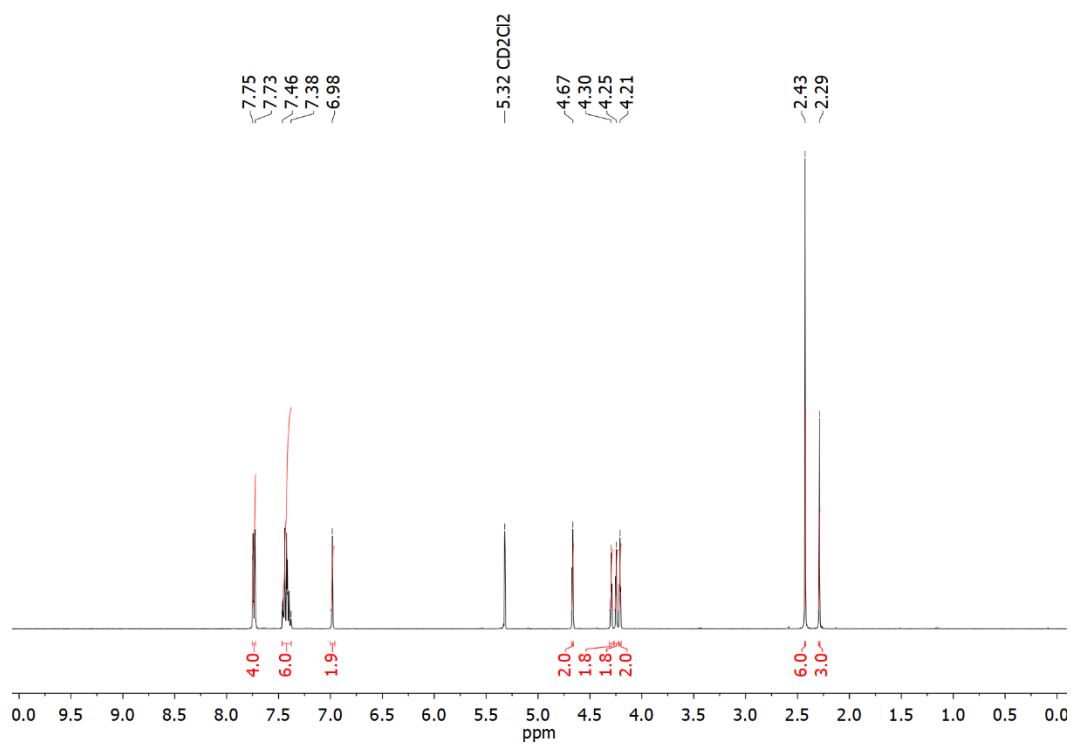


Figure S50. ^1H NMR spectrum (400 MHz, CD_2Cl_2) of $[\text{AuCl}(\mathbf{8}^{\text{Mes}})]$.

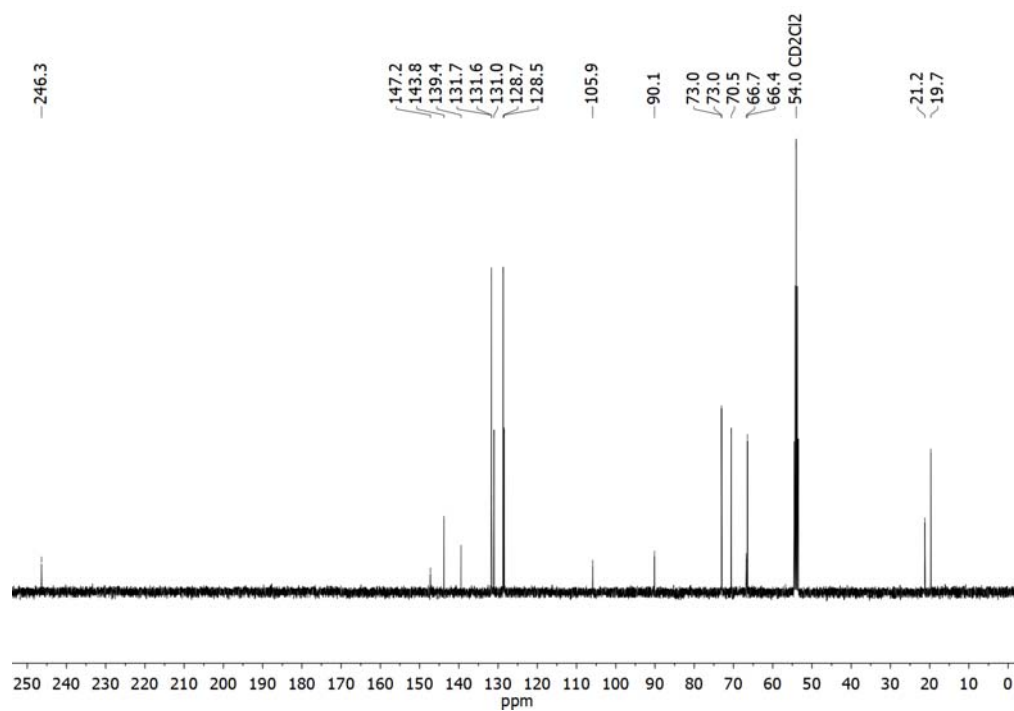


Figure S51. $^{13}\text{C}\{^1\text{H}\}$ NMR spectrum (101 MHz, CD_2Cl_2) of $[\text{AuCl}(\mathbf{8}^{\text{Mes}})]$.

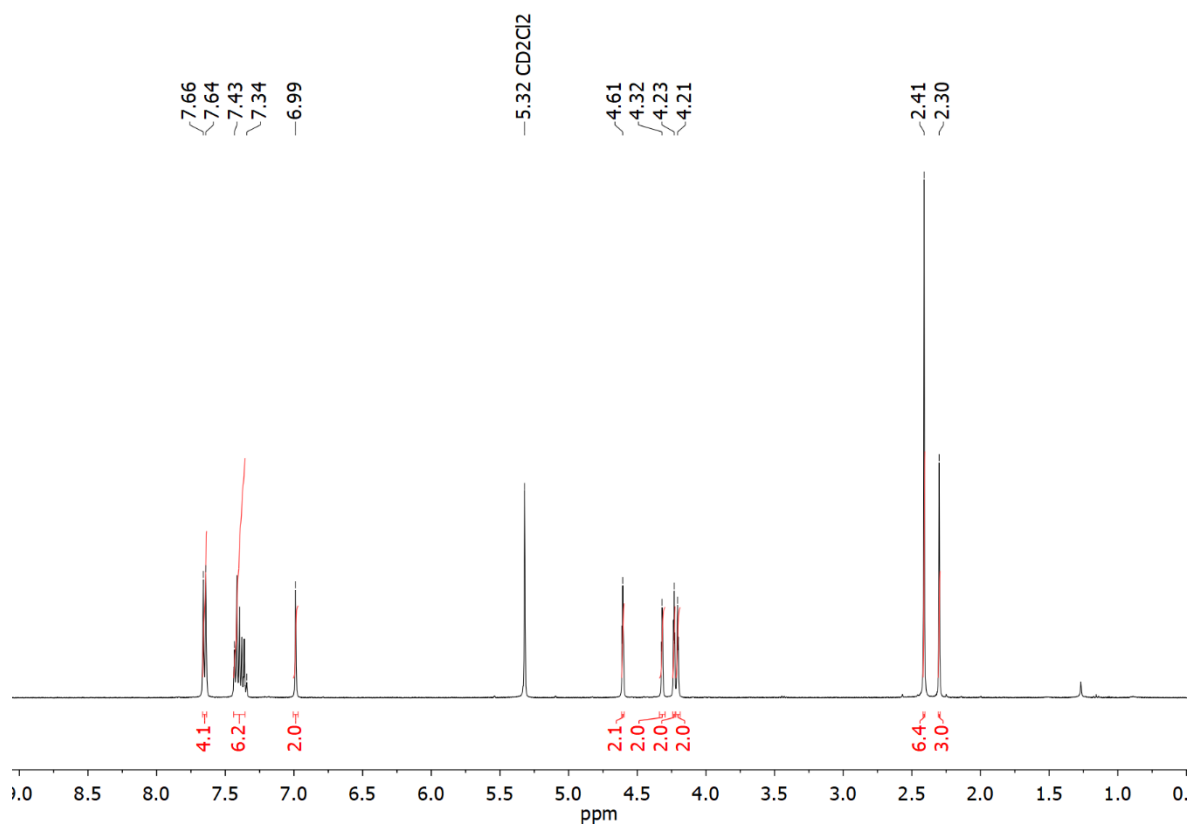


Figure S52. ^1H NMR spectrum (400 MHz, CD_2Cl_2) of $[\text{CuCl}(\mathbf{8}^{\text{Mes}})]$.

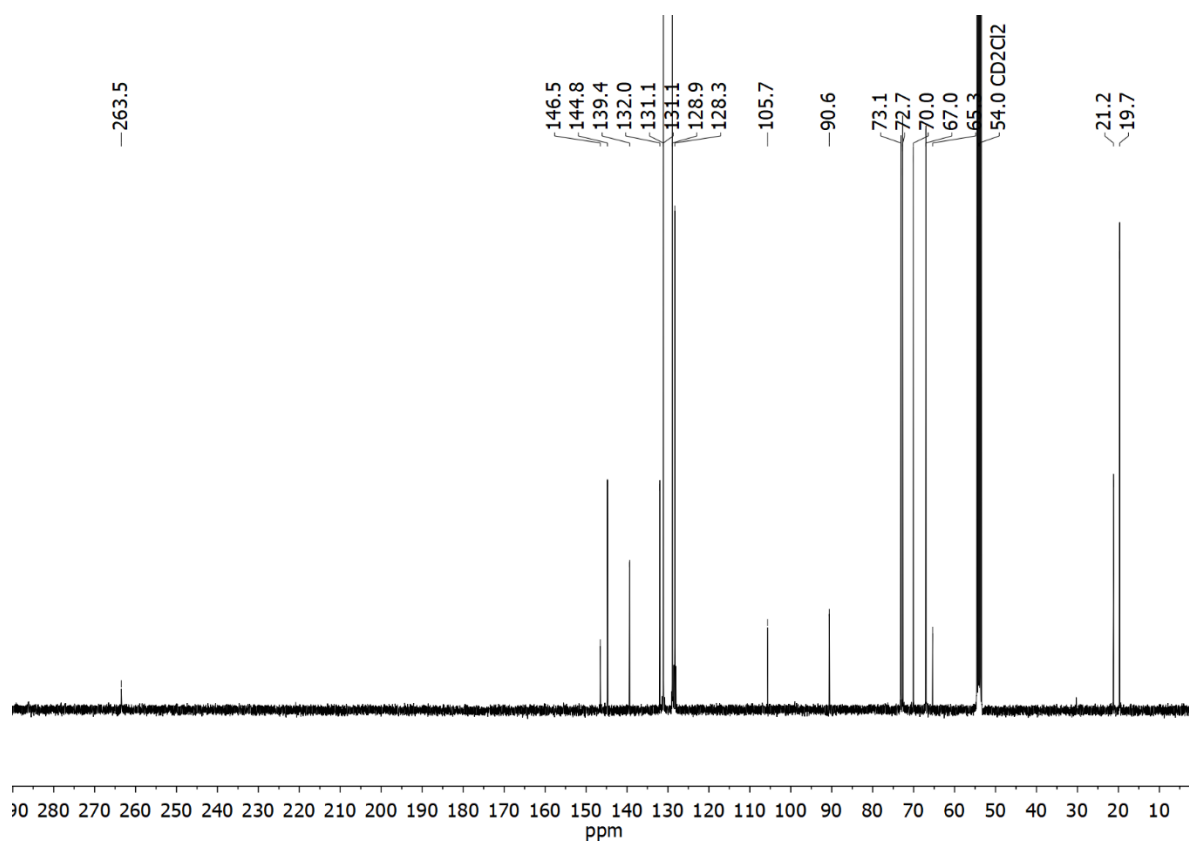


Figure S53. $^{13}\text{C}\{^1\text{H}\}$ NMR spectrum (101 MHz, CD_2Cl_2) of $[\text{CuCl}(\mathbf{8}^{\text{Mes}})]$.

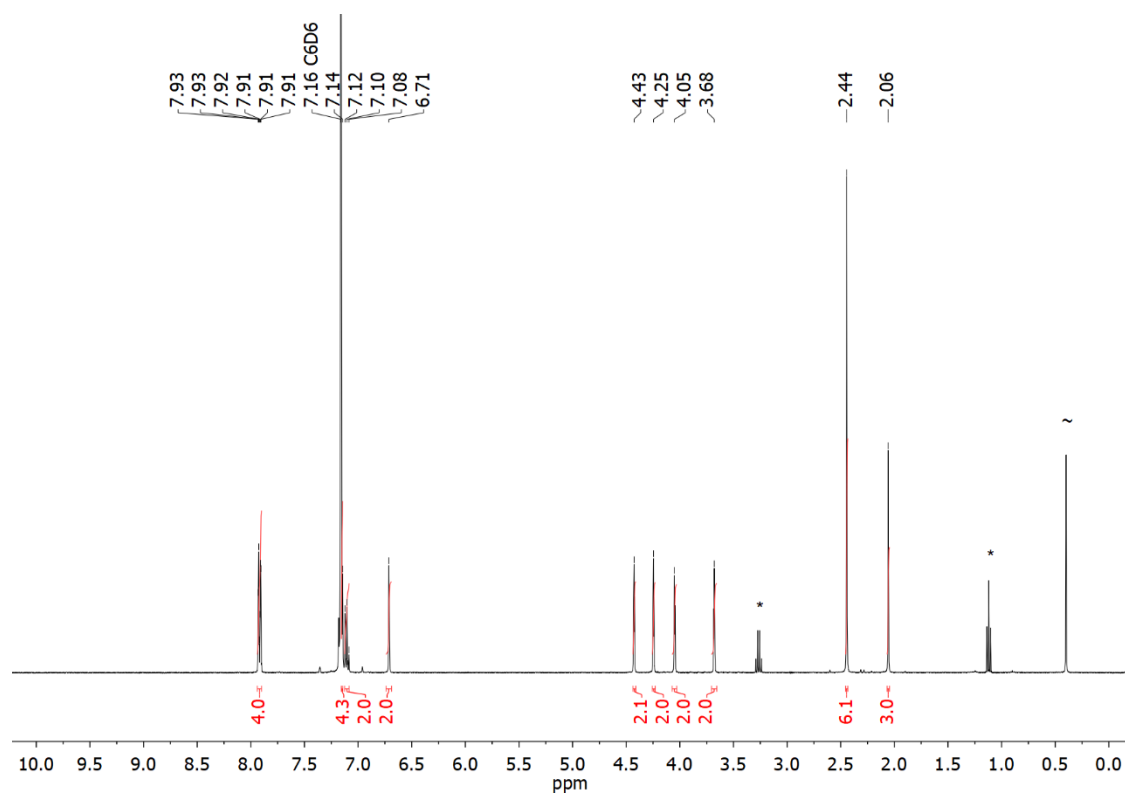


Figure S54. ^1H NMR spectrum (400 MHz, C_6D_6) of $\mathbf{8}^{\text{Mes}}\text{Se}$. Signals marked belong to residual diethyl ether (*) and water (~).

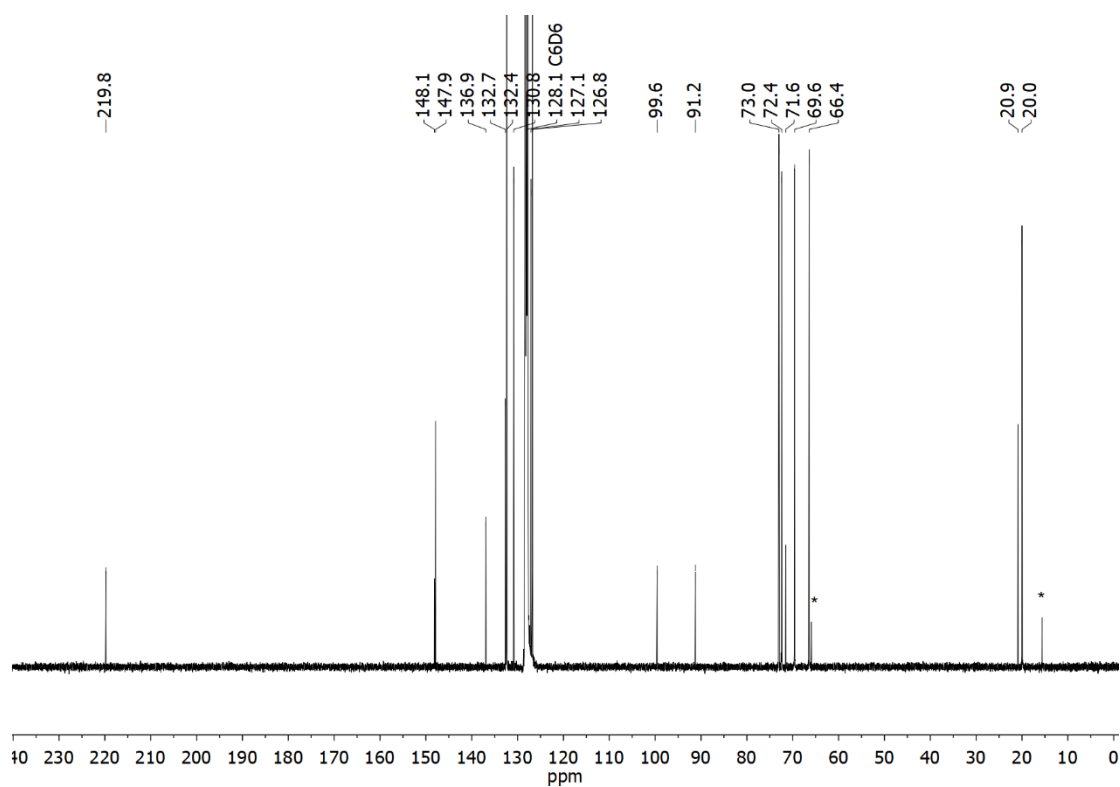


Figure S55. $^{13}\text{C}\{^1\text{H}\}$ NMR spectrum (101 MHz, C_6D_6) of 8^{Mes}Se . Signals marked (*) belong to residual diethyl ether.

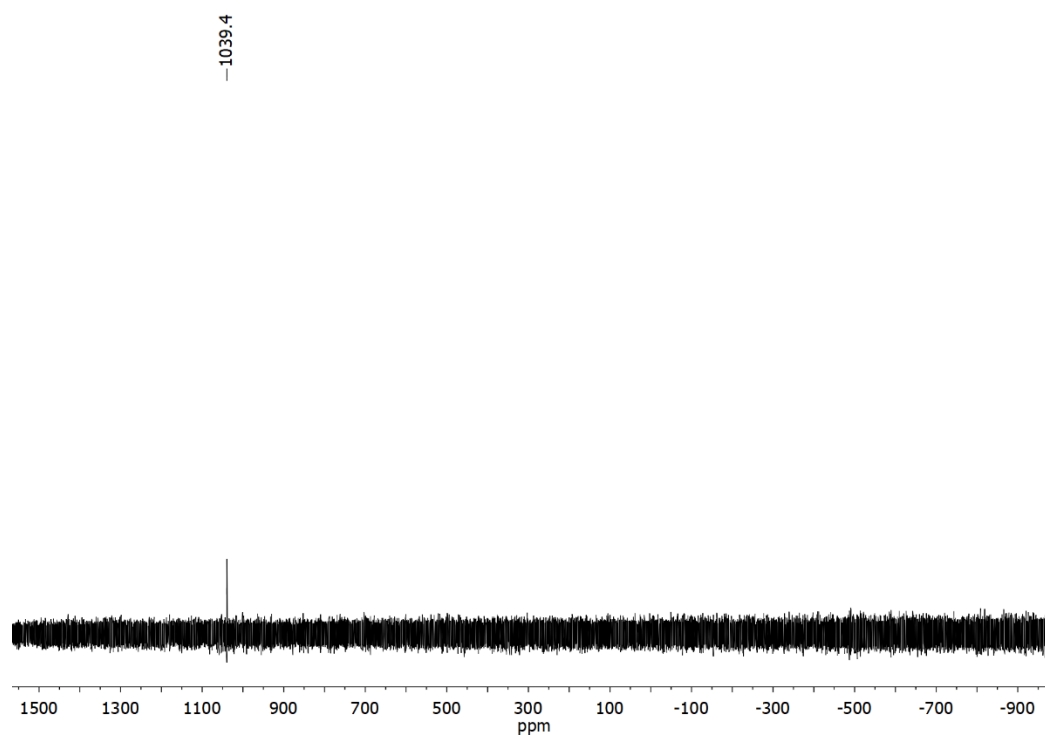


Figure S56. ^{77}Se NMR spectrum (95 MHz, $\text{acetone-}d_6$) of 8^{Mes}Se .

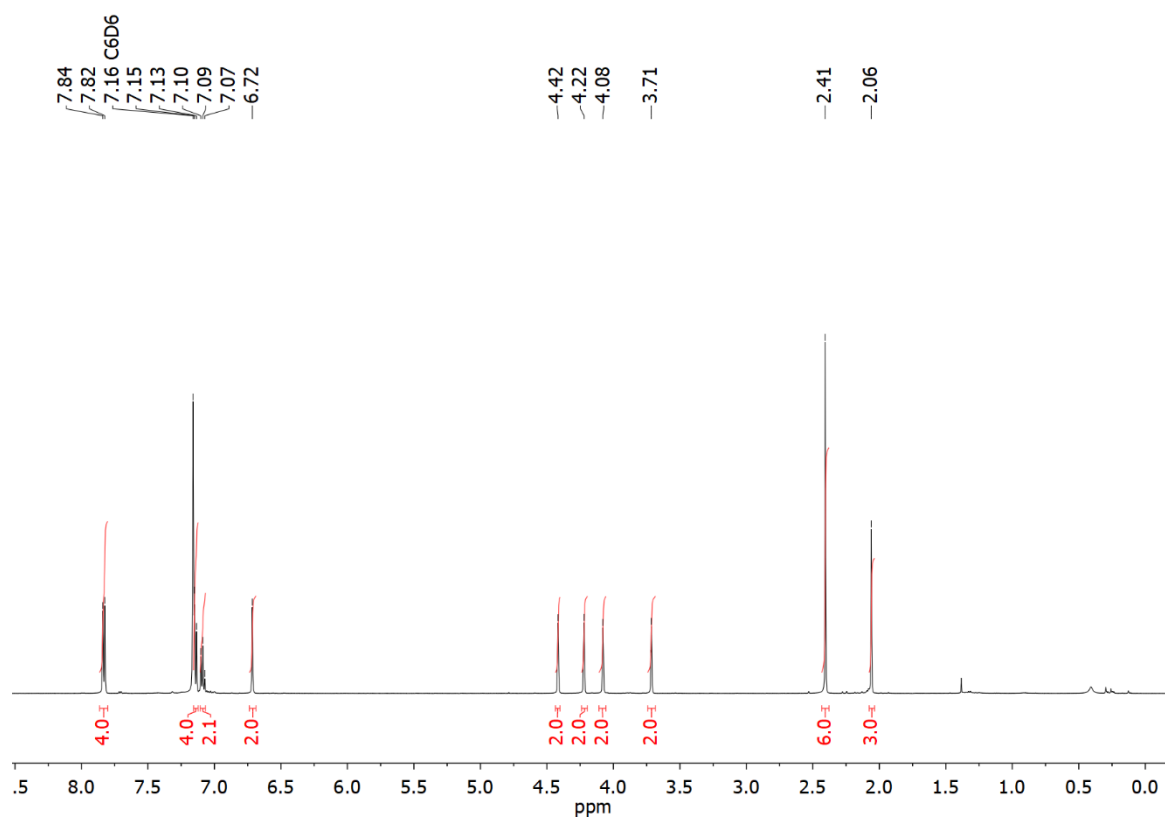


Figure S57. ^1H NMR spectrum (500 MHz, C_6D_6) of $\mathbf{8}^{\text{MesS}}$.

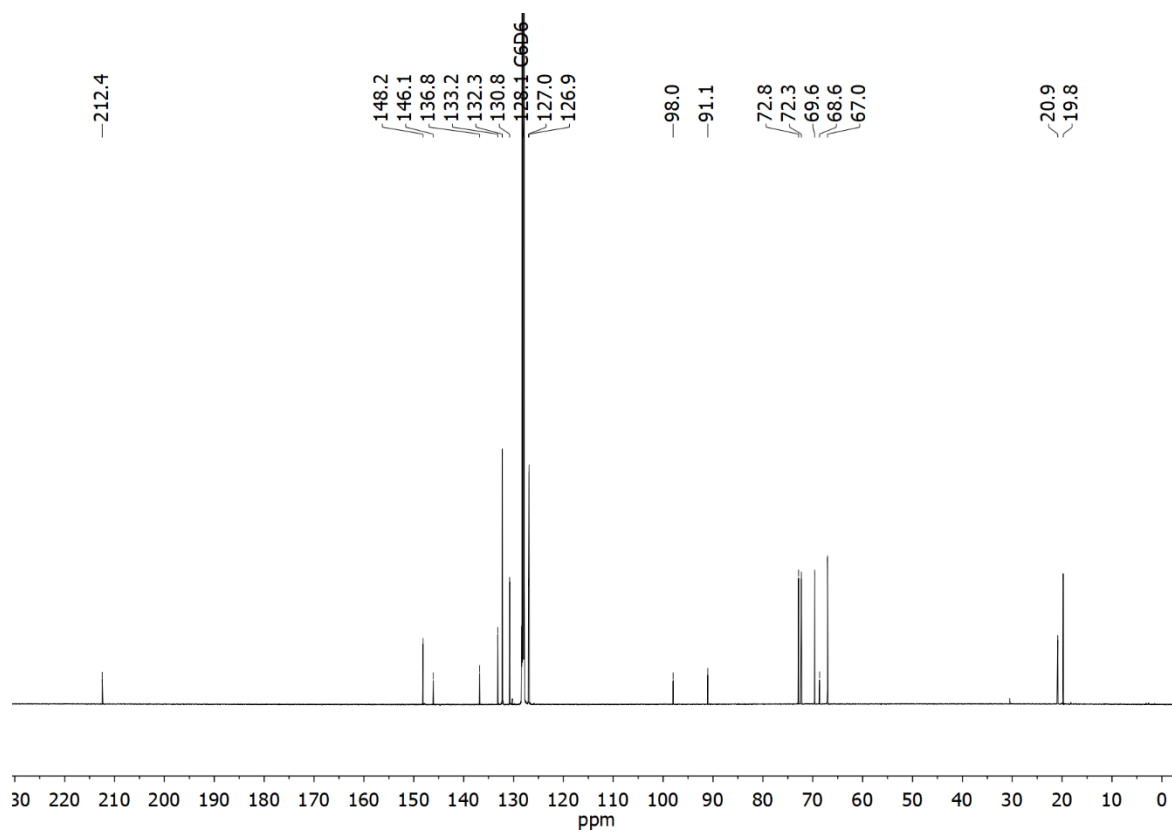


Figure S58. $^{13}\text{C}\{^1\text{H}\}$ NMR spectrum (126 MHz, C_6D_6) of $\mathbf{8}^{\text{MesS}}$.

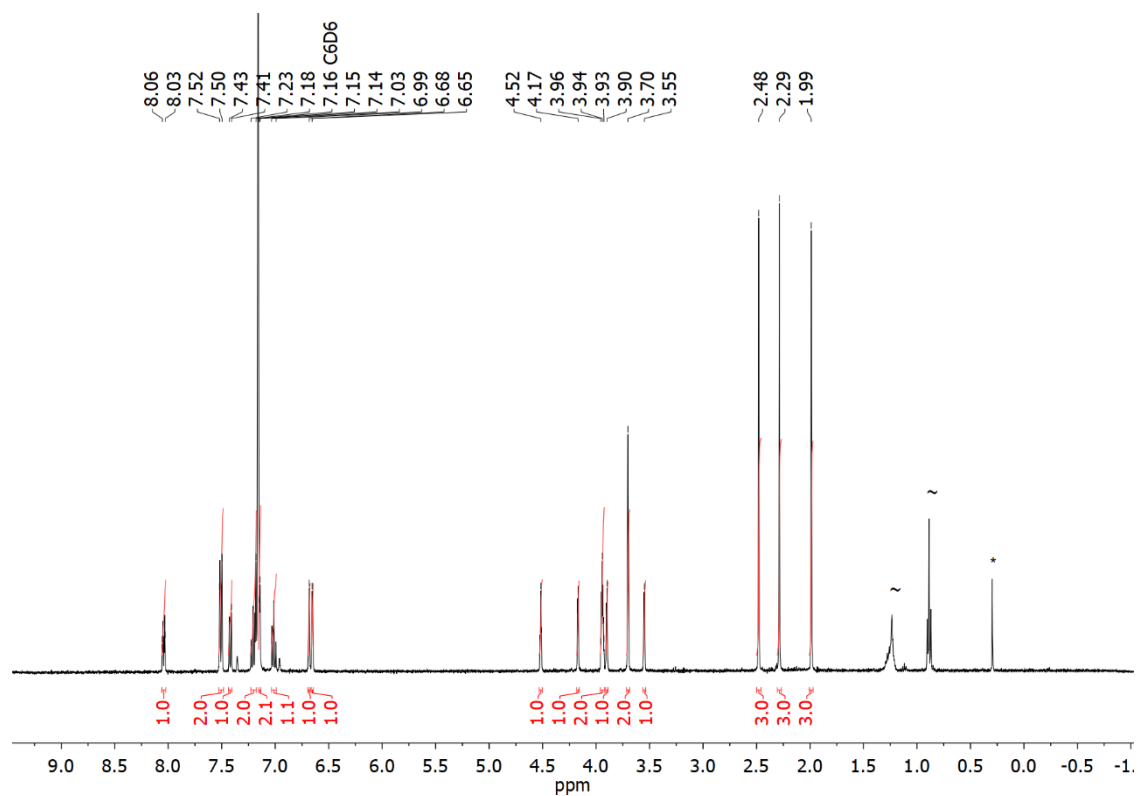


Figure S59. ^1H NMR spectrum (400 MHz, C_6D_6) of $[\text{Rh}(\mathbf{9})(\text{CO})_2]$. Signals marked belong to residual *n*-hexane (~) and silicon grease (*).

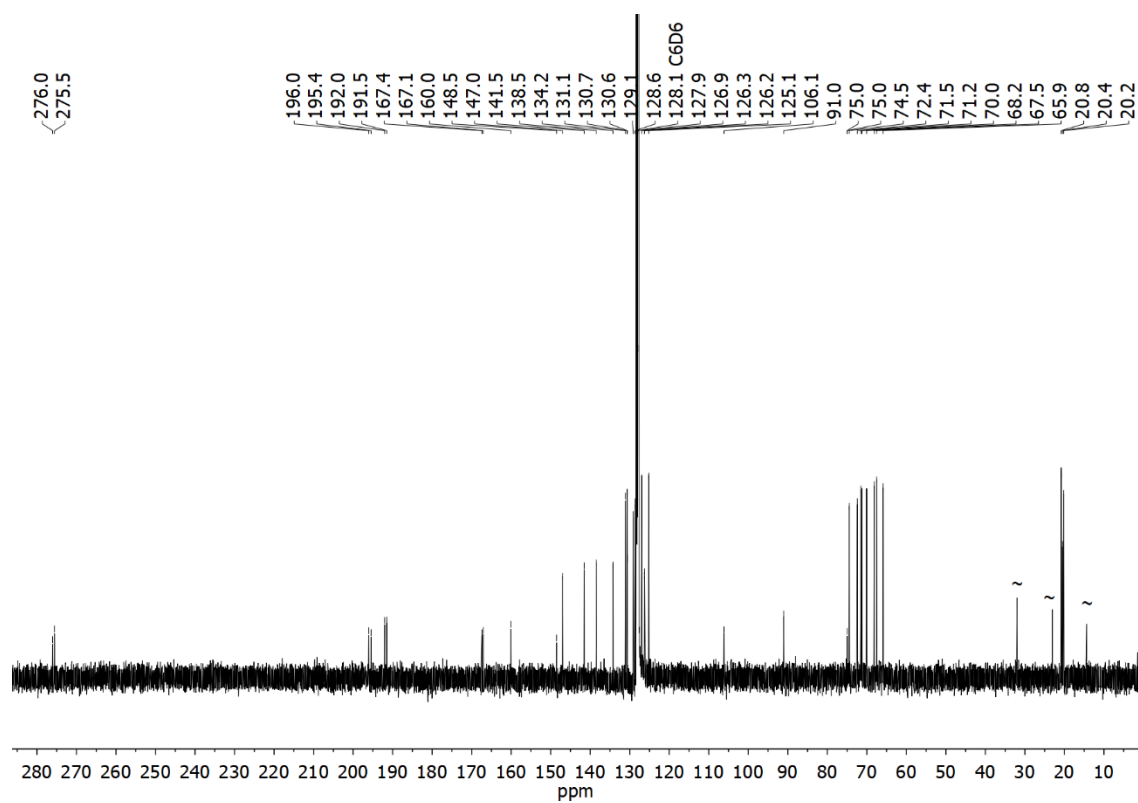


Figure S60. $^{13}\text{C}\{^1\text{H}\}$ NMR spectrum (101 MHz, C_6D_6) of $[\text{Rh}(\mathbf{9})(\text{CO})_2]$. Signals marked (~) belong to residual *n*-hexane.

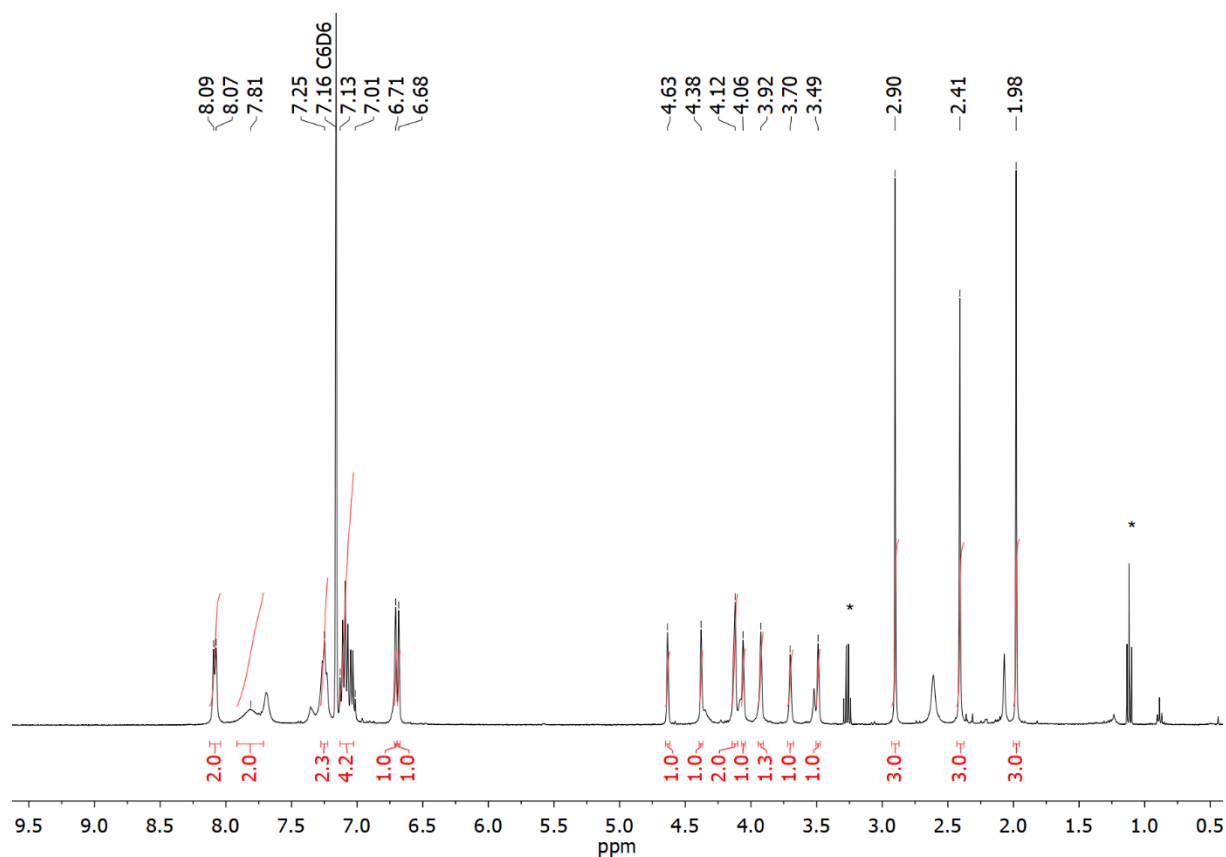


Figure S61. ^1H NMR spectrum (400 MHz, C_6D_6) of $[\text{RhCl}(\text{CO})_2(\mathbf{8}^{\text{Mes}})]$. Signals marked (*) belong to residual diethyl ether.

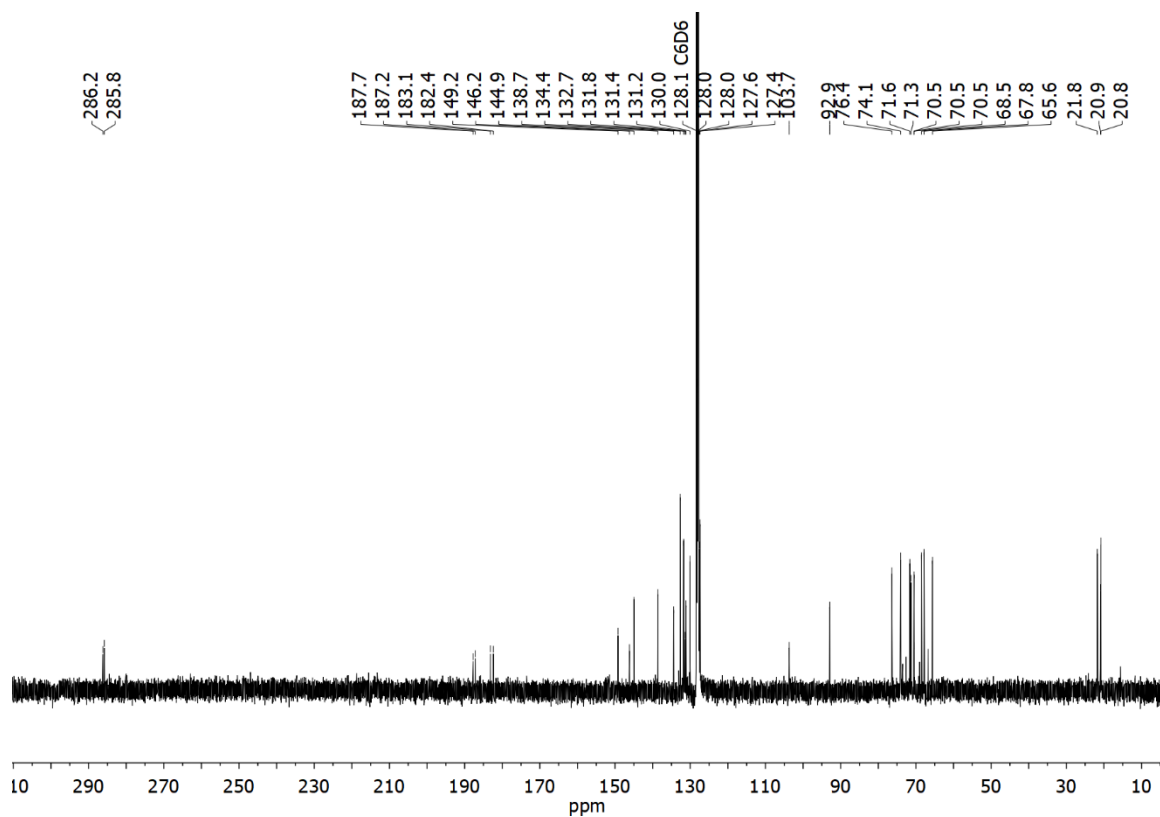


Figure S62. $^{13}\text{C}\{^1\text{H}\}$ NMR spectrum (101 MHz, C_6D_6) of $[\text{RhCl}(\text{CO})_2(\mathbf{8}^{\text{Mes}})]$. Signals marked (*) belong to residual diethyl ether.

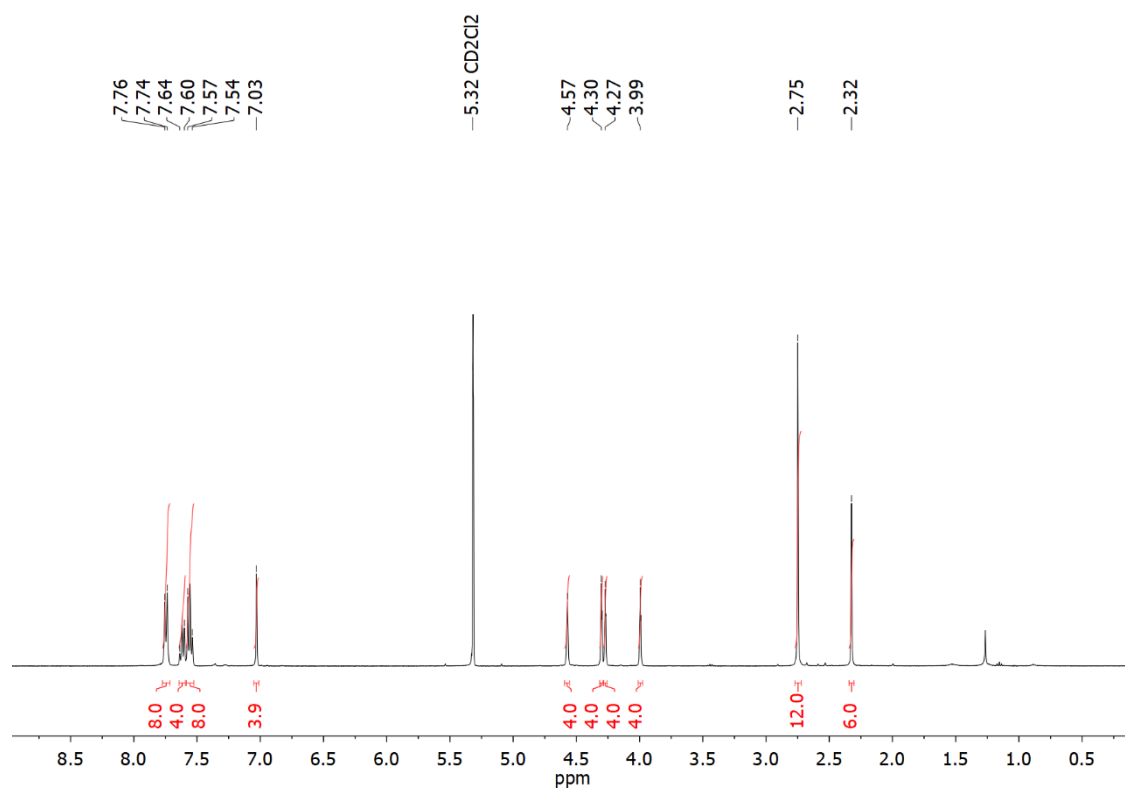


Figure S63. ^1H NMR spectrum (400 MHz, CD_2Cl_2) of $[\text{Rh}(\mu\text{-Cl})(\text{CO})(\mathbf{8}^{\text{Mes}})]_2$.

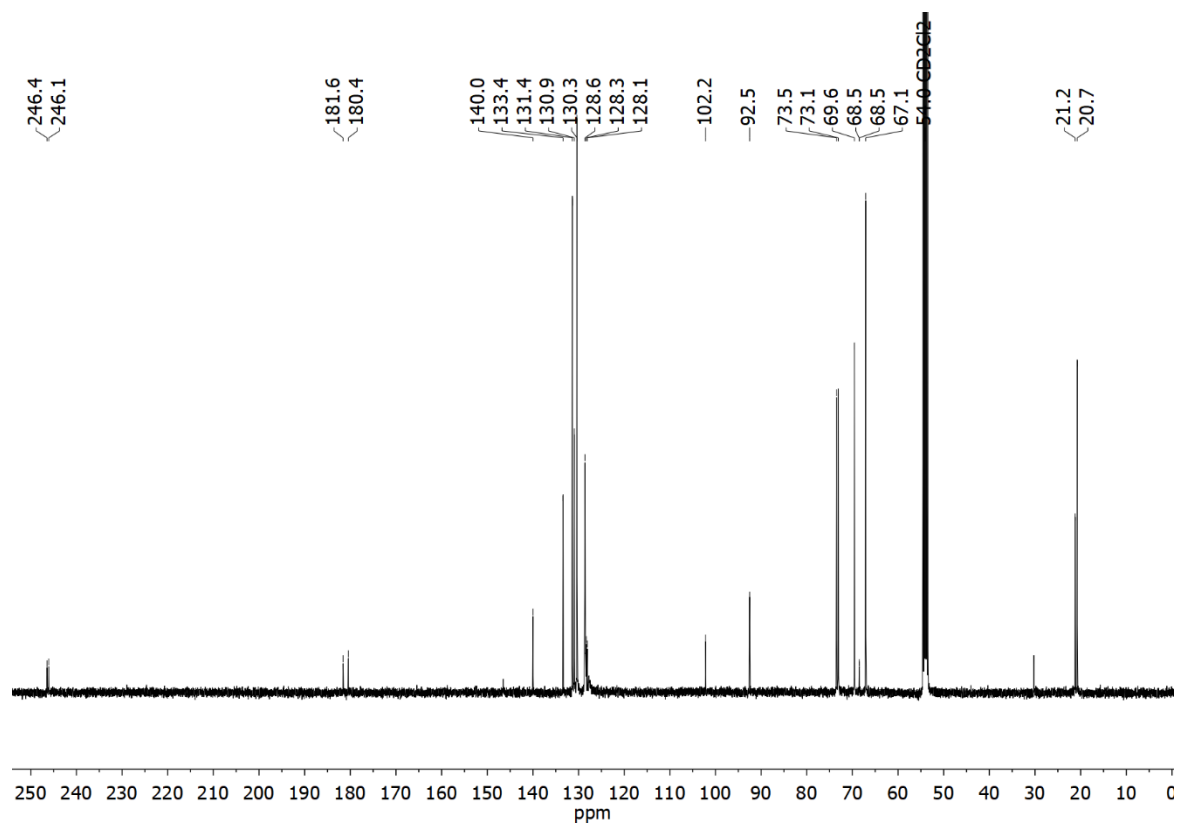


Figure S64. $^{13}\text{C}\{^1\text{H}\}$ NMR spectrum (101 MHz, CD_2Cl_2) of $[\text{Rh}(\mu\text{-Cl})(\text{CO})(\mathbf{8}^{\text{Mes}})]_2$.

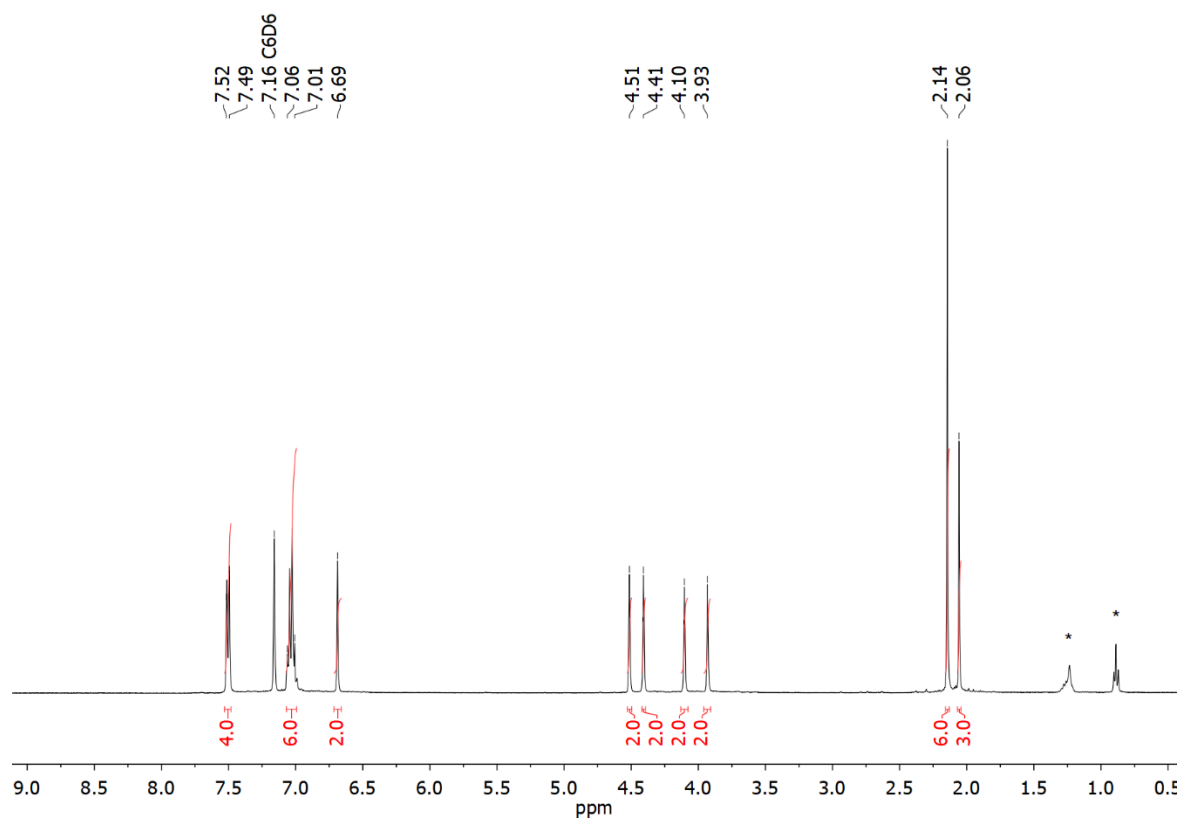


Figure S65. ^1H NMR spectrum (400 MHz, C_6D_6) of $\mathbf{8}^{\text{Mes}}\text{CO}$. Signals marked (*) belong to residual *n*-hexane.

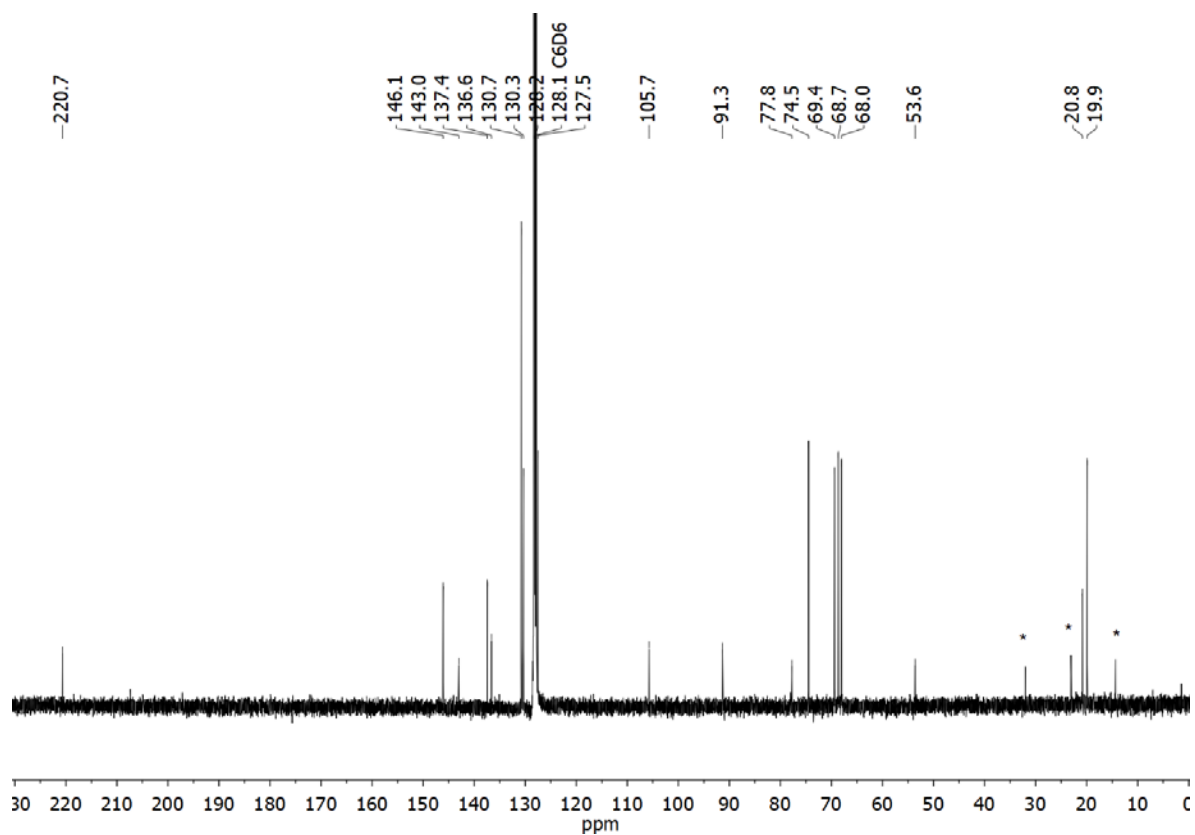


Figure S66. $^{13}\text{C}\{^1\text{H}\}$ NMR spectrum (101 MHz, C_6D_6) of $\mathbf{8}^{\text{Mes}}\text{CO}$. Signals marked (*) belong to residual *n*-hexane.

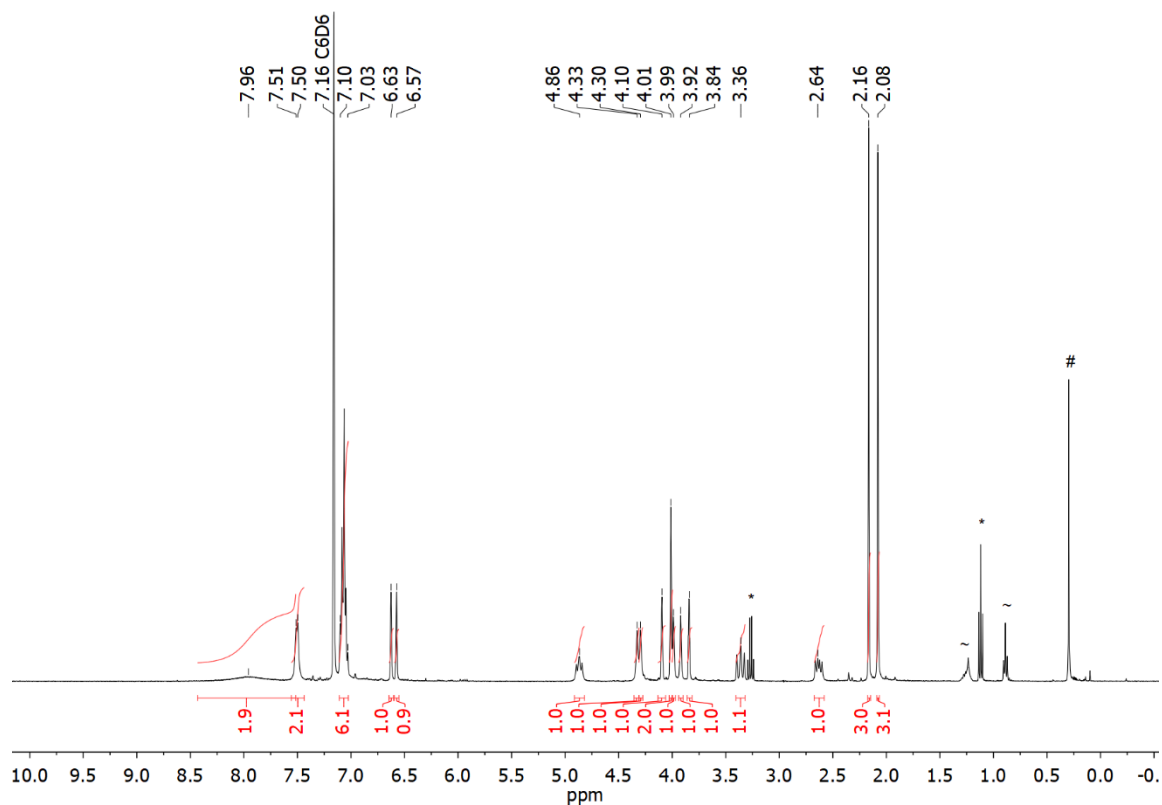


Figure S67. ^1H NMR spectrum (400 MHz, C_6D_6) of **10**. Signals marked belong to residual diethyl ether (*), *n*-hexane (~) and silicon grease (*).

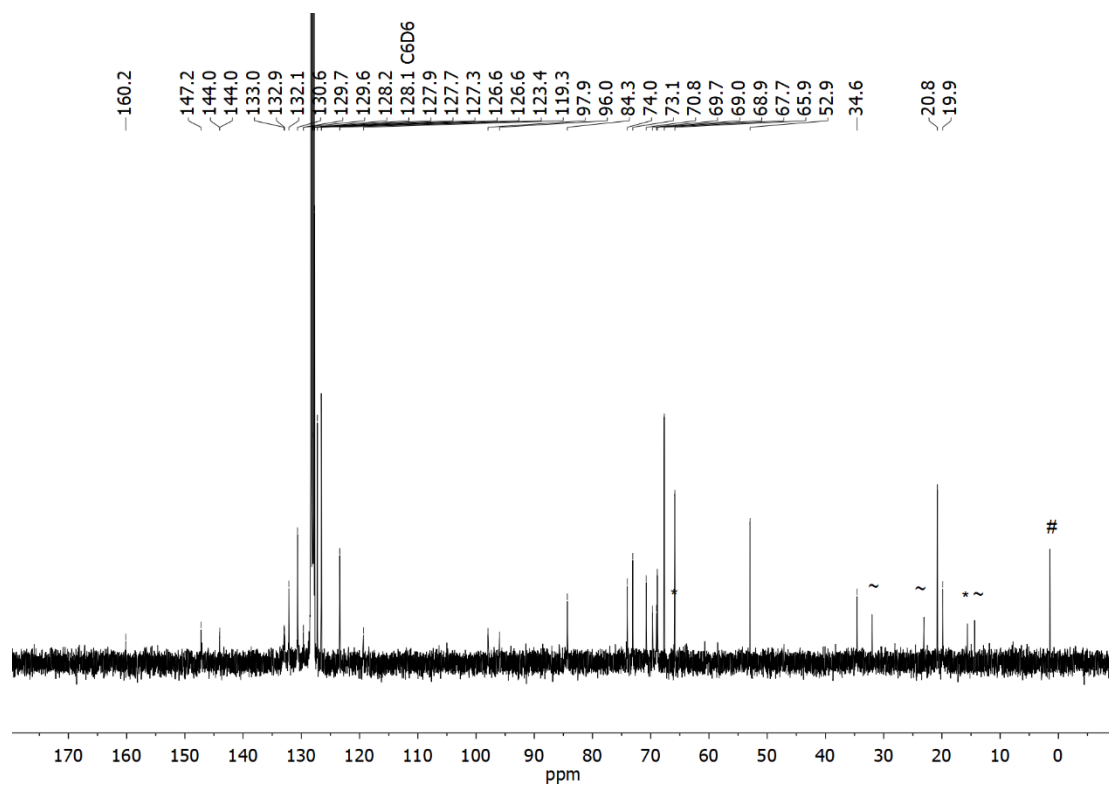
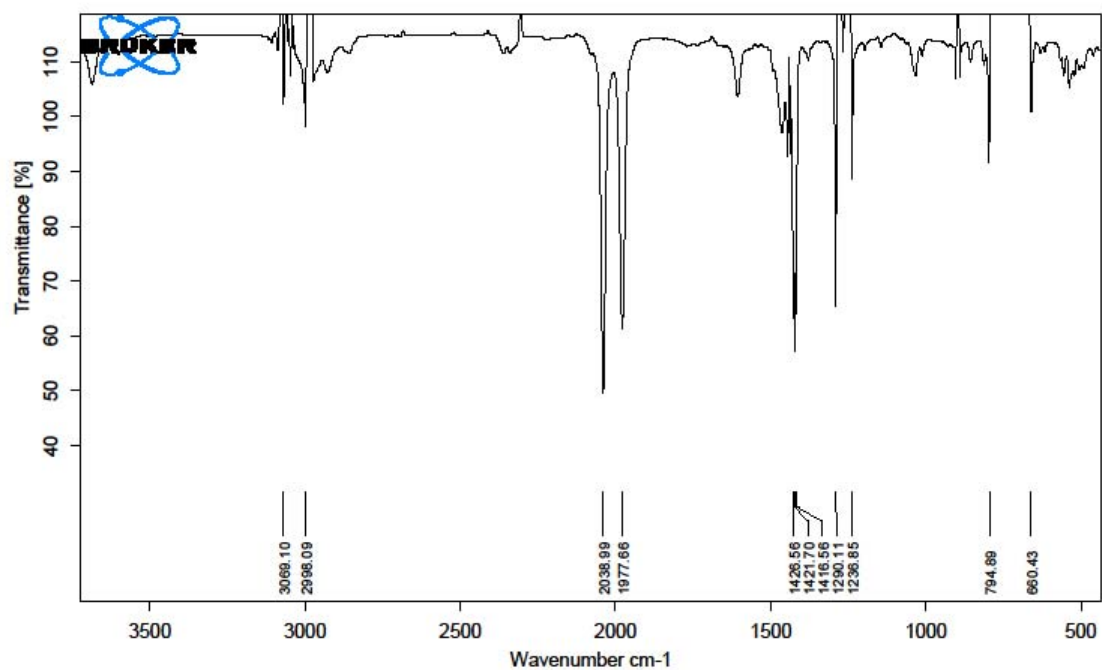
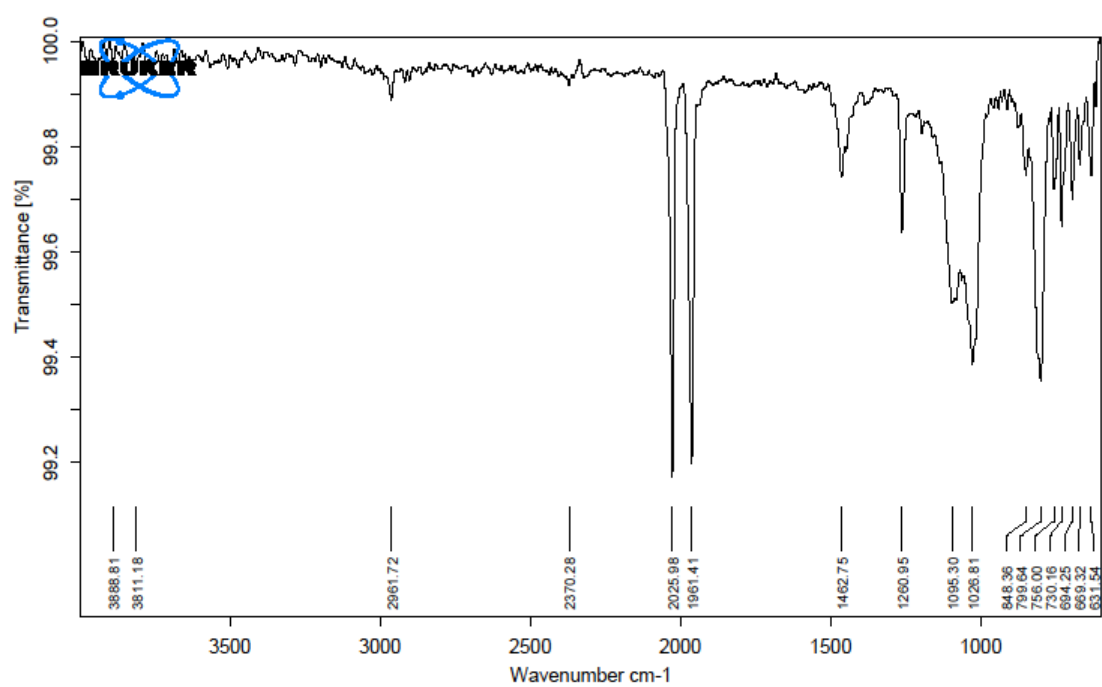


Figure S68. $^{13}\text{C}\{^1\text{H}\}$ NMR spectrum (101 MHz, C_6D_6) of **10**. Signals marked belong to residual diethyl ether (*), *n*-hexane (~) and silicon grease (*).

F Plots of IR Spectra

Figure S69. IR spectrum (dichloromethane) of $[\text{Rh}(\mathbf{9})(\text{CO})_2]$.Figure S70. IR spectrum (ATR) of $[\text{Rh}(\mathbf{9})(\text{CO})_2]$.

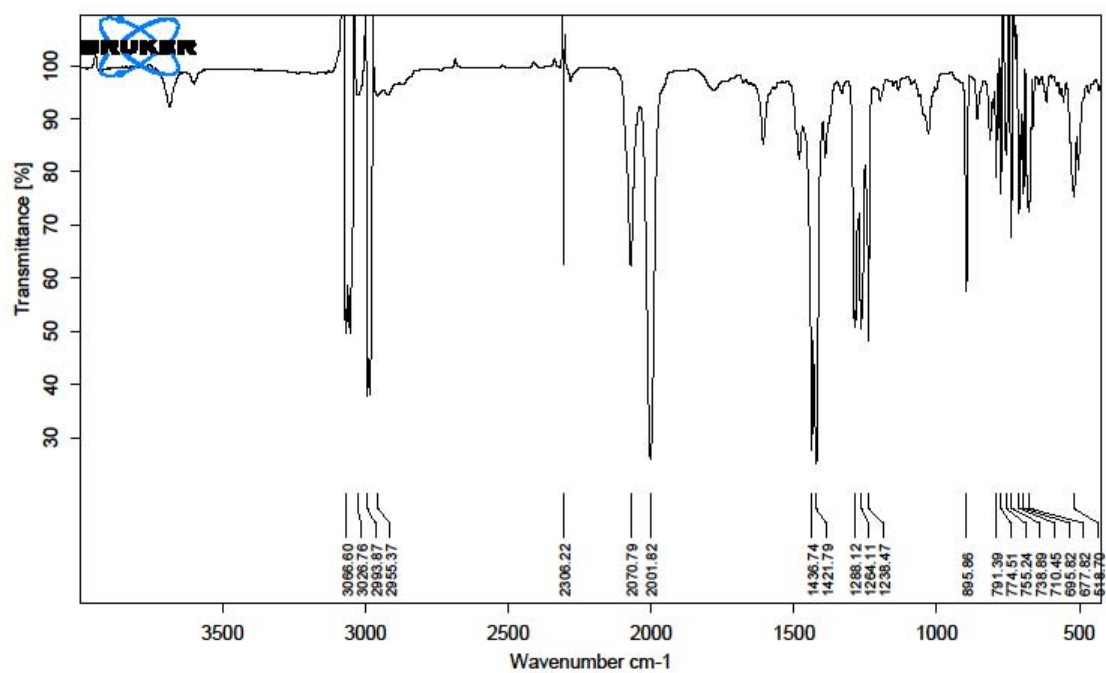


Figure S71. IR spectrum (dichloromethane) of $[\text{RhCl}(\text{CO})_2(\mathbf{8}^{\text{Mes}})]$.

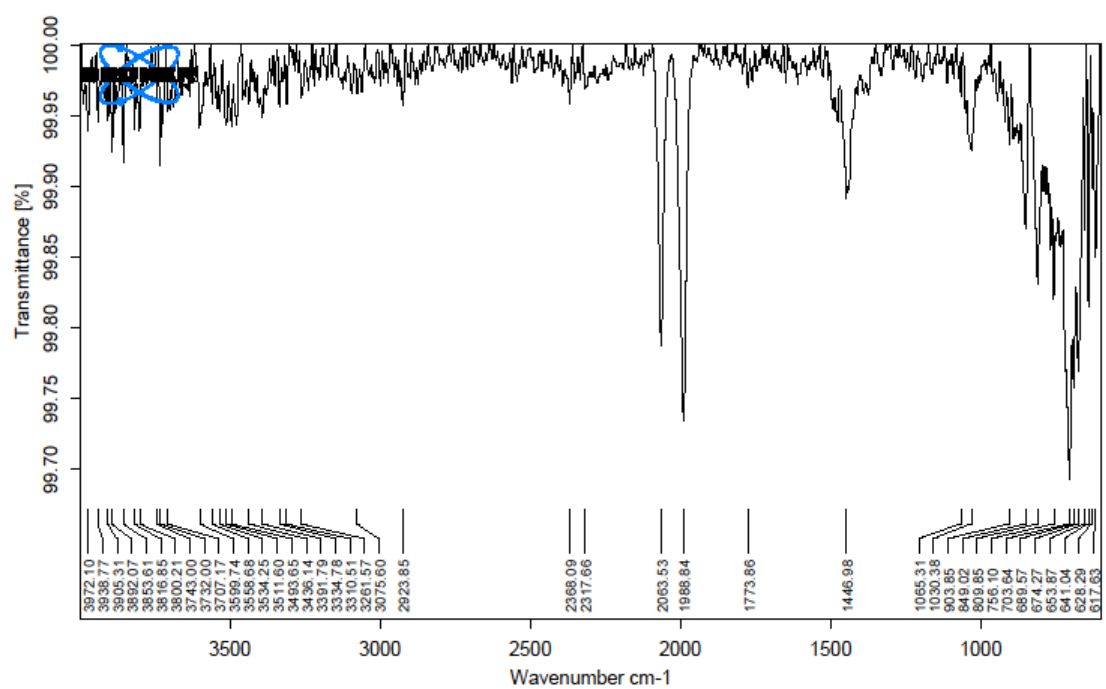


Figure S72. IR spectrum (ATR) of $[\text{RhCl}(\text{CO})_2(\mathbf{8}^{\text{Mes}})]$.

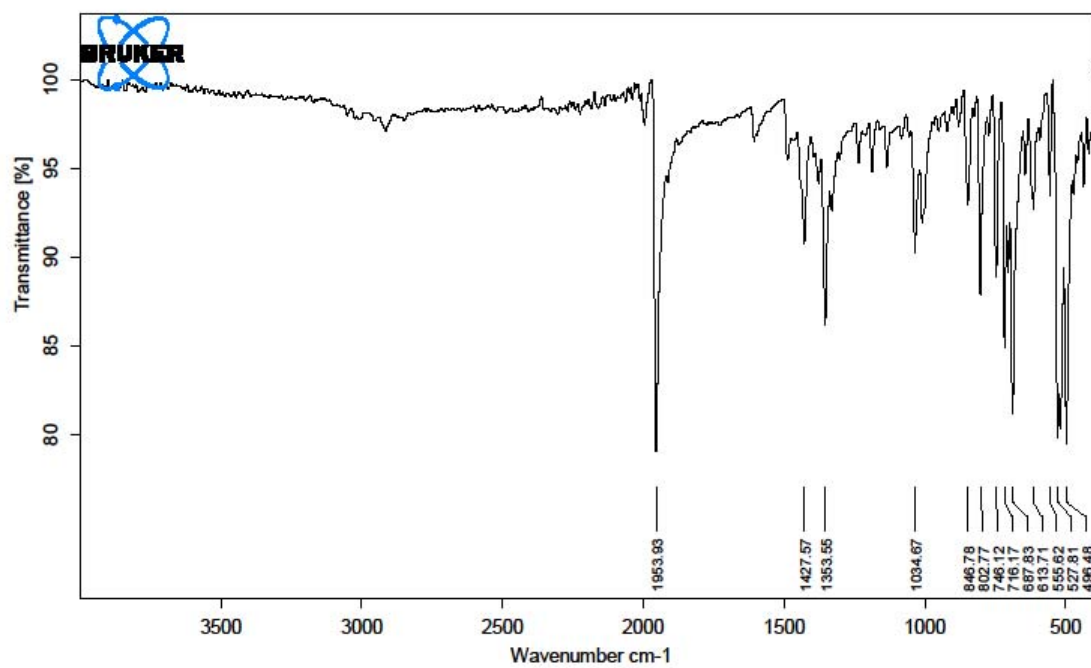


Figure S73. IR spectrum (ATR) of $[\text{Rh}(\mu\text{-Cl})(\text{CO})(\mathbf{8}^{\text{Mes}})]_2$.

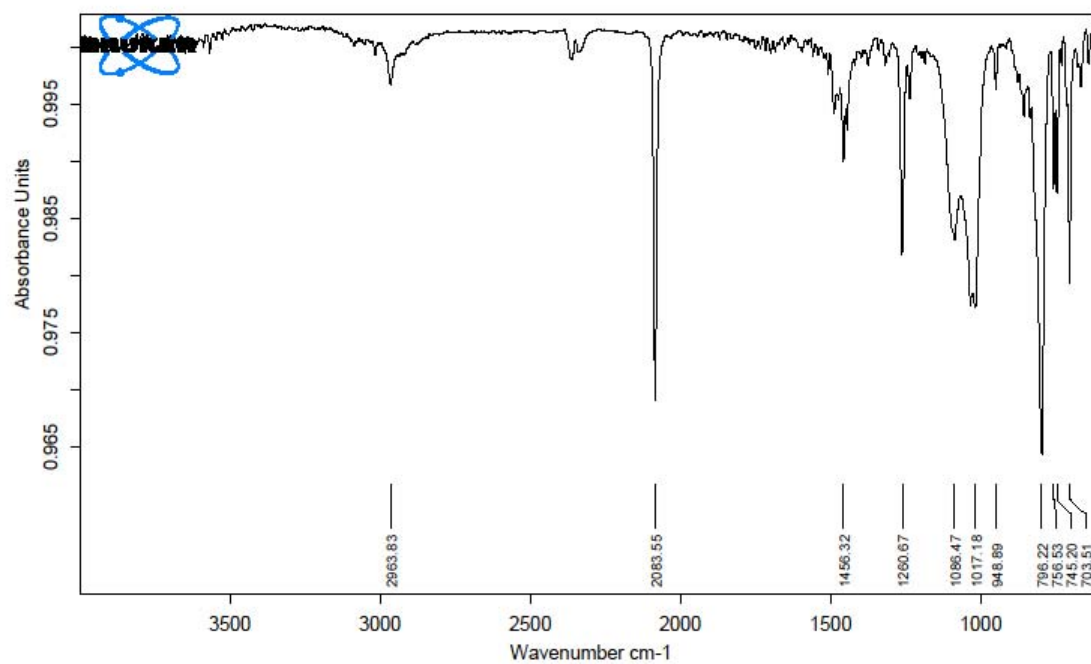
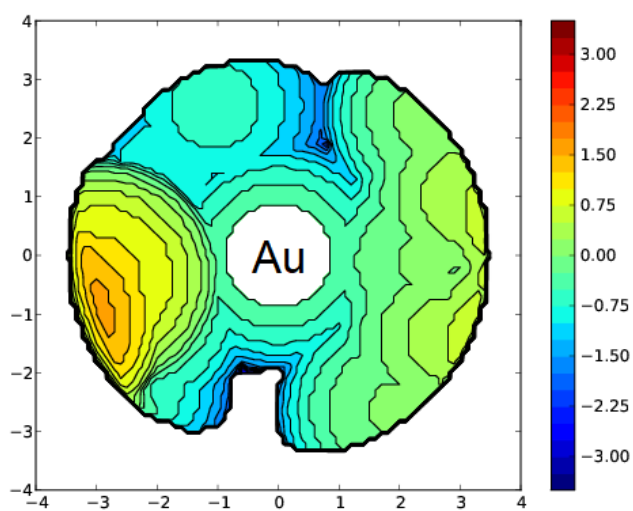
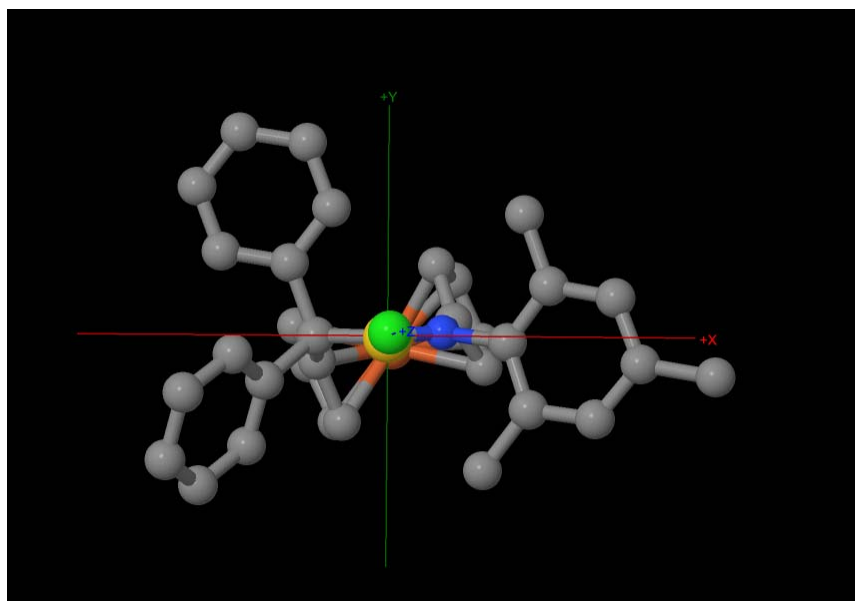
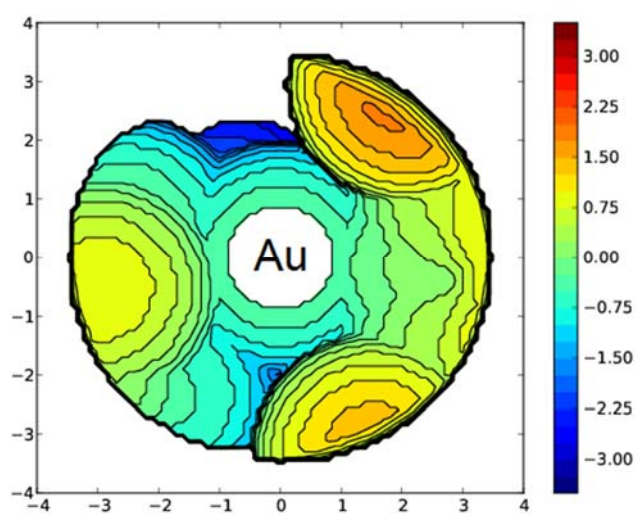
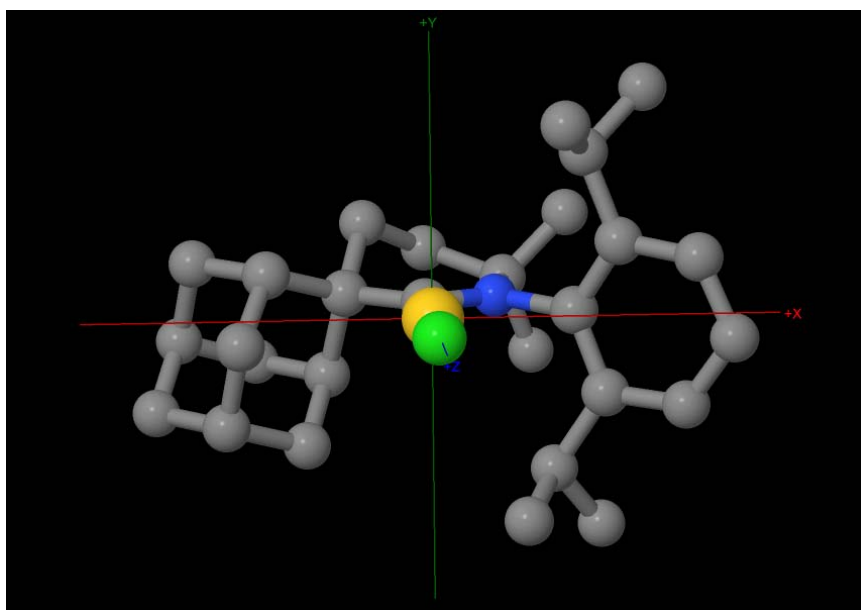


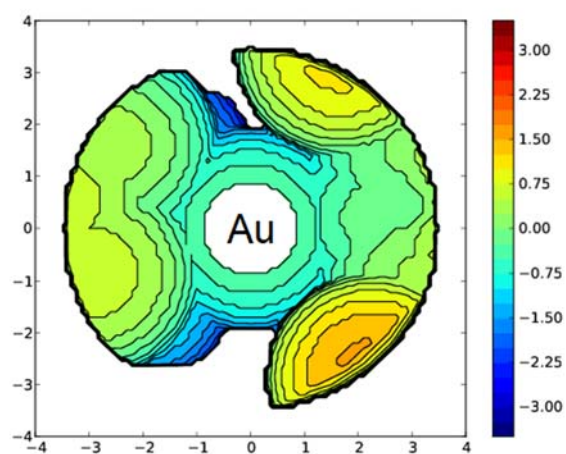
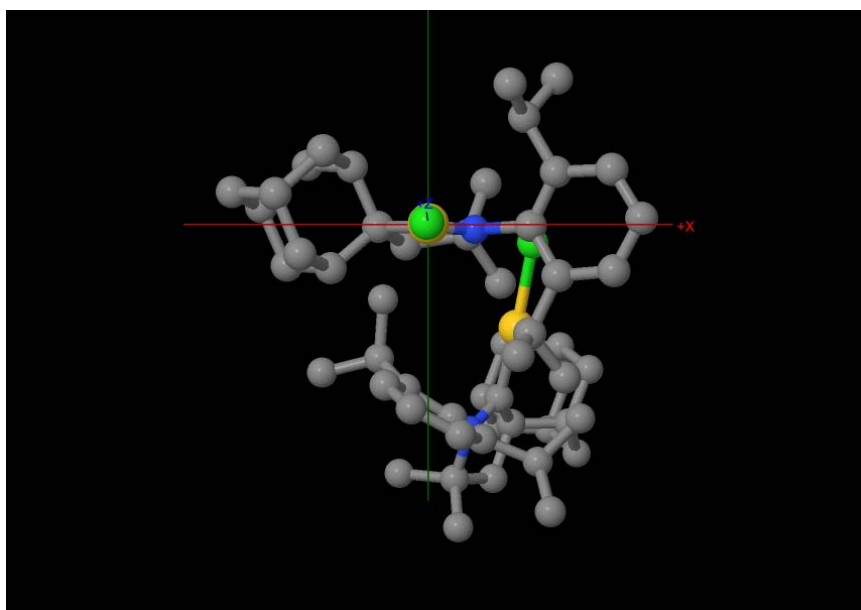
Figure S74. IR spectrum (ATR) of $\mathbf{8}^{\text{Mes}}\text{CO}$.

G Percent Buried Volume ($\%V_{bur}$) as Determined from $[\text{AuCl}(\text{L})]$ ($\text{L} = \mathbf{8}^{\text{Mes}}$, H, I, K) $\%V_{bur} = 45.8$ **Figure S75.** $\%V_{bur}$ determined for $\mathbf{8}^{\text{Mes}}$ from $[\text{AuCl}(\mathbf{8}^{\text{Mes}})]$.



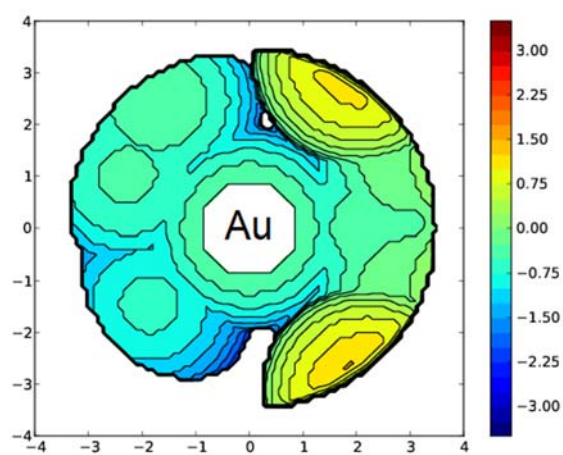
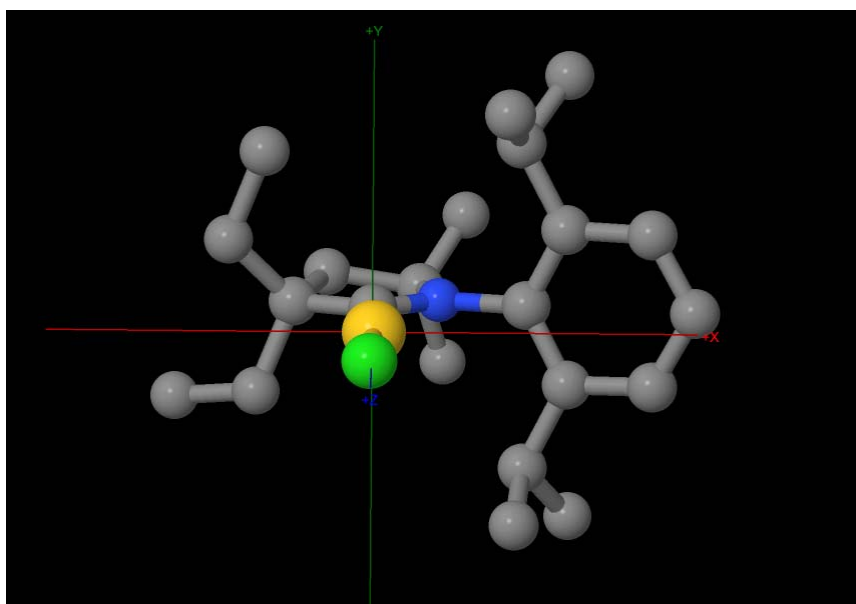
$\%V_{bur} = 51.0$

Figure S76. $\%V_{bur}$ determined for CAAC-6 H from $[\text{AuCl}(\text{H})]$.^{S7}



$\%V_{bur} = 48.3$

Figure S77. $\%V_{bur}$ determined for CAAC-5 I from $[\text{AuCl}(\text{I})]$.⁵⁸



$$\%V_{\text{bur}} = 42.9$$

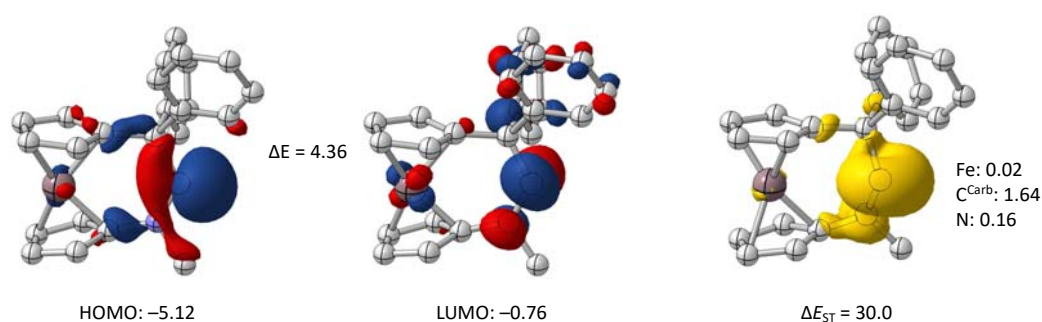
Figure S78. $\%V_{\text{bur}}$ determined for CAAC-5 K from $[\text{AuCl}(\text{K})]$.^{S9}

II Computational Details

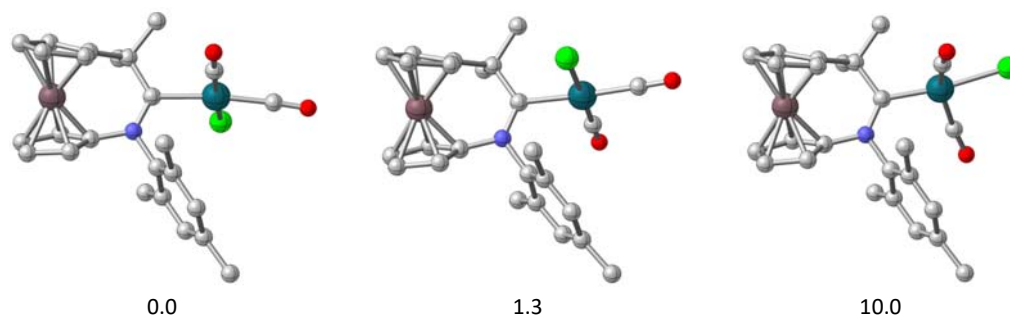
All geometry optimizations and harmonic frequency calculations were performed using the Gaussian16^{S10} program package (Rev. B.01). For comparison of frontier orbitals and singlet-triplet gaps the B3LYP^{S11-S13} functional combined with the def2-TZVPP^{S14} basis set was used. For mechanistic investigations the M06L^{S15} density functional combined with the def2-SVP^{S14} basis set and the D3 dispersion correction was used.^{S16} Zero-point vibrational energies and thermal contributions to Gibbs free energies at 298.15 K were obtained at this level of theory. Additional single point calculations on optimized geometries were performed using the same functional and the def2-TZVPP^{S14} basis set. Optimised structures were characterised as minima or first order saddle points by eigenvalue analysis of the computed Hessians. Connectivities between minima and the corresponding transition states were validated by intrinsic reaction coordinate (IRC) calculations^{S17} or by displacing the transition-state geometries along both directions of the transition mode, followed by unconstrained optimisations to the respective minima. Bonds formed or broken in transition states are shown dashed, unreactive H atoms are omitted and the orientation of Ph substituents is indicated by showing the C_{ipso} atom only.

Pictures of molecular structures were generated with the Cylview^{S18} and Chemcraft^{S19} program. All energies given are relative free energies at 298.15 K and 1 atm (ΔG^{298}) in kcal mol⁻¹.

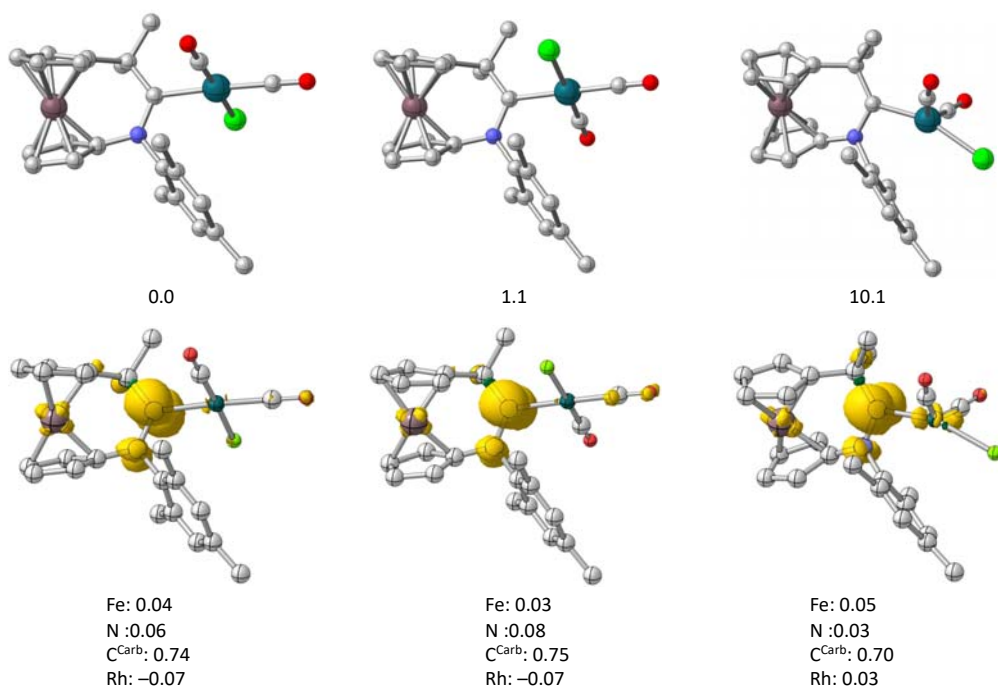
Additional Information



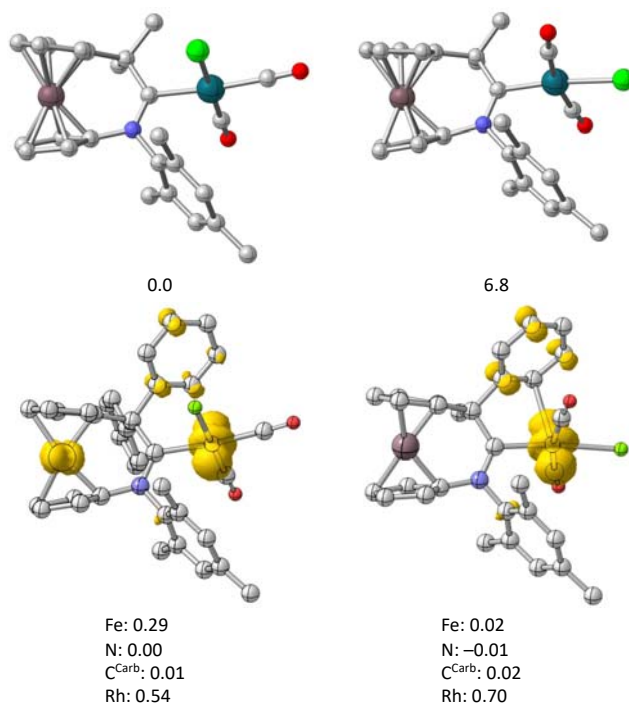
Scheme S1. Frontier orbitals of **8**^{Me} (orbital energies in eV) and spin density of the triplet (computed $\Delta E_{S/T}$ in kcal/mol) and Mulliken spin populations (right).



Scheme S2. Top: structure of $[\text{RhCl}(\mathbf{8}^{\text{Mes}})(\text{CO})_2]$, its conformer (middle) and isomer (right) with relative energies ΔE in kcal mol⁻¹.



Scheme S3. Top: structure of the radical anion $[\text{RhCl}(\mathbf{8}^{\text{Mes}})(\text{CO})_2]^{-\bullet}$, its conformer (middle) and isomer (right) with relative energies ΔE in kcal mol^{-1} . Bottom: spin densities with Mulliken spin populations.

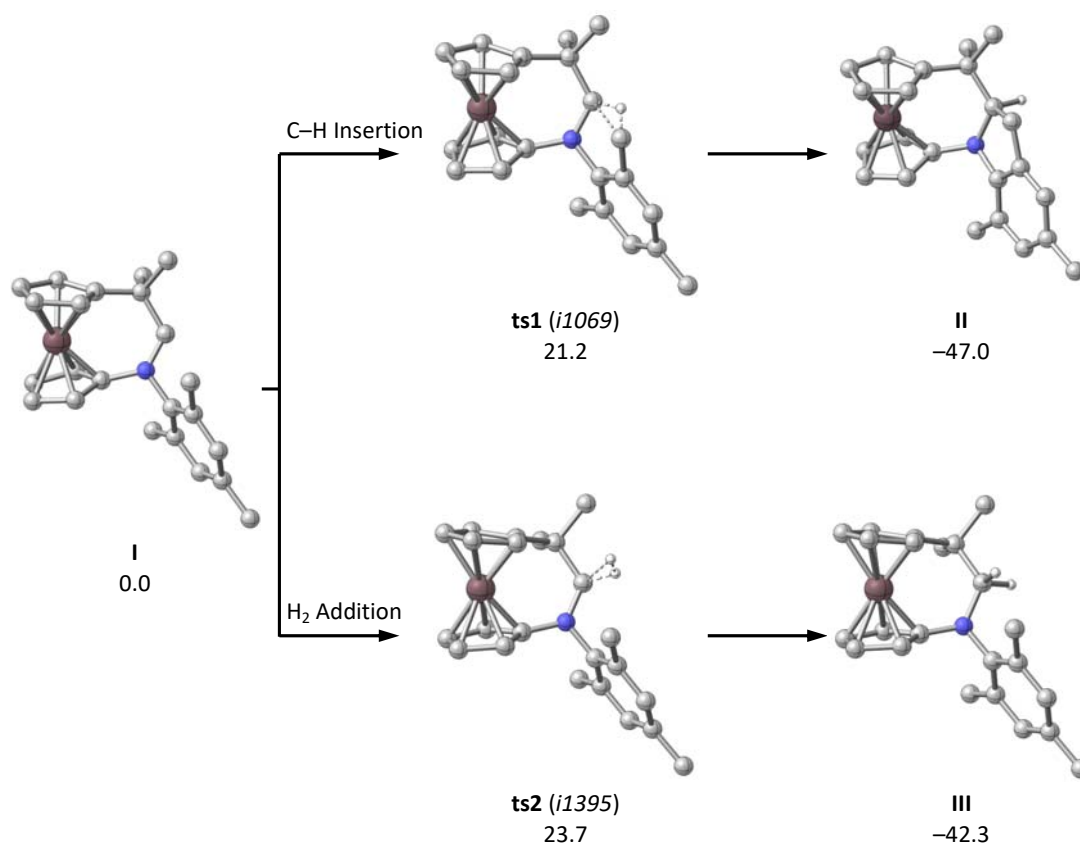


Scheme S4. Top: structure of the radical cation $[\text{RhCl}(\mathbf{8}^{\text{Mes}})(\text{CO})_2]^{\bullet+}$ and its isomer (right) with relative energies ΔE in kcal mol^{-1} . Bottom: spin densities with Mulliken spin populations.

Table S5. Calculated CO vibrations for $[\text{RhCl}(\mathbf{8}^{\text{Mes}})(\text{CO})_2]$ and the radical anion/cation. Shift $\Delta\tilde{\nu}$ relative to the neutral complex (free CO: 2229 cm^{-1}).

	CO vibration (cm^{-1})	$\Delta\tilde{\nu}$ (cm^{-1})
$[\text{RhCl}(\mathbf{8}^{\text{Mes}})(\text{CO})_2]$		
asymmetric	2065	
symmetric	2139	
$[\text{RhCl}(\mathbf{8}^{\text{Mes}})(\text{CO})_2]^{\bullet+}$		
asymmetric	2111	46
symmetric	2184	45
$[\text{RhCl}(\mathbf{8}^{\text{Mes}})(\text{CO})_2]^{\bullet-}$		
asymmetric	2019	-46
symmetric	2078	-61

I is the full molecular system $\mathbf{8}^{\text{Mes}}$ and **II** is the experimentally observed product **10**. Unreactive hydrogen atoms are omitted and the orientation of the phenyl substituents is indicated by showing the respective C_{ipso} atom only.



Scheme S5. Computed reaction paths for intramolecular C–H insertion (top) and H₂ addition (bottom) for **I** (relative free energies in kcal/mol).

H	7.07382	-1.78320	-1.08895
C	2.54895	-0.74860	2.56545
H	1.91281	0.14305	2.64792
H	3.29347	-0.70558	3.37006
H	1.91212	-1.62382	2.76816
C	-1.84628	-0.66524	1.30270
C	-1.01777	-0.89060	2.40203
H	0.05615	-0.97300	2.25017
C	-1.54241	-1.01288	3.69066
H	-0.86689	-1.18768	4.53230
C	-2.91474	-0.91831	3.90043
H	-3.32909	-1.01544	4.90648
C	-3.75816	-0.70942	2.80728
H	-4.83923	-0.64697	2.95290
C	-3.22963	-0.59273	1.52575
H	-3.90080	-0.44820	0.67421
C	-2.06445	-1.64038	-0.93365
C	-2.99545	-1.35483	-1.93619
H	-3.20059	-0.31877	-2.21454
C	-3.67019	-2.38476	-2.59410
H	-4.39121	-2.13992	-3.37793
C	-3.42616	-3.71425	-2.26008
H	-3.95314	-4.51905	-2.77794
C	-2.51215	-4.00744	-1.24684
H	-2.32241	-5.04572	-0.96357
C	-1.84973	-2.98015	-0.58282
H	-1.14608	-3.20795	0.22267
H	0.37897	-1.65385	-1.16234
H	0.10953	-1.30803	-2.05060

References

- S1 A. Shafir, M. P. Power, G. D. Whitener and J. Arnold, *Organometallics*, 2000, **19**, 3978.
- S2 D. P. Day, T. Dann, R. J. Blagg and G. G. Wildgoose, *J. Organomet. Chem.*, 2014, **770**, 29.
- S3 Q.-S. Liu, D.-Y. Wang, J.-F. Wang, Z.-Y. Ma and M. Ye, *Tetrahedron*, 2017, **73**, 3591.
- S4 R. Uson, A. Laguna, M. Laguna, D. A. Briggs, H. H. Murray and J. P. Fackler, Jr., *Inorg. Synth.*, 1989, **26**, 85.
- S5 (a) J. Klein, A. Stuckmann, S. Sobottka, L. Suntrup, M. van der Meer, P. Hommes, H.-U. Reissig and B. Sarkar, *Chem. Eur. J.*, 2017, **23**, 12314; (b) M. Krejčík, M. Daněk and F. Hartl, *J. Electroanal. Chem. Interfacial Electrochem.*, 1991, **317**, 179.
- S6 G. M. Sheldrick, *Acta Crystallogr. Sect. A*, 2008, **64**, 112.
- S7 C. M. Weinstein, G. P. Junor, D. R. Tolentino, R. Jazzar, M. Melaimi and G. Bertrand, *J. Am. Chem. Soc.*, 2018, **140**, 9255.
- S8 V. Lavallo, G. D. Frey, S. Kousar, B. Donnadiu and G. Bertrand, *Proc. Natl. Acad. Sci. U. S. A.*, 2007, **104**, 13569.
- S9 M. T. Proetto, K. Alexander, M. Melaimi, G. Bertrand and N. C. Gianneschi, *Chem. Eur. J.*, 2021, **27**, 3772.
- S10 M. J. Frisch, G. W. Trucks, H. B. Schlegel, G. E. Scuseria, M. A. Robb, J. R. Cheeseman, G. Scalmani, V. Barone, G. A. Petersson, H. Nakatsuji, X. Li, M. Caricato, A. V. Marenich, J. Bloino, B. G. Janesko, R. Gomperts, B. Mennucci, H. P. Hratchian, J. V. Ortiz, A. F. Izmaylov, J. L. Sonnenberg, Williams, F. Ding, F. Lipparini, F. Egidi, J. Goings, B. Peng, A. Petrone, T. Henderson, D. Ranasinghe, V. G. Zakrzewski, J. Gao, N. Rega, G. Zheng, W. Liang, M. Hada, M. Ehara, K. Toyota, R. Fukuda, J. Hasegawa, M. Ishida, T. Nakajima, Y. Honda, O. Kitao, H. Nakai, T. Vreven, K. Throssell, J. A. Montgomery Jr., J. E. Peralta, F. Ogliaro, M. J. Bearpark, J. J. Heyd, E. N. Brothers, K. N. Kudin, V. N. Staroverov, T. A. Keith, R. Kobayashi, J. Normand, K. Raghavachari, A. P. Rendell, J. C. Burant, S. S. Iyengar, J. Tomasi, M. Cossi, J. M. Millam, M. Klene, C. Adamo, R. Cammi, J. W. Ochterski, R. L. Martin, K. Morokuma, O. Farkas, J. B. Foresman and D. J. Fox, Wallingford, CT, 2016.
- S11 A. D. Becke, *J. Chem. Phys.*, 1993, **98**, 5648.
- S12 A. D. Becke, *Phys. Rev. A*, 1988, **38**, 3098.
- S13 C. Lee, W. Yang and R. G. Parr, *Phys. Rev. B*, 1988, **37**, 785.
- S14 F. Weigend and R. Ahlrichs, *Phys. Chem. Chem. Phys.*, 2005, **7**, 3297.
- S15 Y. Zhao, D. G. Truhlar, *J. Chem. Phys.*, 2006, **125**, 194101.
- S16 S. Grimme, J. Antony, S. Ehrlich and H. Krieg, *J. Chem. Phys.*, 2010, **132**, 154104.
- S17 K. Fukui, *Acc. Chem. Res.*, 1981, **14**, 363.
- S18 C. Y. Legault, Université de Sherbrooke, <http://www.cylview.org>, 2009.
- S19 G. A. Andrienko, 2015.